UNIVERSITÀ DEGLI STUDI DI PALERMO

Dottorato di Ricerca in Oncologia e Chirurgia Sperimentali

Dipartimento di Medicina di Precisione in Area Medica, Chirurgica e Critica (Me.Pre.C.C.)

"Characterization of the secretome from Spheroids of Adipose derived Stem Cells (SASCs) and its potential for tissue regeneration"

Doctoral Dissertation of:
Valentina Urrata

Supervisor:
Prof. Michele Rosario Colonna
Prof. Rosario Emanuele Perrotta

Tutor:
Prof. Francesca Toia

Co-Tutor:
Dr. Anna Barbara Di Stefano

The Chair of the Doctoral Program:
Prof. Antonio Russo

Years 2021/2024 - Cycle XXXVI

Index

Abstract

Introduction: Adipose-derived Stem Cells (ADSCs), a population of Mesenchymal Stem Cells (MSCs), showed very important features in the field of regenerative medicine such as high multilineage differentiation potential and immunomodulatory activity. In the last years, MSC properties have been attributed to their secreted factors such as soluble proteins, cytokines and growth factors. Moreover, a key role is played by the extracellular vesicles (EVs) which lead a heterogeneous *cargo* of proteins, lipids, mRNAs and small and long non-coding RNAs that interfere with the pathways of the recipient cells.

Purpose: The aim of this work was to characterize the composition of the secretome from 3D Spheroids of Adipose-derived Stem Cells (SASCs) by screening it for a pool of mRNAs and miRNAs. In addition, the effect of the total secretome and the isolated exosomes on endothelial cells, fibroblasts and osteoblasts was tested in *in vitro* wound healing assays.

Material and Methods: Adipose tissue and/or lipoaspirate samples were collected from healthy individuals after signing informed consent. Cells were extracted and cultured for one week. Then, their secretomes were isolated every 72 hours. The exosomes were extracted and characterized by DLS, SEM and Western Blotting analysis and the expression of a panel of mRNAs and miRNAs as internal *cargo* were evaluated through Real-time PCR. Lastly, the wound healing assay was performed to investigate the regenerative potential of the total secretome and/or isolated exosomes on endothelial cells, fibroblasts and osteoblasts.

Results: The exosomes secreted from SASCs showed an up-regulation of NANOG and SOX2 mRNAs, typical of stemness maintenance, as well as miR-126 and miR-146a, related to angiogenic and osteogenic processes. Moreover, the isolated exosomes showed an enhanced pro-regenerative effect on endothelial cells, fibroblasts and osteoblasts if compared to the total secretome in *in vitro* wound healing assay.

Conclusions: The secretome from SASCs carried paracrine signals involved in stemness maintenance, pro-angiogenic and pro-osteogenic differentiation, immune system regulation and regeneration.

Summary

Recently, three-dimensional (3D) cell cultures were developed to mimic better the *in vivo* microenvironment than two-dimensional (2D) conditions [1-3]. In fact, cells 3D cultured do not alter their morphology and their polarity, due to the loss of interaction with the surface of cell culture plates [4] and do not exhibit an altered gene expression and biochemistry [5]. Cells seeded in a three-dimensional environment generate aggregates in suspension, as spheroids, called 'SASCs' [6]. Several techniques have been applied to obtain spheroids but, currently, there is no standardized one [7]. Anyway, we showed that spheroids can be obtained directly from liposuction fat or adipose tissue digestion, seeding Adipose derived Stem Cells in ultra-low adhesion conditions without additional steps [8]. In addition, several studies proved that all cells secrete soluble factors and extracellular vesicles (EVs), called 'secretome', as paracrine signalling to communicate with the surrounding environment [9-11]. We have already evaluated the composition of the soluble fraction of the secretome from SASCs for a panel of 52 analytes [12]. In this work we screened exosomes from SASCs for a pool of mRNAs and miRNAs as their internal *cargo* and, finally, the regenerative effects of the exosomes were evaluated on three cell lineages through *in vitro* wound healing assays.

Introduction

1.1 Stem Cells

A stem-cell is a self-renewal and undifferentiated cell able to generate the different specialized cell types found in the body [13]. Stem cells can be divided into embryonic and adult stem cells. Embryonic stem cells are totipotent, so they can generate any kind of cell line of the body while adult stem cells can only form certain types of specialized cells [14]. They can make symmetric or asymmetric division. In the first one, a stem cell divides and both cells stay undifferentiated in the form of stem cells. Instead, in the asymmetric division one generated stem cell goes on to proliferate and differentiate into the progeny, and the other one stays as a stem cell [15].

1.2 Mesenchymal Stem Cells

Mesenchymal stem cells (MSCs) were initially identified in the bone marrow stroma in the late 1960s by Friedenstein [16]. They are multipotent cells able to differentiate into several mesenchymal lineages such as adipocytes, osteoblasts, chondrocytes, myocytes [17, 18] and also neuron-like [19]. MSCs were found in almost all tissues and are highly mobile in response to tissue damage signals [20, 21]. Moreover, they are responsible of several cell functions such as pro-angiogenesis [22], immunomodulation [23], anti-inflammation [24], anti-apoptosis [25], neuro-protection and regulation [26] but several studies showed that these functions are not mainly exerted by cells but by their secreted paracrine factors [10, 27-30].

1.3 Adipose-derived Stem Cells (ADSCs)

Adipose tissue derives from mesenchyme [31] and it is divided into white (WAT) and brown (BAT) adipose tissue. WAT is critical for energy storage, endocrine communication, and insulin sensitivity while BAT is critical for body temperature maintenance [32]. Adipose tissue is homogeneously distributed throughout the body and, due to its abundance and the easiness of surgical accessibility, it became the new primary source of MSCs. Adipose-derived Stem Cells (ADSCs) exhibit high multilineage differentiation potential and immunomodulatory activity, very important features in the field of regenerative medicine [33].

1.4 Spheroids of Adipose-derived Stem Cells (SASCs)

Although, for a long time, 2D cell cultures have been used from researches as *in vitro* models, the attention has recently shifted towards 3D cell cultures as they better mimic *in vivo* cell microenvironment [1, 2, 34, 35]. Two-dimensional culture conditions lead cells to alter their morphology and surface adhesion molecules [4] but they also show unlimited access to the nutrients of culture medium due to their arrangement on a monolayer [36] and could alter their gene and protein expression [5]. Thus, recently, several studies were performed on 3D cultures, demonstrating their effective superiority. Although to date there is still no standardized technique to obtain 3D spheroids [7, 37, 38], our recent study showed that spheroids can be directly obtained from liposuction fat or adipose tissue digestion, seeding ADSCs in ultra-low adhesion conditions without any additional step, forming the so called 'SASCs' [8]. They show a higher multilineage differentiation potential, the ability of maintaining stemness until 28 days and better regenerative abilities in *in vitro* and *in vivo* experiments if compared to 2D cultured cells [39, 40] [41].

1.5 Secretome

Cells need to communicate between each other and to exchange information not only through a direct cell-cell interaction but also through an indirect way as the endocrine, autocrine and paracrine signalling [42]. In particular, paracrine signalling can occur through a set of soluble factors and/or extracellular vesicles (EVs) secreted by the cells and released in the culture medium, called 'conditioned medium'. The pool of secreted factors together

with EVs is called 'secretome'. Amongst the main components of the soluble fraction there are proteins, cytokines, chemokines and growth factors [43], whilst EVs are distinguished into exosomes, microvesicles (MVs) and apoptotic bodies, according to their size and biogenesis.

1.6 Extracellular Vesicles (EVs)

Extracellular vesicles (EVs) are mainly classified in: exosomes, microvesicles and apoptotic bodies. Exosomes are spheroidal shape vesicles of 30-150 nm in size. They derive from multivesicular bodies (MVBs) generated by the early endosomes. MVBs are rich in intraluminal vesicles (ILVs), generated by the inward budding of endosomal membranes. MVBs fate can be dual: they can fuse with lysosomes being degraded or they can be transported to plasma membrane and, after fusion with it, they can release their EVs content outside the cells. In this case, released ILVs are called exosomes. The proteins mainly expressed on the exosomes surface are CD63, CD9 and CD81 [44]. Microvesicles are 100-1000 nm in size and derive by plasma membrane shedding. They are directly released into the extracellular space and their surface is characterized by membrane components typical of the cell of origin. They are characterized by an irregular shape [45]. Both exosomes and microvesicles are enriched in small and long non-coding RNAs, mRNAs, lipid and proteins by conveying specific information to the recipient cells [46, 47]. Apoptotic bodies are 1-3 µm in size and derive from apoptotic cells. Apoptosis is a programmed cell death which involves a cascade of tightly regulated processes. At the end of them, apoptotic cells disassemble themselves and release apoptotic bodies (ApoBDs) [48]. They have a variable shape and group cytosolic fragments and proteins as well as nuclear fragments (such as DNA and histones) or even organelles to protect the neighbouring cells [49, 50].

1.7 Secretome advantages

It has been proved that the secretome has a higher safety profile if compared to cell engrafting due to its reduced possibility of neoplastic transformation [51] and a better ease of storage with the use of natural and non-toxic agents such as the trehalose, a natural disaccharide found in many foods [52]. Moreover, in the last few years, vesicles have been engineered for a controlled drug delivery and the simultaneous overcoming of drug

resistances which is a widespread problem to date [53-56]. Exosomes have generated considerable interest for clinical application as diagnostic biomarkers and therapeutic *cargo* carriers [16]. Reduced immunogenicity due to their biocompatibility and a bi-layered lipid structure, which protects the genetic *cargo* from degradation, makes them attractive as therapeutic vectors. Their small size and membrane composition allow them to cross major biological membranes including the blood brain barrier [44].

1.8 mRNAs and microRNAs

Messenger RNA (mRNA) is a single-stranded RNA synthesized from a DNA template during the transcription process. It carries protein information from the DNA, located in the cell's nucleus, to the cell's cytoplasm. Here, it will be decodified by ribosomes that, together with tRNAs, add the corresponding aminoacid for each three-base (codon) of mRNA and translated it into a protein. MicroRNAs (miRNAs) are a class of small non coding RNAs of 21–25 nucleotide single-stranded RNAs (ssRNAs), produced from precursors through several steps. The first step consists in pri-miRNA processing, within the nucleus, to a pre-miRNA. This step is performed by the RNAse III endonucleases, Drosha. pre-miRNAs is carried to the cytoplasm by exportin-5 (EXP-5). Here, it is again processed to become a mature miRNA by Dicer, an RNase III endonucleases loaded onto the Argonaute (ago) protein. A miRNA duplex is generated and it is divided into a single strand miRNA by an helicase. Mature single strand miRNA is complexed with RISC and thus it can targets the mRNAs [57, 58].

1.9 Rationale and Objectives

Recently our research group demonstrated that ADSCs cultured in 3D ultra-low adhesion conditions to form spheroids of ADSCs (SASCs) show better stemness properties than 2D cultured ASCs together with a higher expression of stemness-associated mRNAs. Moreover, SASCs cultured in Integra scaffold and implanted in an *in vivo* T8 laminectomy mice models showed a significant participation in bone tissue regeneration [39] as well as SASCs implanted in an *in vivo* calvaria rabbit model also induced neo-vessels formation [41].

SASCs are directly isolated in ultra-low conditions in the way to do not alter their properties. Since cells communicate each other also through a paracrine signalling, our aim was to characterize the secretome from SASCs. In our previous study we performed the Luminex Assay to screen the secretome from SASCs for a panel of soluble factors.

In this work, we isolated the exosomal population from SASCs by performing:

- Characterization analysis (DLS, SEM and Western Blotting)
- Analysis of a pool of EVs mRNAs and miRNAs as internal *cargo*
- Wound healing assay on endothelial cells, fibroblasts and osteoblasts to evaluate the regenerative effects of exosomes.

CHAPTER 2

Materials and Methods

2.1 Cells extraction and culture

Adipose tissue or liposuction fat were collected from healthy individuals after signing informed consent at the Plastic and Reconstructive Surgery Unit of Palermo. The Hospital ethical committee approved the study so an informed consent was collected from each patient. Adipose tissue or liposuction fat were enzymatically and mechanically digested. Adipose tissue was digested with Collagenase (150 mg/ml; Gibco) and Hyaluronidase (20 mg/ml; Sigma) through mechanical agitation for 1 hour at 37°C while liposuction samples were digested with collagenase (150 mg/ml; Gibco) through mechanical agitation for 30 minutes at 37°C. The samples were then centrifuged at 1200 x g for 5 minutes and the Stromal Vascular Fraction (SVF) was divided into two parts: a half was seeded with serum-free stem cell specific medium (SCM) added with basic fibroblast growth factor (bFGF; 10 ng/ml; Sigma) and epidermal growth factor (EGF; 20 ng/ml) and plated in ultra-low adhesion flasks (Corning). The other half was seeded in adhesion flasks (Corning) with Dulbecco's Modified Eagle's Medium High Glucose (DMEM) (Sigma) complemented with 10% Fetal Bovine Serum (FBS) (EuroClone) and were called ADSCs. Both the cell media were replaced twice a week. Endothelial cells, Fibroblasts and Osteoblasts were cultured in adhesion flasks (Corning). Endothelial cells and osteoblasts were differentiated from SASCs for 21 days with a specific differentiation medium: Endothelial Cell Growth Medium (PromoCell) and Osteoblast Growth Medium (PromoCell). Normal Human Dermal Fibroblasts (NHDF) were provided by PromoCell and cultured with Fibroblast Growth Medium (PromoCell). Cells were maintained at 37°C in a 5% CO_2 humidified incubator.

2.2 Secretome collection and exosomes extraction

Cells were cultured for one week and then the media were collected each 72 hours and centrifuged at 2000 x g per 30 minutes to remove cells and debris, according to the Total Exosome Isolation (from cell culture media) protocol (Invitrogen). The cell-free culture medium was transferred in a new tube and 0.5 volumes of Total Exosome Isolation Reagent were added. The solution was mixed and the samples were incubated at 4°C overnight. Then, the samples were centrifuged at 10.000 x g for 1 hour at 4°C. The supernatant was discarded and the pellet was appropriately resuspended in 200 µl 1X PBS for RNA extraction or in 50 µl of Exosome Resuspension Buffer for protein extraction.

2.3 Protein extraction and quantification

EVs protein extraction was performed by Total Exosome RNA and Protein Isolation Kit (Invitrogen). After having resuspended the exosome pellet in 50 µl of Exosome Resuspension Buffer for protein extraction, the total protein amount was analysed through Qubit™ Protein Assay Kit (Termofisher) according to the manufacturer protocol, and then read using the Qubit™ 4 Fluorometer instrument.

2.4 Exosomes characterization

Exosomes were characterized by Dynamic Light Scattering (DLS), Scanning Electron Microscopy (SEM) and Western Blotting analyses. DLS was performed through the Zetasizer nano ZSP 2 (MALVERN) instrument and Scanning Electron Microscopy through FEI – Versa 3D Dual Beam Microscope. In the DLS technique a laser strikes the solution and the intensity of the scattered light as a function of time is measured. Light is scattered due to the Brownian motion of particles that correlates with their hydrodynamic diameter. The smaller the particle, the faster it will diffuse. The bigger the particle, the slower it will diffuse. DLS instrument will generate a correlation function that is mathematically linked with particle size and its time-dependent light scattering capacity. SEM uses a focused beam of high-energy electrons to investigate the surface of solid samples. Electrons are generated by an electron source and are accelerated. When they impact against the sample, decelerated. The electron-sample interactions produce a variety of signals such as backscattered electrons, secondary electrons, photons, visible light and heat. All of them give information about the sample external morphology and crystalline structure and orientation at micro and nano scale.

For Western Blotting, after protein extraction and quantification, 40 µg of proteins from SASCs-derived exosomes were complexed with 2x Laemmli Sample Buffer (BioRad) and added with 2-mercaptoethanol (BioRad). The same protein amount from 3D SASCs and 2D ASCs as control was prepared. Samples were loaded in the Mini-PROTEAN® TGX Stain-Free™ Gels (BioRad). The gel was blotted on the Trans-Blot® Turbo™ Transfer Pack (BioRad) through the Trans-Blot Turbo instrument (BioRad) in 7 minutes. The membrane was then incubated with 1x TBS 1% Casein Blocker (BioRad) for 1 hour at RT during shaking and then incubated overnight at 4°C with the primary antibody CD63 (Invitrogen) diluted 1:250. The day after, the membrane was washed three-times with tTBS 0.05% and then incubated for 2 hours with the Goat Anti Mouse IgG antibody (HRP) (Prodotti Gianni Srl) diluted 1:5000. Membrane was washed with tTBS 0.05% twice and TBS 1x once and then the Clarity MaxTM Western ECL substrate (BioRad) was prepared by mixing in a 1:1 ratio the Clarity Western Peroxide Reagent and the Clarity Western Luminol/Enhancer Reagent. The membrane was incubated in the substrate solution for 5 minutes and then exposed to the ChemiDoc Imaging System (BioRad).

2.5 mRNA extraction from exosomes

mRNAs from exosomes were extracted by RNeasy Mini Kit (Qiagen). 350 µl of Buffer RLT previously completed with 2-mercaptoethanol (BioRad), were added to the pellet. The mix was vortexed for 1 minute and passed through a 1 ml syringe with needle. Then, 1 volume of 70% ethanol was added and the mixture was transferred to an RNeasy Mini Spin column and centrifuged at 12.000 rpm for 15 seconds. The flow through was discarded and a new centrifuge with the addition of 700 µl of Buffer RW1 onto the RNeasy Mini Spin column was performed for 15 seconds at 12.000 rpm. The flow-through was discarded and two other centrifugations with the addition of 500 µl of Buffer RPE were performed at the same velocity of 12.000 rpm but respectively for 15 seconds and 2 minutes. Then, the RNeasy Mini Spin column was centrifuged at the full speed (14.000 rpm) for 1 minute to dry the membrane. Finally, 30 µl of RNase free water were added directly to the column membrane and centrifuged for 1 minute at 10.000 rpm. The total mRNA was eluted.

2.6 miRNA extraction from exosomes

miRNAs from exosomes were extracted by miRNeasy Mini Kit (Qiagen). The exosome pellet was disrupted by adding QIAzol Lysis Reagent and homogenized by vortexing for 1

minute and by passing it through a 1 ml syringe with needle. After incubating the homogenate for 5 minutes at RT, 140 µl of chloroform were added and shaked for 15 seconds. The sample was incubated for 3 minutes at RT and then centrifuged at 12.000 x g for 15 minutes at 4°C. The upper aqueous phase was recovered and 1.5 volumes of 100% ethanol were added. 700 µl of sample were transferred on the RNeasy Mini Spin column and centrifuged at 12.000 rpm for 15 seconds at RT. The flow-through was discarded. To wash the column, 700 µl of Buffer RWT were added and centrifuged at 12.000 rpm for 15 seconds. 500 µl Buffer RPE were pipetted onto the RNeasy Mini spin column and centrifuged for 15 seconds at 12.000 rpm to wash the column. The flowthrough was discarded and the previous step was performed again. A full speed centrifuge for 1 minute was executed to eliminate any possible contaminant inside the RNeasy Mini spin column. Finally, the RNeasy Mini spin column was transferred into a new 1.5 ml collection tube and 30 µl RNase-free water were pipetted directly onto the membrane. It was centrifuged for 1 minute at 12.000 rpm to elute the RNA.

2.7 RNA quantification

RNA was quantified by Qubit™ RNA HS Assay Kit (Termofisher) according to the manufacter protocol and then read using the Qubit™ 4 Fluorometer instrument.

2.8 mRNA Reverse Transcription and Real-time PCR

To perform mRNA reverse transcription, High Capacity cDNA Reverse Transcription Kit (Termofisher) was used. The sample was mixed as follows: 10X RT buffer 5 µl, 25 X dNTP Mix 2 µl, 10x RT Random Primers 5 µl, H_2O 10.5 µl, MultiScribe™ Reverse Transcriptase 2.5 µl and 25 µl of sample. The reverse transcription was performed by the MiniAmp Plus Thermal Cycler (Termofisher) and the protocol for cDNA obtaining was the following: 10 minutes at 25°C, 2 hours at 37°C and 5 minutes at 85°C followed by the decrease at 4°C to remove the sample.

To perform Real-time PCR, a master mix was prepared as follows: 10 µl of TaqMan™ Fast Advanced Master Mix (Termofisher), 7 µl of H_2O, 1 µl of primer and 2 µl of sample for a total of 20 µl per well. The amplification protocol was the following: step 1 consisting of 2 minutes at 50°C and 2 minutes at 95°C and step 2 consisting of 40 cycles, each one made by 1 second at 95°C and 20 seconds at 60°C. Real-time PCR was executed through the StepOnePlus instrument (Termofisher). The evaluated mRNAs were: SOX2

(Hs01053049_s1), NANOG (Hs04399610_g1), POU5F1 (Hs00999632_g1), PROM1 (Hs01009259_m1), SOX9 (Hs01001343_g1), VEGFA (Hs00900054_m1), HIF1A (Hs00153153_m1), PPARG (Hs01115513_m1), RUNX2 (Hs00231692_m1), VEGFR2 (Hs00911700_m1), IGF1 (Hs01547656_m1), CD31 (Hs00169777_m1), GAPDH (Hs02758991_g1). Results have been standardized to the relative expression of GAPDH.

2.9 miRNA Reverse Transcription and Real-time PCR

To perform miRNA reverse transcription, TaqMan^{TM} MicroRNA Reverse Transcription Kit (Termofisher) was used. Firstly, a primer pool containing 10 primers was generated. The primer pool was a mixture made by 2.5 µl of each primer and 225 µl of H$_2$O. Then, the reaction mix was prepared as follows: 6 µl of primer pool, 0.30 µl of dNTP mix w/dTTp, 1,5 µl of 10X RT Buffer, 0.19 µl of RNase Inhibitor, 3 µl of MultiScribe^{TM} RT enzyme and 4.04 µl of sample, corresponding to 19 ng of RNA for a total volume of 15 µl for the reverse transcription.

The reverse transcription protocol for miRNAs was the following: 30 minutes at 16°C, 30 minutes at 42°C and 5 minutes at 85°C. Then, the temperature decreased at 4°C to allow the removal of the sample. To perform Real-time PCR, a master mix was prepared as follows: 5 µl of TaqMan^{TM} Fast Advanced Master Mix (Termofisher), 3.84 µl of H$_2$O, 0.67 µl of sample and 0.50 µl of primer for a total of 10 µl per well. The amplification protocol was divided into two steps: 20 seconds at 95°C was the first step and then 3 seconds at 95°C and 30 seconds at 60°C both repeated 40 times was the second one. Real-time PCR was executed through the StepOnePlus instrument (Termofisher).

The evaluated miRNAs were: hsa-miR-191 (TM/RT:002299), mmu-miR-451 (TM/RT:001141), hsa-miR-126 (TM/RT:002228), hsa-miR-100 (TM/RT:000437), hsa-miR-221 (TM/RT:000524), mmu-miR-495 (TM/RT:001663), mmu-miR-140 (TM/RT:001187), hsa-miR-30c (TM/RT: 000419), hsa-miR-143 (TM/RT: 002249), hsa-miR-146a (TM/RT: 000468), hsa-miR-142-3p (TM/RT: 000464), hsa-miR-182 (TM/RT: 002334). Results have been standardized to the relative expression of miR-191.

2.10 Wound healing assay

Endothelial cells, Fibroblasts and Osteoblasts were seeded in a 24-well plate at the concentration of 15.000 cells/well until they reached confluence. The experimental conditions were the following: control exosomes (specific cell culture medium + PBS),

control secretome (specific cell culture medium + SCM), total exosomes (specific cell culture medium + isolated exosomes) and total secretome (specific cell culture medium + total secretome from 3D cultured SASCs). Image J software was used to measure the percentage of wounded area.
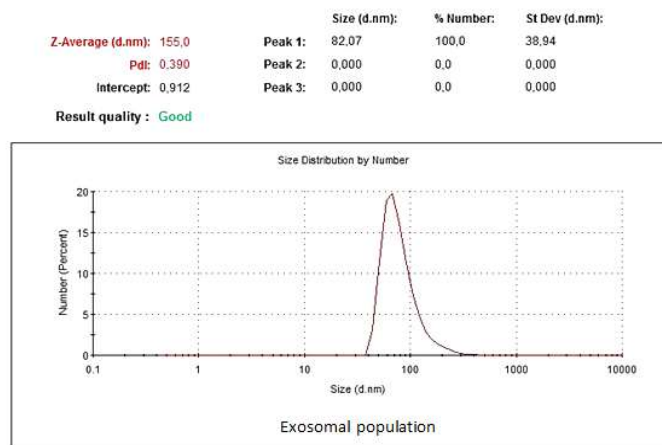
2.11 Statistical analysis

Data are expressed as mean ± standard deviation of three independent experiments. Statistical significance was calculated using one way analysis of variance (ANOVA), followed by either a Tukey's or Bonferroni's multiple comparison post hoc test. Significance levels were analysed with GraphPad Prism 8 statistical software and indicated as p values (*p<0.05, **p<0.01, ***p<0.001).

CHAPTER 3

Results

3.1 Exosomes characterization

DLS analysis was performed to evaluate the homogeneity of the extracted exosomal population from SASCs secretome. Results (Fig. 2) showed that all the analysed populations were homogeneous in size and ranged between 80 and 120 nm, in agreement with the exosomal dimensions amongst 30 and 150 nm [59]. SEM analysis was executed to investigate exosomes morphology and dimensions. Results (Fig. 3) demonstrated a round shape and a size between 90 and 120 nm, typical of exosomes and in agreement with DLS results.
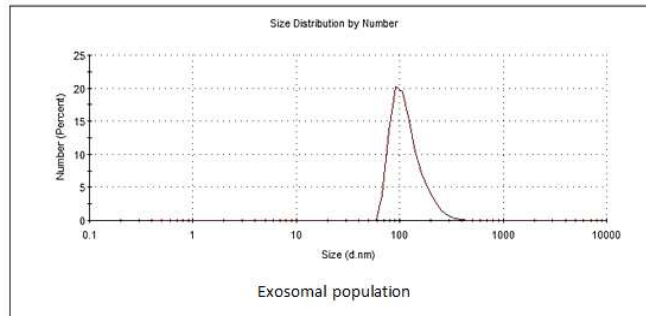
Fig. 2 – DLS analysis of three exosomal populations
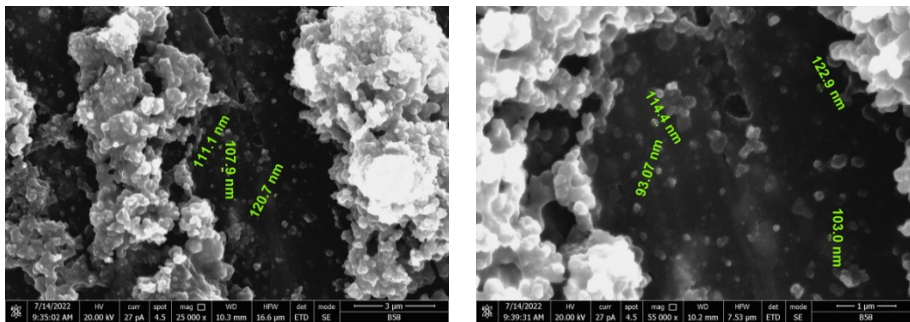
Fig. 3 – SEM analysis of two exosomal populations

The protein expression analysis was performed to demonstrate the presence of an exosomal population through anti-CD63. Results (Fig.4) showed the presence of a rich exosomal population derived from SASCs. The proteins from cell lysates of 2D ASC and 3D SASC were used as control.
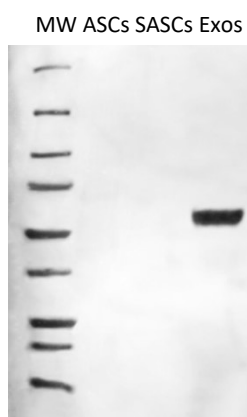
Fig. 4 – CD63 exosomal expression on: 2D ASC lysates, 3D SASC lysates and exosomes.

3.2 mRNA analysis

The gene expression analysis was performed to screen exosomes for a pool of mRNAs as their internal *cargo*. Results (Fig.5) showed that exosomes significantly expressed stemness-related mRNAs if compared to the ones related to angiogenesis or mesenchymal differentiation. In detail, NANOG was the most expressed mRNA amongst the stemness-related ones, followed by SOX2 and POU5F1. The expression of angiogenesis-related mRNAs and mesenchymal differentiation related mRNAs were considered negligible (Fig.5C).

(A)

EVs mRNA related to stemness

(B)

EVs mRNA related to angiogenesis

(C)

EVs mRNA related to mesenchymal differentiation
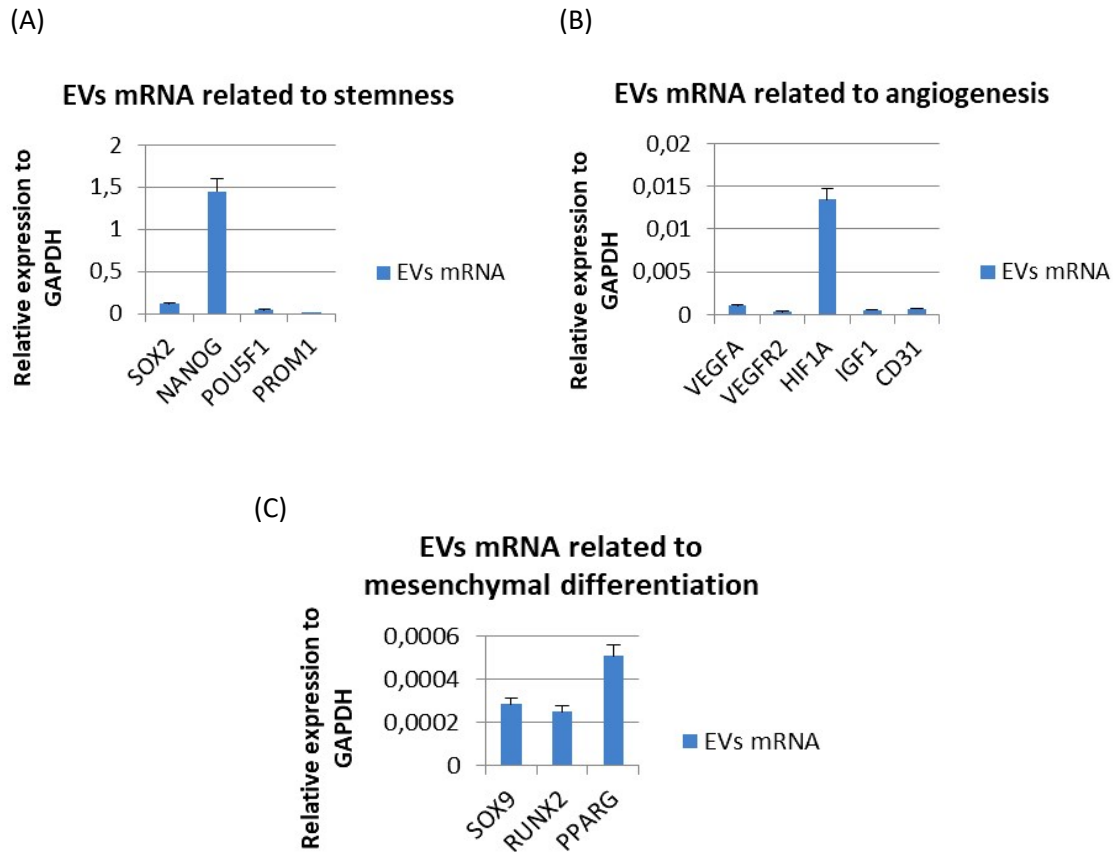
Fig. 5 – Exosomal internal *cargo*: analysis of 12 mRNAs. (A) stemness-related mRNAs; (B) angiogenesis-related mRNAs; (C) mesenchymal differentiation-related mRNAs.

3.3 miRNA analysis

A pool of 11 microRNAs (miRNAs), small endogenous non-coding RNAs of approximately 22 nt in length, was analysed as exosomal internal *cargo* [60, 61]. The higher miRNA expression was found for miR-126 and miR-146a. Then, a lower expression was found for miR-451 followed by miR-100, miR-143, miR-221, miR-140 and miR-30c (Fig. 6).
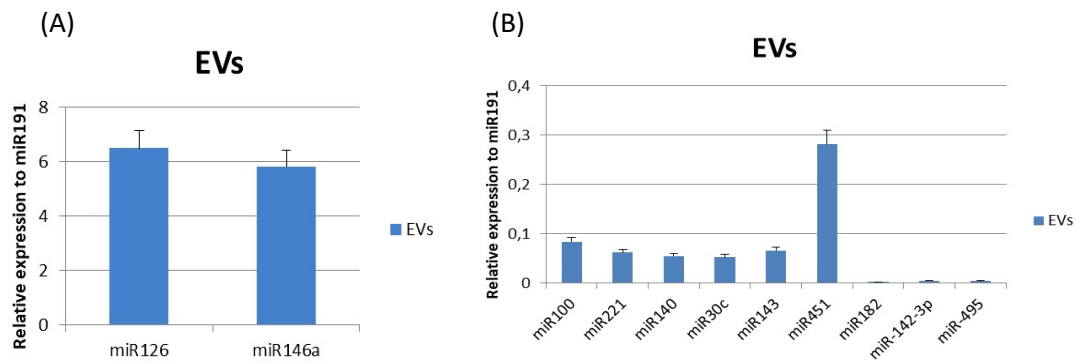
Fig. 6 – Exosomal internal *cargo*: analysis of 11 miRNAs. (A) Over-expressed miRNAs; (B) Less-expressed miRNAs.

3.4 Wound healing assay

Wound healing assay was performed to investigate if the total secretome or the exosomes exerted a more regenerative potential compared to the normal cell culture media. Results showed that endothelial cells treated with the secretome did not show a significant wounded area closure after 1 day of treatment, compared to the control. A different result was obtained after the total exosomes treatment. In fact, after 1 day, the percentage of wounded area was significantly decreased (Fig. 7A-7D). Similarly, after 1 day of treatment with the secretome, fibroblasts did not show a significant wound closure if compared to the control, whilst with the total exosomes there was a significant decrease of the wounded area that was almost completely closed after 2 days (Fig. 7B-7E). Osteoblasts treated with the secretome showed a comparable trend to the control while the use of the total exosomes led to a complete wound closure already after 1 day of treatment (Fig. 7C-7F).
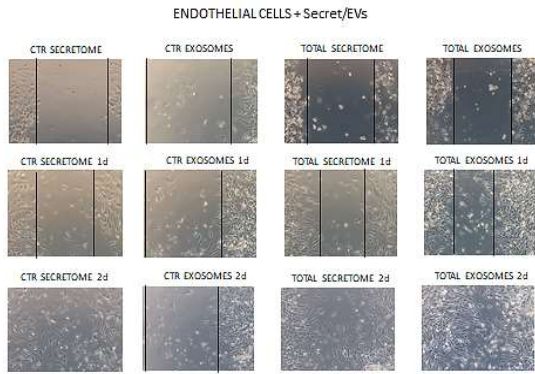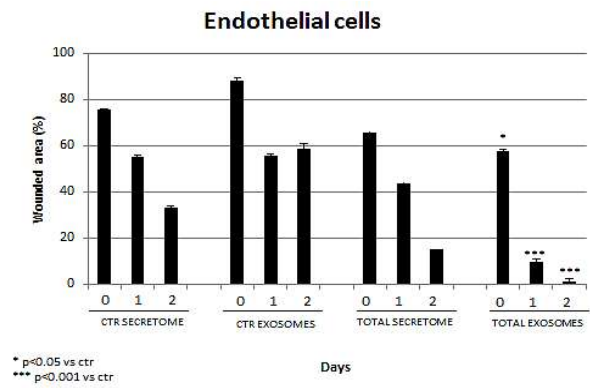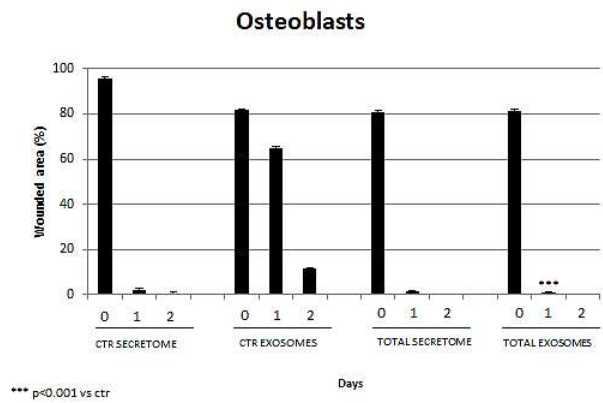
Fig. 7 – Wound healing assay on: (A) endothelial cells (B) fibroblasts (C) osteoblasts. Percentage of wounded area of: (D) endothelial cells (E) fibroblasts (F) osteoblasts.

CHAPTER 4

Discussion

It has been already proved that cells cultured in 3D conditions show better properties than the same ones cultured in 2D adhesion conditions. In fact, cells cultured in 3D conditions mimic better the native conditions thus they don't alter their surface characteristics and their gene and protein expression, due to the loss of interactions with the surface of the culture plate [5].

Several techniques have been applied to obtain spheroids even if, to date, there is no standardized one [7, 37, 38]. In this paper, spheroids have been directly obtained from liposuction fat or adipose tissue digestion, seeding ADSCs in ultra-low adhesion conditions without an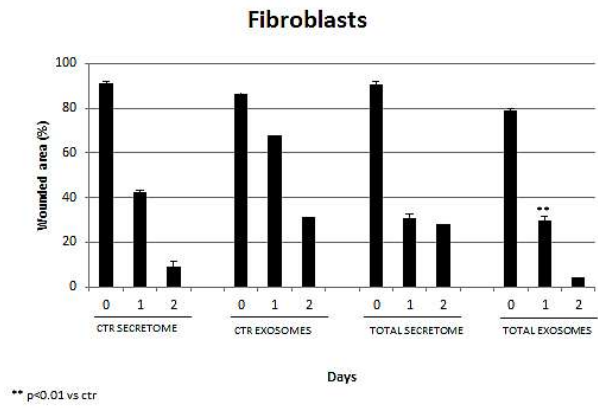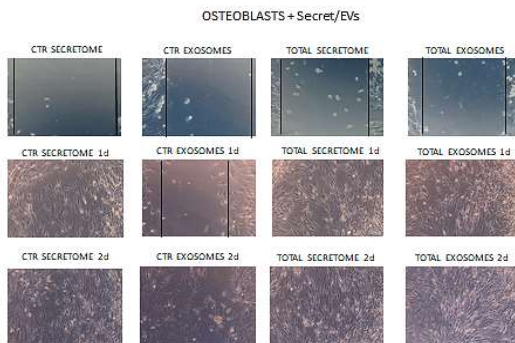y additional step, forming the so called 'SASCs'. They have been already characterized, showing the ability of maintaining stemness until 28 days with a higher expression of stemness-associated mRNAs as well as better regenerative abilities if compared to 2D cultured cells [39, 40]. Cells need to exchange information between each other and, to do so, they communicate not only through a direct cell-cell interaction but also through the endocrine, autocrine and paracrine signalling [42]. Paracrine signalling can occur through a set of soluble factors and/or extracellular vesicles (EVs) secreted by the cells and released in the culture medium, called 'conditioned medium'. The pool of secreted factors together with EVs is called 'secretome'. It has been proved that the secretome has a higher safety profile if compared to cell engrafting due to its reduced possibility of neoplastic transformation [51] and a better ease of storage with the use of natural and non-toxic agents such as trehalose, a natural disaccharide found in many foods [52]. Moreover, in the last few years, the focus has shifted on extracellular vesicles (EVs), such as exosomes, that showed great utility for clinical application as diagnostic biomarkers and therapeutic *cargo* carriers [16]. Exosomes exhibit a reduced immunogenicity due to their biocompatibility and the bi-layered lipid structure, which also protects their *cargo* from

degradation. In addition, their small size and membrane composition allows them to cross major biological membranes including the blood brain barrier [44].

A study recently performed by our group investigated the composition of the secretome from SASCs by screening it for a panel of soluble factors [12].We found that SASCs secreted a significant concentration of growth factors related to angiogenesis or stemness maintenance such as: PIGF-1, HGF and FGF-2 but also several interleukines related to the immune system modulation such as IL-5, IL-1Ra, IL-8, IL-2, IL-7, IL-23, IL-15, IL-13, IL-10 and the chemokine CCL-4. In addition, typical endothelial factors such as VEGFR2, CD31, CD62E and ICAM-1 were over-expressed. Scientific literature demonstrated that PIGF-1 (placental-derived growth factor) played a role in inducing angiogenesis *in vivo* and proliferation and migration of endothelial cells *in vitro* [62]. Other studies demonstrated that HGF (hepatocyte growth factor) played an important role in maintaining the stemness of hBM-MSCs [63] as well as in inducing angiogenesis [64]. Similarly, FGF-2 (fibroblast growth factor 2) showed a role in stemness maintenance of BM-MSCs [65] and in maintaining cells far from senescence [66]. Thus, our previous data already demonstrated that SASCs are able to communicate with each other through paracrine signaling and probably promote the stemness maintenance even through the secretion of typical growth factors involved in this process. In addition, amongst the most expressed interleukines (ILs), they can be conventionally grouped as pro- and anti-inflammatory or adaptive immunity but all of them are involved in the immune system modulation. Additionally, a review demonstrated that interleukines are able to exert a pro- or anti-inflammatory function according to their amount as well as the nature of the target cell and the activating signal or its timing [67]. Thus, the secretion of all these immunomodulatory molecules makes possible to ascribe to SASCs' secreted factors an important role in balancing the immune system activation and its shutting down, also hypothesizing that a different concentration of cells or cultivation time could lead to a different concentration of released interleukins that could change their role on the immune response. The expression of typical endothelial analytes as soluble factors secreted by SASCs could suggest an enrichment of extracellular vesicles (EVs) in the conditioned medium and their expression of typical endothelial markers. This could be due to the high angiogenic potential of SASCs [68] that might lead cells to generate EVs that carry typical angiogenic molecules. DLS, SEM and Western Blotting analyses demonstrated the presence of an exosomal population with dimensions into the range of 30-150 nm, a round shape and the enrichment in CD63 as membrane marker. A pool of mRNAs was then analyzed as exosomal internal *cargo*,

showing a high expression of NANOG, followed by SOX2 and POU5F1. All of them are involved in stemness maintenance. NANOG is a gene located on chromosome 12 and codify for a transcription factor that plays a key role in stemness maintenance of embryonic pluripotent cells as well as adult MSCs [69, 70]. Moreover, it regulates the expression of several factors involved in the maintenance of the immunomodulatory functions of MSCs [71]. Similarly, SOX2 codify for a transcription factor with a key role in MSC stemness maintenance and proliferation [72]. In addition, it is responsible of cell growth and differentiation towards adipogenic, osteogenic and chondrogenic lineages in hMSCs [73]. POU5F1 is usually expressed by embryonic stem cells and codify for a key transcription factor involved in the maintenance of self-renewal and undifferentiated state [74]. These results are in agreement with the stemness condition of SASCs that, probably, regulate their self-renewal and maintenance of the undifferentiated state also through paracrine signaling. In the perspective of using their exosomes for regenerative purposes, it might be important to carry stemness messages that could be directly injected in the damaged site and diffuse into the neighboring tissues in the way to promote the proliferation of the stem cells that reside in it. Moreover, it could be advantageous the simultaneous use of both NANOG and SOX2 mRNAs to modulate also the immune system. The analysis of a pool of 11 miRNAs as exosomal internal *cargo* showed a high miR-126 and miR-146a expression. Then, a lower expression was found for miR-451 followed by miR-100, miR-143, miR-221, miR-140 and miR-30c. Several studies showed that miR-126 played a positive role in endothelial cells for angiogenesis regulation [75] by promoting endothelial differentiation of BMSCs by increasing CD31, eNOS and VE-cadherin levels or directly inhibiting PIK3R2 (phosphoinositol-3 kinase regulatory subunit 2) and SPRED1 (Sprouty-related protein), two negative regulators of VEGF signaling pathway [76]. Another study proved the synergistic role of miR-126 and miR-146a, vehiculated by exosomes, in inducing cardiac regeneration. miR-126 was involved in cellular migration and angiogenesis whilst miR-146a in the anti-inflammatory activity. In the study, exosomes from ADSCs loaded with miR-126 and miR-146a were encapsulated in injectable Alg hydrogel and injected in myocardial infarction animal models. The authors found that miRNAs combination led to the improvement of HUVECs migration and proliferation as well as angiogenesis, promoting an over-expression of Connexin 43 (CX43) and VEGFR2 together with PI3K-AKT pathway activation and a decrease of inflammation mediated by miR-146a via inhibiting TRAF-6 and IRAK-1 [77]. In addition, miR-146a was positively involved in osteogenic differentiation. In fact, by analyzing the effects of miR-146a-mimic group in

BMSCs, an increased deposition of calcium and an enhanced osteogenic differentiation ability were found, also proved by mRNA expression of ALP and Ocn [78]. Similarly, the overexpression of miR-146a in BMSCs transfected with miR-146, enhanced cell proliferation, migration, and osteogenic differentiation in canine right mandibular distraction osteogenesis (DO) models [79]. Moreover, several studies proved that miR-146a also was a negative regulator of inflammation [80-82]. These results suggest that, probably, the balancing amongst miR-146a and miR-126 inside exosomes could give an equal contribution to proliferation, migration and differentiation of endothelial cells and osteoblasts and they also could modulate the immune system responses if the exosomes would be used in *in vivo* applications. Amongst the less expressed miRNAs, miR-451 was studied in the tumor field as a suppressor of osteosarcoma and hepatocellular carcinoma growth and angiogenesis [83, 84]. miR-100 was negatively related to angiogenesis in endothelial and vascular smooth muscle cells, due to its negative regulation of VEGF [85] and mTOR signaling, responsible of sprouting phenomena, tube formation and proliferation of endothelial cells [86]. In SASCs, the expression of miR-100 increased during the late osteogenic differentiation while miR-221 was down-regulated [40]. miR-143 was positively related to osteoblasts differentiation and pro-angiogenic activity [87], while miR-140 was only studied in chondrocytes where it was expressed during embryonic bone development [88]. It played a key role in the stability and maintenance of the cartilage matrix and in inhibiting chondrocytes senescence [89]. miR-30c targeted IL-6, a typically pro-inflammatory cytokine [90]. Since it has not yet been done, all these findings open new perspectives for the more in-depth study of the effects of each of these miRNAs on angiogenesis and osteogenesis in the regenerative field. Anyway, we could speculate that the high concentration of miRNA 126 with pro-angiogenic functions within SASCs-derived exosomes could probably induce some cells to show their angiogenic differentiation potential, already widely demonstrated [68]. This could explain why SASCs could generate exosomes with typical endothelial membrane markers. Finally, the wound healing assay on endothelial cells, fibroblasts and osteoblasts demonstrated that in all the three cell lineages the use of total exosomes led to a significant reduction of the percentage of wounded area as early as one day after treatment to reach an almost complete wound closure after two days. These preliminary *in vitro* results are promising for the use of exosomes from SASCs for tissue regeneration applications, together with vascularization. Moreover, they also showed a positive regenerative effect on fibroblasts. This could allow the formation of new connective tissue and new extracellular matrix in *in vivo* treatments, enabling the

maintenance of the homeostasis of regenerated cells in a damaged tissue. Altogether, these results suggest that spheroids of adipose derived stem cells secrete factors involved in stemness maintenance, immunomodulation and pro-differentiation signals towards endothelial or osteoblastic lineages making them promising for future *in vivo* studies for regenerative purposes.

References

1. Langhans, S. A. (2018) Three-Dimensional, *Front Pharmacol.* **9**, 6.

2. Chen, H., Seaman, L., Liu, S., Ried, T. & Rajapakse, I. (2017) Chromosome conformation and gene expression patterns differ profoundly in human fibroblasts grown in spheroids versus monolayers, *Nucleus.* **8**, 383-391.

3. Nipha, C., Phongsakorn, K. & Parinya, N. (2019) Three-dimensional cell culture systems as an in vitro platform for cancer and stem cell modeling in pp. 1065-1083, World J Stem Cells,

4. Duval, K., Grover , H., Han , L.-H., Mou , Y., Pegoraro , A. F., Fredberg , J. & Zi, C. (2017) Modeling Physiological Events in 2D vs. 3D Cell Culture in pp. 266-277, *Physiology*,

5. Birgersdotter, A., Sandberg, R. & Ernberg, I. (2005) Gene expression perturbation in vitro--a growing case for three-dimensional (3D) culture systems, *Semin Cancer Biol.* **15**, 405-12.

6. Mueller-Klieser, W. (1997) Three-dimensional cell cultures: from molecular mechanisms to clinical applications, *Am J Physiol.* **273**, C1109-23.

7. Di Stefano, A. B., Urrata, V., Trapani, M., Moschella, F., Cordova, A. & Toia, F. (2022) Systematic review on spheroids from adipose-derived stem cells: Spontaneous or artefact state?, *J Cell Physiol*.

8. Di Stefano, A. B., Grisafi, F., Perez-Alea, M., Castiglia, M., Di Simone, M., Meraviglia, S., Cordova, A., Moschella, F. & Toia, F. (2021) Cell quality evaluation with gene expression analysis of spheroids (3D) and adherent (2D) adipose stem cells, *Gene.* **768**, 145269.

9. Xiaoting, L., Yue, D., Yuelin, Z., Hung-Fat, T. & Qizhlou, L. (2014) Paracrine Mechanisms of Mesenchymal Stem Cell-Based Therapy: Current Status and Perspectives in pp. 1045-1059, *Cell Transplantation*,

10. Huang, W., Lv, B., Zeng, H., Shi, D., Liu, Y., Chen, F., Li, F., Liu, X., Zhu, R., Yu, L. & Jiang, X. (2015) Paracrine Factors Secreted by MSCs Promote Astrocyte Survival Associated With GFAP Downregulation After Ischemic Stroke via p38 MAPK and JNK, *J Cell Physiol.* **230**, 2461-75.

11. Mabotuwana, N. S., Rech, L., Lim, J., Hardy, S. A., Murtha, L. A., Rainer, P. P. & Boyle, A. J. (2022) Paracrine Factors Released by Stem Cells of Mesenchymal Origin and their Effects in Cardiovascular Disease: A Systematic Review of Pre-clinical Studies. in pp. 2606-2628, *Stem Cell Rev and Rep*,

12. Toia, F., Lo Presti, E., Di Stefano, A. B., Di Simone, M., Trapani, M., Corsale, A. M., Picone, C., Moschella, F., Dieli, F., Cordova, A. & Meraviglia, S. (2023) An analysis of the immunomodulatory properties of human spheroids from adipose-derived stem cells, *Life Sci.* **321**, 121610.

13. Zakrzewski, W., Dobrzyński, M., Szymonowicz, M. & Rybak, Z. (2019) Stem cells: past, present, and future, *Stem Cell Res Ther.* **10**, 68.

14. Condic, M. L. (2014) Totipotency: what it is and what it is not, *Stem Cells Dev.* **23**, 796-812.

15. Morrison, S. J. & Kimble, J. (2006) Asymmetric and symmetric stem-cell divisions in development and cancer, *Nature.* **441**, 1068-74.

16. Friedenstein, A. J., Chailakhjan, R. K. & Lalykina, K. S. (1970) The development of fibroblast colonies in monolayer cultures of guinea-pig bone marrow and spleen cells, *Cell Tissue Kinet.* **3**, 393-403.

17. Pittenger, M. F., Mackay, A. M., Beck, S. C., Jaiswal, R. K., Douglas, R., Mosca, J. D., Moorman, M. A., Simonetti, D. W., Craig, S. & Marshak, D. R. (1999) Multilineage potential of adult human mesenchymal stem cells, *Science.* **284**, 143-7.

18. Khan, A. A., Huat, T. J., Al Mutery, A., El-Serafi, A. T., Kacem, H. H., Abdallah, S. H., Reza, M. F., Abdullah, J. M. & Jaafar, H. (2020) Significant transcriptomic changes are associated with differentiation of bone marrow-derived mesenchymal stem cells into neural progenitor-like cells in the presence of bFGF and EGF, *Cell Biosci.* **10**, 126.

19. Bae, K. S., Park, J. B., Kim, H. S., Kim, D. S., Park, D. J. & Kang, S. J. (2011) Neuron-like differentiation of bone marrow-derived mesenchymal stem cells, *Yonsei Med J.* **52**, 401-12.

20. Wang, Y., Fang, J., Liu, B., Shao, C. & Shi, Y. (2022) Reciprocal regulation of mesenchymal stem cells and immune responses, *Cell Stem Cell.* **29**, 1515-1530.

21. Zhou, J. & Shi, Y. (2023) Mesenchymal stem/stromal cells (MSCs): origin, immune regulation, and clinical applications, *Cell Mol Immunol.* **20**, 555-557.

22. Huang, W. H., Chang, M. C., Tsai, K. S., Hung, M. C., Chen, H. L. & Hung, S. C. (2013) Mesenchymal stem cells promote growth and angiogenesis of tumors in mice, *Oncogene.* **32**, 4343-54.

23. Weiss, A. R. R. & Dahlke, M. H. (2019) Immunomodulation by Mesenchymal Stem Cells (MSCs): Mechanisms of Action of Living, Apoptotic, and Dead MSCs, *Front Immunol.* **10**, 1191.

24. Huang, P., Gebhart, N., Richelson, E., Brott, T. G., Meschia, J. F. & Zubair, A. C. (2014) Mechanism of mesenchymal stem cell-induced neuron recovery and anti-inflammation, *Cytotherapy.* **16**, 1336-44.

25. Kossl, J., Bohacova, P., Hermankova, B., Javorkova, E., Zajicova, A. & Holan, V. (2021) Antiapoptotic Properties of Mesenchymal Stem Cells in a Mouse Model of Corneal Inflammation, *Stem Cells Dev.* **30**, 418-427.

26. Papazian, I., Kyrargyri, V., Evangelidou, M., Voulgari-Kokota, A. & Probert, L. (2018) Mesenchymal Stem Cell Protection of Neurons against Glutamate Excitotoxicity Involves Reduction of NMDA-Triggered Calcium Responses and Surface GluR1, and Is Partly Mediated by TNF, *Int J Mol Sci.* **19**.

27. Chen, L., Tredget, E. E., Wu, P. Y. & Wu, Y. (2008) Paracrine factors of mesenchymal stem cells recruit macrophages and endothelial lineage cells and enhance wound healing, *PLoS One.* **3**, e1886.

28. Kwon, H. M., Hur, S. M., Park, K. Y., Kim, C. K., Kim, Y. M., Kim, H. S., Shin, H. C., Won, M. H., Ha, K. S., Kwon, Y. G. & Lee, D. H. (2014) Multiple paracrine factors secreted by mesenchymal stem cells contribute to angiogenesis, *Vascul Pharmacol.* **63**, 19-28.

29. Kuchroo, P., Dave, V., Vijayan, A., Viswanathan, C. & Ghosh, D. (2015) Paracrine factors secreted by umbilical cord-derived mesenchymal stem cells induce angiogenesis in vitro by a VEGF-independent pathway, *Stem Cells Dev.* **24**, 437-50.

30. Pankajakshan, D. & Agrawal, D. K. (2014) Mesenchymal Stem Cell Paracrine Factors in Vascular Repair and Regeneration, *J Biomed Technol Res.* **1**.

31. Zuk, , P. A., Zhu, , M., Ashjian, , P., Ugarte, D., , D. A., Huang, , J. I., Mizuno, , H., Alfonso, , Z. C., Fraser, , J. K., Benhaim, , P., Hedrick & H., M. (2002) Human Adipose Tissue Is a Source of Multipotent Stem Cells in, Molecular Biology of the Cell,

32. J. Richard , A., White , U., Elks , C. M. & Stephens , J. M. Adipose Tissue: Physiology to Metabolic Dysfunction in, Endotext [Internet],

33. Krawczenko, A. & Klimczak, A. (2022) Adipose Tissue-Derived Mesenchymal Stem/Stromal Cells and Their Contribution to Angiogenic Processes in Tissue Regeneration, *Int J Mol Sci.* **23**.

34. Koledova, Z. (2017) 3D Cell Culture: An Introduction in, Springer Nature,

35. Jauković, A., Abadjieva, D., Trivanović, D., Stoyanova, E., Kostadinova, M., Pashova, S., Kestendjieva, S., Kukolj, T., Jeseta, M., Kistanova, E. & Mourdjeva, M. (2020) Specificity of 3D MSC Spheroids Microenvironment: Impact on MSC Behavior and Properties, *Stem Cell Rev Rep.* **16**, 853-875.

36. Kapałczyńska, M., Kolenda, T., Przybyła, W., Zajączkowska, M., Teresiak, A., Filas, V., Ibbs, M., Bliźniak, R., Łuczewski, Ł. & Lamperska, K. (2018) 2D and 3D cell cultures – a comparison of different types of cancer cell cultures in pp. 910-919, Arch Med Sci

37. Redondo-Castro, E., Cunningham, C. J., Miller, J., Brown, H., Allan, S. M. & Pinteaux, E. (2018) Changes in the secretome of tridimensional spheroid-cultured human mesenchymal stem cells in vitro by interleukin-1 priming in, Stem Cell Research & Therapy,

38. Bartosh, T. J., Ylöstalo, J. H., Mohammadipoor, A., Bazhanov, N., Coble, K., Claypool, K., Lee, R. H., Choi, H. & Prockop, D. J. (2010) Aggregation of human mesenchymal stromal cells (MSCs) into 3D spheroids enhances their antiinflammatory properties, *Proc Natl Acad Sci U S A.* **107**, 13724-9.

39. Di Stefano, A., Leto Barone, A., Giammona, A., Apuzzo, T., Moschella, P., Di Franco, S., Giunta, G., Carmisciano, M., Eleuteri, C., Todaro, M., Dieli, F., Cordova, A., Stassi, G. & Moschella, F. (2015) Identification and Expansion of Adipose Stem Cells with Enhanced Bone Regeneration Properties in, J Regen Med,

40. Di Stefano, A. B., Grisafi, F., Castiglia, M., Perez, A., Montesano, L., Gulino, A., Toia, F., Fanale, D., Russo, A., Moschella, F., Leto Barone, A. A. & Cordova, A. (2018) Spheroids from adipose-derived stem cells exhibit an miRNA profile of highly undifferentiated cells, *J Cell Physiol.* **233**, 8778-8789.

41. Di Stefano, A. B., Montesano, L., Belmonte, B., Gulino, A., Gagliardo, C., Florena, A. M., Bilello, G., Moschella, F., Cordova, A., Leto Barone, A. A. & Toia, F. (2021) Human Spheroids from Adipose-Derived Stem Cells Induce Calvarial Bone Production in a Xenogeneic Rabbit Model, *Ann Plast Surg.* **86**, 714-720.

42. Lee, G. H., Kim, S. H., Kang, A., Takayama, S., Lee, S. H. & Park, J. Y. (2015) Deformable L-shaped microwell array for trapping pairs of heterogeneous cells in, Journal of Micromechanics and Microengineering,

43. Driscoll, J. & Patel, T. (2019) The mesenchymal stem cell secretome as an acellular regenerative therapy for liver disease, *J Gastroenterol.* **54**, 763-773.

44. Gurung, S., Perocheau, D., Touramanidou, L. & Baruteau, J. (2021) The exosome journey: from biogenesis to uptake and intracellular signalling, *Cell Commun Signal.* **19**, 47.

45. Tricarico, C., Clancy, J. & D'Souza-Schorey, C. (2017) Biology and biogenesis of shed microvesicles, *Small GTPases.* **8**, 220-232.

46. Zhou, X., Xie, F., Wang, L., Zhang, L., Zhang, S., Fang, M. & Zhou, F. (2020) The function and clinical application of extracellular vesicles in innate immune regulation, *Cell Mol Immunol.* **17**, 323-334.

47. Borges, F. T., Reis, L. A. & Schor, N. (2013) Extracellular vesicles: structure, function, and potential clinical uses in renal diseases in, Brazilian Journal of Medical and Biological Research,

48. Santavanond, J. P., Rutter, S. F., Atkin-Smith, G. K. & Poon, I. K. H. (2021) Apoptotic Bodies: Mechanism of Formation, Isolation and Functional Relevance, *Subcell Biochem.* **97**, 61-88.

49. Battistelli, M. & Falcieri, E. (2020) Apoptotic Bodies: Particular Extracellular Vesicles Involved in Intercellular Communication, *Biology (Basel).* **9**.

50. Haddad, Y. B., Robert, S., Salers, P., Zekraoui, L., Farnarier, C., Dinarello, C. A., George, F. D. & G., K. (2011) Sterile inflammation of endothelial cell-derived apoptotic bodies is mediated by interleukin-1α in, PNAS,

51. Théry, C.Witwer, K. W.Aikawa, E.Alcaraz, M. J.Anderson, J. D.Andriantsitohaina, R.Antoniou, A.Arab, T.Archer, F.Atkin-Smith, G. K.Ayre, D. C.Bach, J. M.Bachurski, D.Baharvand, H.Balaj, L.Baldacchino, S.Bauer, N. N.Baxter, A. A.Bebawy, M.Beckham, C.Bedina Zavec, A.Benmoussa, A.Berardi, A. C.Bergese, P.Bielska, E.Blenkiron, C.Bobis-Wozowicz, S.Boilard, E.Boireau, W.Bongiovanni, A.Borràs, F. E.Bosch, S.Boulanger, C. M.Breakefield, X.Breglio, A. M.Brennan, M.Brigstock, D. R.Brisson, A.Broekman, M. L.Bromberg, J. F.Bryl-Górecka, P.Buch, S.Buck, A. H.Burger, D.Busatto, S.Buschmann, D.Bussolati, B.Buzás, E. I.Byrd, J. B.Camussi, G.Carter, D. R.Caruso, S.Chamley, L. W.Chang, Y. T.Chen, C.Chen, S.Cheng, L.Chin, A. R.Clayton, A.Clerici, S. P.Cocks, A.Cocucci, E.Coffey, R. J.Cordeiro-da-Silva, A.Couch, Y.Coumans, F. A.Coyle, B.Crescitelli, R.Criado, M. F.D'Souza-Schorey, C.Das, S.Datta Chaudhuri, A.de Candia, P.De Santana, E. F.De Wever, O.Del Portillo, H. A.Demaret, T.Deville, S.Devitt, A.Dhondt, B.Di Vizio, D.Dieterich, L. C.Dolo, V.Dominguez Rubio, A. P.Dominici, M.Dourado, M. R.Driedonks, T. A.Duarte, F. V.Duncan, H. M.Eichenberger, R. M.Ekström, K.El Andaloussi, S.Elie-Caille, C.Erdbrügger, U.Falcón-Pérez, J. M.Fatima, F.Fish, J. E.Flores-Bellver, M.Försönits, A.Frelet-Barrand, A., et al. (2018) Minimal information for studies of extracellular vesicles 2018 (MISEV2018): a position statement of the International Society for Extracellular Vesicles and update of the MISEV2014 guidelines, *J Extracell Vesicles.* **7**, 1535750.

52. Jeyaram, A. & Jay, S. M. (2017) Preservation and Storage Stability of Extracellular Vesicles for Therapeutic Applications, *AAPS J.* **20**, 1.

53. Nikhil, A. & Kumar, A. (2022) Evaluating potential of tissue-engineered cryogels and chondrocyte derived exosomes in articular cartilage repair, *Biotechnol Bioeng.* **119**, 605-625.

54. Huang, L., Rong, Y., Tang, X., Yi, K., Qi, P., Hou, J., Liu, W., He, Y., Gao, X., Yuan, C. & Wang, F. (2022) Engineered exosomes as an in situ DC-primed vaccine to boost antitumor immunity in breast cancer, *Mol Cancer.* **21**, 45.

55. Liang, G., Zhu, Y., Ali, D. J., Tian, T., Xu, H., Si, K., Sun, B., Chen, B. & Xiao, Z. (2020) Engineered exosomes for targeted co-delivery of miR-21 inhibitor and chemotherapeutics to reverse drug resistance in colon cancer, *J Nanobiotechnology.* **18**, 10.

56. Hui, B., Lu, C., Wang, J., Xu, Y., Yang, Y., Ji, H., Li, X., Xu, L., Wang, J., Tang, W., Wang, K. & Gu, Y. (2022) Engineered exosomes for co-delivery of PGM5-AS1 and oxaliplatin to reverse drug resistance in colon cancer in, Journal of Cellular Physiology,

57. Wahid, F., Shehzad, A., Khan, T. & Kim, Y. Y. (2010) MicroRNAs: synthesis, mechanism, function, and recent clinical trials, *Biochim Biophys Acta.* **1803**, 1231-43.

58. Bartel, D. P. (2004) MicroRNAs: Genomics, Biogenesis, Mechanism, and Function in, Cell,

59. Li, N., Huang, Z., Zhang, X., Song, X. & Xiao, Y. (2019) Reflecting Size Differences of Exosomes by Using the Combination of Membrane-Targeting Viscosity Probe and Fluorescence Lifetime Imaging Microscopy, *Anal Chem.* **91**, 15308-15316.

60. Huang, Y., Shen, X. J., Zou, Q., Wang, S. P., Tang, S. M. & Zhang, G. Z. (2011) Biological functions of microRNAs: a review, *J Physiol Biochem.* **67**, 129-39.

61. O'Brien, J., Hayder, H., Zayed, Y. & Peng, C. (2018) Overview of MicroRNA Biogenesis, Mechanisms of Actions, and Circulation, *Front Endocrinol (Lausanne).* **9**, 402.

62. Ziche, M., Maglione, D., Ribatti, D., Morbidelli, L., Lago, C. T., Battisti, M., Paoletti, I., Barra, A., Tucci, M., Parise, G., Vincenti, V., Granger, H. J., Viglietto, G. & Persico, M. G. (1997) Placenta growth factor-1 is chemotactic, mitogenic, and angiogenic, *Lab Invest.* **76**, 517-31.

63. Cao, Z., Xie, Y., Yu, L., Li, Y. & Wang, Y. (2020) Hepatocyte growth factor (HGF) and stem cell factor (SCF) maintained the stemness of human bone marrow mesenchymal stem cells (hBMSCs) during long-term expansion by preserving mitochondrial function via the PI3K/AKT, ERK1/2, and STAT3 signaling pathways, *Stem Cell Res Ther.* **11**, 329.

64. Hayashi, S., Morishita, R., Nakamura, S., Yamamoto, K., Moriguchi, A., Nagano, T., Taiji, M., Noguchi, H., Matsumoto, K., Nakamura, T., Higaki, J. & Ogihara, T. (1999) Potential role of hepatocyte growth factor, a novel angiogenic growth factor, in peripheral arterial disease: downregulation of HGF in response to hypoxia in vascular cells, *Circulation.* **100**, II301-8.

65. Chen, L., Carlton, M., Chen, X., Kaur, N., Ryan, H., Parker, T. J., Lin, Z., Xiao, Y. & Zhou, Y. (2021) Effect of fibronectin, FGF-2, and BMP4 in the stemness maintenance of BMSCs and the metabolic and proteomic cues involved, *Stem Cell Res Ther.* **12**, 165.

66. Li, J., Song, S., Li, X., Zhu, J., Li, W., Du, B., Guo, Y., Xi, X. & Han, R. (2020) Down-Regulation of Fibroblast Growth Factor 2 (FGF2) Contributes to the Premature Senescence of Mouse Embryonic Fibroblast, *Med Sci Monit.* **26**, e920520.

67. Cavaillon, J. M. (2001) Pro- versus anti-inflammatory cytokines: myth or reality, *Cell Mol Biol (Noisy-le-grand).* **47**, 695-702.

68. Barbara Di Stefano, A., Toia, F., Urrata, V., Trapani, M., Montesano, L., Cammarata, E., Moschella, F. & Cordova, A. (2023) Spheroids of adipose derived stem cells show their potential in differentiating towards the angiogenic lineage, *Gene.* **878**, 147578.

69. Pitrone, M., Pizzolanti, G., Tomasello, L., Coppola, A., Morini, L., Pantuso, G., Ficarella, R., Guarnotta, V., Perrini, S., Giorgino, F. & Giordano, C. (2017) NANOG Plays a Hierarchical Role in the Transcription Network Regulating the Pluripotency and Plasticity of Adipose Tissue-Derived Stem Cells, *Int J Mol Sci.* **18**.

70. Gawlik-Rzemieniewska, N. & Bednarek, I. (2016) The role of NANOG transcriptional factor in the development of malignant phenotype of cancer cells, *Cancer Biol Ther.* **17**, 1-10.

71. Sun, Z., Han, Q., Zhu, Y., Li, Z., Chen, B., Liao, L., Bian, C., Li, J., Shao, C. & Zhao, R. C. (2011) NANOG has a role in mesenchymal stem cells' immunomodulatory effect, *Stem Cells Dev.* **20**, 1521-8.

72. Yoon, D. S., Kim, Y. H., Jung, H. S., Paik, S. & Lee, J. W. (2011) Importance of Sox2 in maintenance of cell proliferation and multipotency of mesenchymal stem cells in low-density culture, *Cell Prolif.* **44**, 428-40.

73. Park, S. B., Seo, K. W., So, A. Y., Seo, M. S., Yu, K. R., Kang, S. K. & Kang, K. S. (2012) SOX2 has a crucial role in the lineage determination and proliferation of mesenchymal stem cells through Dickkopf-1 and c-MYC, *Cell Death Differ.* **19**, 534-45.

74. Niknejad, P., Azizi, H. & Sojoudi, K. (2021) Protein and Gene Expression Analysis in Neonate and Adult Mouse Testicular Germ Cells by Immunohistochemistry and Immunocytochemistry, *Cell Reprogram.* **23**, 349-358.

75. Kong, R., Gao, J., Ji, L. & Zhao, D. (2020) MicroRNA-126 promotes proliferation, migration, invasion and endothelial differentiation while inhibits apoptosis and osteogenic differentiation of bone marrow-derived mesenchymal stem cells, *Cell Cycle.* **19**, 2119-2138.

76. Fish, J. E., Santoro, M. M., Morton, S. U., Yu, S., Yeh, R. F., Wythe, J. D., Ivey, K. N., Bruneau, B. G., Stainier, D. Y. & Srivastava, D. (2008) miR-126 regulates angiogenic signaling and vascular integrity, *Dev Cell.* **15**, 272-84.

77. Shafei, S., Khanmohammadi, M., Ghanbari, H., Nooshabadi, V. T., Tafti, S. H. A., Rabbani, S., Kasaiyan, M., Basiri, M. & Tavoosidana, G. (2022) Effectiveness of exosome mediated miR-126 and miR-146a delivery on cardiac tissue regeneration, *Cell Tissue Res.* **390**, 71-92.

78. Kong, Y. & Chen, Z. T. (2019) MiR-146a regulates osteogenic differentiation and proliferation of bone marrow stromal cells in traumatic femoral head necrosis, *Eur Rev Med Pharmacol Sci.* **23**, 441-448.

79. Shen, H., Jiang, W., Yu, Y., Feng, Y., Zhang, T., Liu, Y., Guo, L., Zhou, N. & Huang, X. (2022) microRNA-146a mediates distraction osteogenesis via bone mesenchymal stem cell inflammatory response, *Acta Histochem.* **124**, 151913.

80. Han, R., Gao, J., Wang, L., Hao, P., Chen, X., Wang, Y., Jiang, Z., Jiang, L., Wang, T., Zhu, L. & Li, X. (2023) MicroRNA-146a negatively regulates inflammation via the IRAK1/TRAF6/NF-κB signaling pathway in dry eye, *Scientific Reports.* **13**, 11192.

81. Dull, K., Fazekas, F., Deák, D., Kovács, D., Póliska, S., Szegedi, A., Zouboulis, C. C. & Törőcsik, D. (2021) miR-146a modulates TLR1/2 and 4 induced inflammation and links it with proliferation and lipid production via the indirect regulation of GNG7 in human SZ95 sebocytes, *Sci Rep.* **11**, 21510.

82. Taganov, K. D., Boldin, M. P., Chang, K. J. & Baltimore, D. (2006) NF-kappaB-dependent induction of microRNA miR-146, an inhibitor targeted to signaling proteins of innate immune responses, *Proc Natl Acad Sci U S A.* **103**, 12481-6.

83. Liu, S. Y., Deng, S. Y., He, Y. B. & Ni, G. X. (2017) miR-451 inhibits cell growth, migration and angiogenesis in human osteosarcoma via down-regulating IL 6R, *Biochem Biophys Res Commun.* **482**, 987-993.

84. Liu, X., Zhang, A., Xiang, J., Lv, Y. & Zhang, X. (2016) miR-451 acts as a suppressor of angiogenesis in hepatocellular carcinoma by targeting the IL-6R-STAT3 pathway, *Oncol Rep.* **36**, 1385-92.

85. Pakravan, K., Babashah, S., Sadeghizadeh, M., Mowla, S. J., Mossahebi-Mohammadi, M., Ataei, F., Dana, N. & Javan, M. (2017) MicroRNA-100 shuttled by mesenchymal stem cell-derived exosomes suppresses in vitro angiogenesis through modulating the mTOR/HIF-1α/VEGF signaling axis in breast cancer cells, *Cell Oncol (Dordr).* **40**, 457-470.

86. Grundmann, S., Hans, F. P., Kinniry, S., Heinke, J., Helbing, T., Bluhm, F., Sluijter, J. P., Hoefer, I., Pasterkamp, G., Bode, C. & Moser, M. (2011) MicroRNA-100 regulates neovascularization by suppression of mammalian target of rapamycin in endothelial and vascular smooth muscle cells, *Circulation.* **123**, 999-1009.

87. Wang, R., Zhang, H., Ding, W., Fan, Z., Ji, B., Ding, C., Ji, F. & Tang, H. (2020) miR-143 promotes angiogenesis and osteoblast differentiation by targeting HDAC7, *Cell Death Dis.* **11**, 179.

88. Green, D., Dalmay, T. & Fraser, W. D. (2015) Role of miR-140 in embryonic bone development and cancer, *Clin Sci (Lond).* **129**, 863-73.

89. Duan, L., Liang, Y., Xu, X., Xiao, Y. & Wang, D. (2020) Recent progress on the role of miR-140 in cartilage matrix remodelling and its implications for osteoarthritis treatment, *Arthritis Res Ther.* **22**, 194.

90. Mahjoor, M., Afkhami, H., Najafi, M., Nasr, A. & Khorrami, S. (2023) The role of microRNA-30c in targeting interleukin 6, as an inflammatory cytokine, in the mesenchymal stem cell: a therapeutic approach in colorectal cancer, *J Cancer Res Clin Oncol.* **149**, 3149-3160.

Scientific Papers

REVIEW ARTICLE

Systematic review on spheroids from adipose-derived stem cells: Spontaneous or artefact state?

Anna Barbara Di Stefano[1] 🔘 | Valentina Urrata[1] | Marco Trapani[1] | Francesco Moschella[1] | Adriana Cordova[1,2,3] | Francesca Toia[1,2,3]

[1]BIOPLAST-Laboratory of BIOlogy and Regenerative Medicine-PLASTic Surgery, Plastic and Reconstructive Surgery Unit, Department of Surgical, Oncological and Oral Sciences, University of Palermo, Palermo, Italy

[2]Department of Surgical, Oncological and Oral Sciences, Unit of Plastic and Reconstructive Surgery, University of Palermo, Palermo, Italy

[3]Department of D.A.I. Chirurgico, Plastic and Reconstructive Unit, Azienda Ospedaliera Universitaria Policlinico "Paolo Giaccone", Palermo, Italy

Correspondence
A. B. Di Stefano, University of Palermo, Via Liborio Giuffrè 5, 90127, Palermo, Italy.
Email: annabarbara.distefano@unipa.it

Abstract

Three-dimensional (3D) cell cultures represent the spontaneous state of stem cells with specific gene and protein molecular expression that are more alike the in vivo condition. In vitro two-dimensional (2D) cell adhesion cultures are still commonly employed for various cellular studies such as movement, proliferation and differentiation phenomena; this procedure is standardized and amply used in laboratories, however their representing the original tissue has recently been subject to questioning. Cell cultures in 2D require a support/substrate (flasks, multiwells, etc.) and use of fetal bovine serum as an adjuvant that stimulates adhesion that most likely leads to cellular aging. A 3D environment stimulates cells to grow in suspended aggregates that are defined as "spheroids." In particular, adipose stem cells (ASCs) are traditionally observed in adhesion conditions, but a recent and vast literature offers many strategies that obtain 3D cell spheroids. These cells seem to possess a greater ability in maintaining their stemness and differentiate towards all mesenchymal lineages, as demonstrated in in vitro and in vivo studies compared to adhesion cultures. To date, standardized procedures that form ASC spheroids have not yet been established. This systematic review carries out an in-depth analysis of the 76 articles produced over the past 10 years and discusses the similarities and differences in materials, techniques, and purposes to standardize the methods aimed at obtaining ASC spheroids as already described for 2D cultures.

KEYWORDS
3D cultures, adipose stem cells, biomaterials, hanging drop, spheroids, spinner flask

1 | INTRODUCTION

1.1 | Adipose stem cell (ASCs) spheroids

Two-dimensional (2D) cell cultures are a very useful tool to perform in vitro studies in the field of oncology, stem cell biology and tissue engineering. Adhesion cultures are generally created by means of simple, standardized techniques requiring a support/substrate (flasks, multiwells etc.) and a specific media that employs fetal bovine serum as an adjuvant for cell adhesion and proliferation. Recently, researchers have asked if adhesion cultures manage to properly represent the original cells condition in in vivo tissues.

This questioning has lead to a progressive replacement of 2D cultures in favor of three-dimensional (3D) cell cultures with protein expression patterns and intercellular junctions that are more alike in vivo conditions. Today, these 3D cell cultures have become a very attractive system for the scientific community (Abbott, 2003), however experts do not all agree on these in vitro procedures. ASCs represent promising cell therapies for regenerative medicine and immunomodulation (Agrawal et al., 2014; Pappalardo et al., 2019). Laboratories throughout the world that are currently studying 3D cultures adopt a personal, nonstandardised technique albeit often achieving the same final evaluations, namely that 3D spheroids feature superior characteristics compared to 2D classical ASCs (A. Di Stefano, Montesano et al., 2020; A. B. Di Stefano et al., 2018; A. B. Di Stefano, Grisafi et al. 2020; A. B. Di Stefano et al., 2015; S. Kim, Han, et al., 2018).

Does the spheroid already exist in the tissue or is it the result of a later union or rearrangement of individual cells? This question continues to stand as specialist literature currently available is not conclusive.

This systematic review aims to summarize evidence from studies carried out in the past decade on ASC spheroids. This study reviews all the techniques used for their isolation and/or formation with specific plate, scaffold systems, or nonadhesion methods and discusses the benefits and drawbacks of the different techniques.

2 | MATERIALS AND METHODS

A systematic literature search was conducted in the PubMed database for articles published from April 2011 to February 2021. The following key-words were used: "spheroids [Title/ABSTRACT] AND adipose [Title/ABSTRACT] AND stem cells [Title/ABSTRACT]," species "HUMAN." Selection of the articles was carried out based on the following inclusion and exclusion criteria:

(i) Iinclusion criteria: preclinical or clinical research papers concerning the potential regenerative role of S-ASCs culture.
(ii) Exclusion criteria: reviews and papers that did not directly refer to human ASC spheroids studies.

Two reviewers independently screened all search results, abstracts, and full texts. Further searches included relevant references from selected articles. Data concerning the type of paper, cell isolation, culture methods, and results were extrapolated from the selected articles.

Data were analyzed to summarize current evidence on the following queries:

(i) What technical methods that have been developed in the past decade to create 3D cellular ASC aggregates/spheroids?
(ii) What are the benefits in terms of regenerative capacities of 3D-ASCs compared to traditional 2D-ASC cultures?
(iii) Why does not a standardized method of 3D-ASC isolation and in vitro culture exist today?

3 | RESULTS

3.1 | Common culture methods using specific technical conditions (ultralow/low adhesion or concave multiwell)

Many authors isolate ASCs from liposuction, culture them in traditional adhesion conditions, trypsinize them and then take the cells to 3D conditions. Table 1 lists the selected studies using common culture methods including ultralow/low adhesion or concave multiwell to form ASC spheroids featuring different sizes and oxygen concentrations.

Using agarose micromolds with basic medium, Fennema et al. (2018) generated ASC spheroids adding LG-DMEM (Low-Glucose Dulbecco's Modified Eagle's Medium) and a 400 μm diameter well rubber. Guo et al. instead formed 3D spheroids whose aggregates were then removed and transferred to the nonadhesive plastic Petri dishes called agarose 3D Petri dishes. This innovative method was used to overcome poor post thaw cells and improve the viability and neural differentiation potential of 3D-ASCs (Guo et al., 2015). Likewise, Coyle et al. carried out an analysis on different spheroids sizes (115, 135, 175, and 215 um radius) demonstrating, through in vitro culture and mathematical modeling, that the glucose availability and absence of oxygen improved the spheroids viability through anaerobic glycolysis (Coyle et al., 2019).

Using ultrapure agarose with PDMS (polydimethylsiloxane), De Moor et al. generated spheroids with 7.5×10^5 cells, approximately 262 cells per pore and tested two different fusions: in suspension (in U-shaped wells) and in matrigel. The aim was to evaluate the aggregation behavior in cocultures with ASCs, Human Umbilical Vein Endothelial Cells (HUVECs), and human foreskin fibroblasts in a 10-day time span (De Moor et al., 2018). By means of a similar system, Cho et al. generated spheroids into methylcellulose-coated supports in 96-well plates featuring a diameter of 300 μm, further coated with bovine serum albumin (BSA) aiming to prevent cell attachment (Cho et al., 2017). No and collaborators instead coated the plates with 3% BSA obtaining spheroids with a different diameter (500 μm), fabricating them by employing the soft lithography technique. They also discovered that hepatocyte spheroids acquired an improved liver-specific function when cocultured with hASC spheroids (No et al., 2012). Finally, Lee et al. used concave microwells with PDMS on aluminium plates acting as a mold, placing them into 24-well plates and generating ASCs after 24 h (G. H. Lee et al., 2018).

Rumiński et al. applied a scaffold free, low-adhesion technique to generate spheroids by using plates treated with Pluronic F-127 aqueous solution, but also by employing a common 3D porous polystyrene (PS) scaffold as an additional method. They compared the osteogenic capacity of the two different 3D-ASC models with 2D cultures showing that the ASC proliferation increased in PS scaffolds similar to the control 2D condition, but the osteogenic marker expression was observed in scaffold-free ASC spheroids. Nonetheless, mineral production was higher in 3D PS and in control 2D cultures as the mineralization process required a substrate (Rumiński

TABLE 1 Characteristics of selected studies using common culture methods ultralow/low adhesion or concave multiwall

Author	In vitro culture	Substrates/scaffolds	Results
Fennema et al. (2018)	Liposuction (thighs) I–II passages of 2D	1.5×10^6 cells using agarose micro-molds with basic medium	Study of osteoblastic differentiation
Guo et al. (2015)	Liposuction (abdomen and thighs, female, mean age of 35 years old) N.A. passaged 2D (3.5×10^5 cells)	Agarose micro-molds with LG-DMEM and well rubber of 400 μm diameter, called 3D Petri dishes of agarose. Silicone microwells. 81 wells rubber micro-molds with diameter in 400 μm	Neural differentiation study
Coyle et al. (2019)	Commercially VI–VII passage of 2D (0.5, 1.0, 2.5, and 5.0×10^6 cells/ml)	Agarose hydrogel micro-molds with 35 concave of 800 μm diameter and 800 μm depth	Cell ischemic model
De Moor et al. (2018)	Commercially III–VI passages of 2D (5000 cells/cm²)	High-throughput non-adhesive 3% w/v agarose microwell system in PDMS. One mold contained 2865 pores with a diameter of 200 μm and a depth of 220 μm each. 500 μl of cell suspension containing 7.5×10^5 cells (262 cells per pore). For angiogenic study 1.0×10^6 cells (350 cells per pore).	Angiogenic study in monoculture and coculture ASC/HUVEC/HFF
Cho et al. (2017)	Commercially V passages of 2D (10^5 cells)	PDMS-based concave microwell, located into methylcellulose-coated supports in 96-well plates, with a diameter of 300 μm coated with 3% BSA. Each concave microwell contained 64 holes	Regeneration of lung tissues
No et al. (2012)	Liposuction 2D	PDMS-based concave micromolds of 500 μm diameter coated with 3% BSA overnight.	3D coculture (ASC + hHEP) effect on hepatocyte function and spheroid formation
G. H. et al. (2018)	N.A. passages of 2D (2×10^6 cells)	A microwell array, concave microwells, 30×30 through-hole array, several hundred micrometer-order steel beads, and magnetic force to fabricate 900 microwells in a 3 cm × 3 cm PDMS	Spheroid formation
Rumiński et al. (2019); Rumiński et al. (2020)	Liposuction II–III passages of 2D (1×10^6 cells/cm²)	Pluronic F-127 solution, 3D porous poly PS scaffolds	Osteogenic study
Gimeno et al. (2017)	Liposuction (abdomen)	3.5×10^6 cultured in nonadherent plastic diches	Study of immonomodulatory capacity
Winter et al. (2003)	Liposuction (total hip arthroplasty, mean age 55,3 years)	$3–5 \times 10^5$ cells seeded in culture flasks with a MSC culture medium	chondrocyte differentiation study
Hong et al. (2020)	Commercially V passage 2D 5000 cells cm⁻²	bio-functional matrix PS-MBP-FGF2: polystyrene (PS) surface with basic fibroblast growth factor (FGF2) bound to maltose binding protein (MBP).	Spheroids formation d formation

TABLE 1 (Continued)

Author	In vitro culture	Substrates/scaffolds	Results
Furuhata et al. (2016)	Commercially, III–V passages of 2D (3.2×10^4 cells/cm²)	96-well micropatterned culture plates	Study of cell aggregation effect
Skiles et al. (2013); Skiles et al. (2015)	Commercially III–VI passages of 2D	5000 (5 k), 10,000 (10 k), 20,000 (20 k), or 60,000 (60 k) cells were pipetted into 0.5 ml, siliconized, screw-cap microcentrifuge tubes and centrifuged at 500 rcf for 2 min. encapsulated within the PEG hydrogels	Spheroid size in normoxic (20%) and hypoxic (1% and 2%) condition in monoculture and HUVEC cocultures.
Oberringer et al. (2018)	Commercially V passages of 2D (10,000 cells/ml)	96-well plates with cell-repellent surface	Angiogenic study in monoculture and coculture with HDMEC
Parshyna et al. (2017)	Commercially ASC about 500 cells per spheroid	Nonadherent round bottom 96-well plates, embedded into a collagen matrix (Matrigel) and treated with omega-3 fatty acids for 24 h.	omega-3 fatty acids in angiogenic study of coculture with HUVEC

Abbreviations: ASC, Adipose derived stem cell; BSA, Bovine serum albumin; DMEM, Dulbecco's Modified Eagle's Medium; HDMEC, Human Dermal Microvascular Endothelial Cells; HFF, Human foreskin fibroblasts; HUVEC, Human Umbilical Vein Endothelial Cells; LG-DMEM, Low-Glucose Dulbecco's Modified Eagle's Medium; PDMS: Polydimethylsiloxane; PEG, Plyethylene glycol; PS, polystyrene.

et al., 2019). Consequently, the effect of a cyclic adenosine monophosphate (cAMP) pathway activity on the osteoblastic differentiation of ASC spheroids compared to 2D cultures was also subject to observation. Early osteogenesis was inhibited when cAMP was upregulated. Moreover, the protein kinase A activity may have a role in addressing ASCs to the osteogenic differentiation (Rumiński et al., 2020).

In nonadherent plastic dishes, Gimeno et al. obtained Muse-AT cell spheroids, a pluripotent stem cell subpopulation of adipose derived stem cells (ADSCs), and studied their spontaneous clustering until they reached a diameter between 50 and 150 μm after 72 h in culture (Gimeno et al., 2017). Similarly, Winter et al. (2003) generated spheroids through a spontaneous aggregation of cells plated at a density of $3-5 \times 10^5$ cells on a 48-well plate after 1–2 days.

In a biofunctional matrix of PS coated with basic fibroblast growth factor (FGF2) and maltose binding protein, Hong et al. generated functional 3D hepatocytes with hASCs as supporting cells that were cocultured with mouse induced hepatic precursor cells (miHeps) (Hong et al., 2020).

Small spheroids with average spherical shapes (100 μm diameter) were obtained when a seeding density of 100.000 cells/cm was reached in 96-well plates containing circular adhesive domains. In this study, the 3D condition of the ASCs was associated with an increase of the VEGF-A and IL-8 expressions as regards to wound healing (Furuhata et al., 2016). The capacity to form spheroids in response to different oxygen concentrations is a consolidated fact. Culture geometry, depending on spheroid size, is essential to hypoxia effects; each spheroid counted a different number of cells and was placed at different oxygen concentrations to observe the VEGF expression. An increased VEGF secretion was observed in the spheroids in 2% oxygen conditions compared to a 20% oxygen culture condition (Skiles et al., 2013), (Skiles et al., 2015). Oberringer et al. studied the cocultures of human dermal microvascular endothelial cells (HDMEC) and ASC spheroids using pretreated repellent-surface wells during tissue healing. Tissue reoxygenation appears subject to the strong paracrine role of ASCs and on the 3D cell–cell interaction with HDMECs (Oberringer et al., 2018). Due to the same angiogenic capacity of the 3D-ASCs, Parshyna et al. studied the role of several omega-3 fatty acids. In particular, docosahaenoic acid promoted the sprouting activity of ASCs supporting the formation of microvascular networks in cocultures with HUVECs into a collagen matrix (Parshyna et al., 2017).

3.2 | Common culture methods of ASC spheroids (hanging drop or spinner flask)

Table 2 summarizes the conventional techniques used to form ASC spheroids: hanging drop or spinner flask. A widespread technique is the hanging drop method that is based on the natural predisposition of cells to form 3D aggregates needless of scaffolding. A drop is formed in an inverted plate and held in place due to surface tension. Similar to this case, there are many studies that adopt this technique

TABLE 2 Characteristics of selected studies using common culture methods Hanging drop or Spinner flask for spheroids of adipose stem cells

Author	In vitro culture	Methods	Results
Kapur et al. (2012)	Liposuction (abdomen, average age 42.4 years, BMI of 30.14) V passages of 2D (2000 cells/cm^2)	Hanging drop: 10, 20, 30, and 50 k cells in 24–48 h, then they transferred to ultralow 24-well plates.	Stemness and differentiation study
F. H. Shen et al. (2013)	Liposuction III Passages of 2D (5 × 10^4 cells/cm^2)	Hanging drop: 50 k cells in 40ul of drop for 24 h, then they transferred to Ultralow 96-well plates.	Osteogenic study
Hutton et al. (2013)	Liposuction (female, average age of 46 years, average BM1 of 29.1) II passages of 2D (N.A. cell/cm^2)	Hanging drop: 400 k cells/ml spheroid in 10 μl drop fibrin gel	Vascularized bone tissue formation
Xu et al. (2016)	Liposuction 90% confluence of 2D (N.A. cell/cm^2)	Hanging drop: 25 k cells in 35 μl drop	Vascular regeneration in acute kidney damage
Xu et al. (2020)	Liposuction	Hanging drop: 25 μl were used for 5 days to observe spheroid formation. on the third day, 1000 cells were recovered	Neurogenic erectile dysfunction studies
Berg et al. (2015)	Liposuction (female, age between 28–32 years old) IV passages of 2D (1.6 × 10^5 cells/cm^2)	Hanging drop: 2000 cells in 50 μl drop	Hippocampal neurogenesis and nigral neurodegeneration
Yoon et al. (2012)	Liposuction IV passages of 2D	Siliconized Spinner flask: 1.0 × 10^6 cells/ml in 100 ml volume stirred at 40 rpm for 3 days	Cartilage formation
Williams et al. (2013)	Liposuction (abdominal) N.A. passages of 2D	Siliconized Spinner flask: 3.0 × 10^6 cells/ml in 1,5% alginate at 5 rpm for 2 days and then increased to 10 rpm for 16 days.	Spheroid fabrication
Bhang et al. (2011)	Liposuction V passages of 2D (N.A. cell/cm^2)	Siliconized spinner flasks: 6.0 × 10^5 cells/ml at 70 rpm for 3 days.	Angiogenic study
Hoefner et al. (2020)	Commercially IV–V passage 2D (25,000 cells/cm^2)	Orbital shaker at 50 rpm: 5000 cells/well in 96-well plates coated with 1.5% agarose. Multicellular 3D spheroids obtained through the liquid overlay technique.	Adipogenic study

prooviding for some modifications: spheroid formation times, different drop volumes and abilities to differentiate towards mesenchymal lineages. Kapur et al. demonstrated a homogeneous distribution of the cells inside the spheroids. After 24 h from the drop insertion placed upside down, aggregates were formed and then maintained into a 24-well ultralow attachment plate. Subsequently, the authors showed the upregulation of specific mesenchymal markers (RUNX2, AP, Collagen 1,2, aggregan, LPL, PPARG2, and FABP4) in the spheroids grown in osteoblastic, chondrocytic and adipogenic media compared to the control group (Kapur et al., 2012). Similarly, the Shen group formed multicellular aggregates from forty-microliter droplets containing 50,000 ASCs and plating them in 96-ultralow-adhesion multiwell plates for 2 weeks. The result was a high spheroid capacity of osteoblastic differentiation with deposition of bone matrix in both in vitro and in vivo studies (F. H. Shen et al., 2013). Hutton and colleagues plated the adherent ASCs in 10 μl drops on inverted Petri dishes. After one night, the formation of spheroids was observed and were subsequently seeded on a fibrin gel with osteogenic and vascular media. It was found that spheroidal aggregates presented a greater number of vascular networks than the counterpart in 2D condition (Hutton et al., 2013). Xu et al. used drops with 25,000 cells and a volume of 35 microliters, plating them upside down for 3 days. The generated spheroids featured a greater potential for vascular regeneration in acute kidney damage (Xu et al., 2016). Another study on neurogenic erectile dysfunction evaluated spheroid formation after 5 days from the generation of the drops with 25 μl in volume (Xu et al., 2020).

Berg et al. obtained spheroids in a suspended drop after 4 days of culture and compared them with monolayer cells to study their neural involvement in a Parkinson disease rat model injured by a 6-hydroxydopamine (OHDA) injection. After 8 days, the transplantation of the monolayer ASCs in the substantia nigra of rats showed a significant increase in tyrosine hydroxylase, in the brain-derived neurotrophic factor and in glial fibrillary acid protein levels, while the grafting of spheroids led to an increase in local microgliosis. Consequently, the monolayer culture cells induced a motor function improvement, while the spheroids caused local inflammation and suppression of hippocampal neurogenesis (Berg et al., 2015).

A different strategy for forming spheroids is the spinner flask whereas the fluid is put into turbulence, preventing adhesion and promoting cellular aggregation. Yoon et al. used this method to demonstrate the greater potential of 3D-ASCs cultures compared to the 2D-ASC cultures. Furthermore, they found an improved chondrogenic capacity of hASC spheroids placed in specific differentiation medium added with TGF-b3, confirmed by the greater expression of SOX-9, aggrecan and type II collagen compared to the monolayer culture (Yoon et al., 2012). Williams et al. bioprinted alginate spheroids of ASCs and transferred them into a spinner flask for 2 days. They found the absence of a necrotic core rather than homogenous dissemination of the bioprinted cells (Williams et al., 2013). Bangh et al. placed spheroids in hypoxic culture conditions with 1% oxygen for 3 days. In this condition, spheroids grew faster than monolayer culture and, focusing the attention on the treatment of the ischemic disease, the authors found increased expression levels of survival factors (CXCL12 and HIF-1a) in response to the size of the spheroids. Indeed, apoptosis seems to be involved with the hypoxia phenomenon. The expression of the antiapoptotic factor, Bcl-xL, in the spheroidal culture condition led to an increase of the adhesion molecules such as ICAM-1, VCAM-1, and PECAM-1. These processes enhanced the angiogenic efficacy of stem cells therapy (Bhang et al., 2011).

Hoefner et al. investigated the adipogenic differentiation and the development of ECM in ASC spheroids comparing them to 2D cultures. They were cultured in growth cell medium during shaking at 50 rpm. After only 2 days of induction for the adipogenic lineages, they demonstrated an improved differentiation capacity of the ASC spheroids located in their own ECM (laminin and Col IV) compared to 2D cultures (Hoefner et al., 2020).

3.3 | Novel culture methods to form spheroids of ASCs

Table 3 summarizes selected studies that used novel culture methods to form ASC spheroids.

Several studies tested different hydrogels to form ASC spheroids by employing state of the art materials in the field of tissue engineering such as hyaluronic acid (Feng et al., 2017; Hu et al., 2020) and chitosan (Chen et al., 2018; Cheng, Chang, et al., 2012; Cheng, Wang, et al., 2012; Hsu et al., 2014; Huang et al., 2011; Lin et al., 2020), demonstrating an improved stemness gene expression compared to the traditional cultures in adhesion plates. The combination of these materials, or with other materials (FGF-2 and PVA), was able to form 3D spheroids in a short period of time and showed better properties in stemness maintenance and an increased ability in stimulating angiogenic (Hsu et al., 2014; Hu et al., 2020) and chondrogenic (Huang et al., 2011; Lin et al., 2020) differentiations. Many materials were thermoresponsive such as GNF (glycosyl-nucleosyl-fluorinated) hydrogel (Ziane et al., 2012) or poly-N-isopropylacrylamide (PNIPAAm) (G. Kim, Jung et al., 2020). These allowed an ASC

differentiation, in osteogenic terms, also in the absence of differentiating or water-repellent materials (Pd/Si NWs) (Seo et al., 2014), capable of forming spheroids with a homogeneous size. The chemical and physical properties of the 3D-composite (polyacrylamide [PAAm] with cell mimicking microparticles [CMMPs]) were studied during the adipogenic differentiation of 3D spheroids. The microparticles were distributed into the center of the spheroids for 24–48 h (Labriola et al., 2018).

Fibers of poly-lactic acid (PLLA) (J. Lee et al., 2020) or Poly (L-glutamic acid) (PLGA) (K. Zhang et al., 2017), alone or cross-linked with OEGs (J. Wu et al., 2017), were created with a significant swollen hydrophilic network that weakens cell-scaffold adhesion, leading ASCs to form spheroids. Ahmad et al. investigated fragmented PLLA fibers coated with gelatin fragmented fibers (Ahmad et al., 2018) or adenosine polydopamine intended for bone tissue engineering applications. Moreover, J. Lee et al. (2020) generated 3D spheroids with epigallocatechin gallate (EGCG)-coated PLLA fibers and exposed them to H_2O_2 for 12 h proving that only in EGCG coated spheroids, cell viability and antioxidative enzyme expression were improved.

In the same manner, collagen with oligo(poly(ethylene glycol) fumarate) (OPF) (Ma et al., 2014) or elastin-like polypeptide (ELP) (Newman et al., 2020) was used. The first study demonstrated that ASCs featured higher proliferation and osteogenic properties compared to BM-MSCs into the scaffold when using the dispersed and the spheroid methods (Ma et al., 2014), while with ELP the hASCs differentiation towards the adipogenic lineage is strictly related to the spheroids morphology and scaffold properties (composition, density, and mechanical characteristics) (Newman et al., 2020).

Another study that used polypeptide similar to elastin (ELP), albeit conjugated to polyethylenimine (PEI), demonstrated that the spheroids grew on this support with a differentiation potential toward the osteogenic lineage that was greater compared to 2D-ASC cultures (Gurumurthy et al., 2017). Fitzgerald et al. compared the ELP-PEI method to suspension and ultra-low attachment static cultures evaluating the generation of spheroids and their adipogenic differentiation. A significant reduction of spheroids was observed in both suspension and ultra-low attachment static cultures due to the fusion of spheroids (Fitzgerald et al., 2020). A new strategy for tumor therapy used gold nanorod (AuNR) (photothermal agent)-PEG-PEI (APP) and Chlorin e6 (Ce6) (photodynamic agent)—loaded ADSCs. After irradiation of the APP/Ce6 agents (808 and 660 nm) allowing activation, the role of ASCs was demonstrated in tumor migration, tropism and anticancer properties in in vitro and in vivo models (Chuang et al., 2020).

Oliveira et al. obtained spheroids using Matrigel, a typical scaffold in tumor studies. They examined the involvement of kinin receptors 1 (B1R) in direct cross-talk between two distinct glioblastoma phenotype cells (U87 and U373 cells) and MSCs having two different origins (BM-MSCs and ASCs). The results showed that glioblastoma cells increased their proliferation rate when mixed with BM-MSC spheroids, but not when in contact with ASC ones (Oliveira

TABLE 3 Characteristics of selected studies using novel culture methods to form spheroids of adipose stem cells

Author	In vitro culture	Substrates/scaffolds	Results
Feng et al. (2017)	Liposuction (abdomen or thighs, female, aged 25–27) 1 week of 2D (N.A. cell/cm^2)	3%, 4%, and 5% HA gel in a syringe with (2×10^6, 4×10^6 and 6×10^6) cells and medium	Stemness study
Hu et al. (2020)	Liposuction (abdomen or thighs) for up to IX passage of 2D	Non cross-linked hyaluronic acid (HA) gel	Angiogenic study
Huang et al. (2011); Hsu et al. (2014); Cheng, Wang, et al. (2012); Cheng, Wang, et al. (2012); Chen et al. (2018)	Adipose tissue (abdomen, female, age 30–57, BMI 24.8) III–XIII passages of 2D culture (N.A. cell/cm^2) (1×10^4 cells/cm^2)	Chitosan modified with HA, PVA, gelatin or co-adiuvated with FGF-2	Stemness study
Lin et al. (2020)	Commercially IV passage 2D	Porous 3D hybrid scaffold of chitosan and native cartilage ECM	Chondrogenic study
Ziane et al. (2012)	Adipose tissue (age 20–80) VI passage 2D (40.000 cells/cm^2)	GNF thermosensitive Hydrogel 1.5 million cells/ml of gel	Osteogenic study
G. Kim, Jung et al. (2020)	Commercially V passage 2D	A thermoresponsive poly(N-isopropylacrylamide) (PNIPAAm) hydrogel substrate (PHS) functionalized with poly (ethylene glycol) (PEG) hydrogel	Spheroid formation
Seo et al. (2014)	1.25, 2.5, and 5.0×10^5 cells/ml of 3D	Water adhesive surface of the Pd/Si NWs gas-sensitive Pd, Si, NWs coated DTS	Stemness and angiogenic studies
Labriola et al. (2018)	Liposuction (abdomen and thigh, female, 56 year old) III passages of 2D (N.A. cell/cm^2)	CMMPs formed to developed PAAm	Adipogenic study
J. Lee et al. (2020)	Commercially IV passage 2D	Bio-mineral coated fibers loaded of platelet derived growth factor (PDGF) molecules	Osteogenic and angiogenic studies
K. Zhang et al. (2017)	Liposuction (abdomen, mean age 30 years) III passages of 2D (1×10^6 to 5×10^7 cells/ml)	PLGA	Angiogenic study
J. Wu et al. (2017)	Liposuction (abdomen, mean age 30 years) III passage 2D 5×10^5 cells/ml	PGA cross-linked with OEGs	Angiogenic study
Ahmad et al., 2018	VII passage of 2D	4% PLLA fibers electrospun in a DCM and TFE blend	bone tissue engineering studies
Ma et al. (2014)	Adipose tissue (abdomen) III passages of 2D (N.A. cell/cm^2)	Collagen (3 mg/ml) and OPF (3400 g/mol)	Osteogenic study
Newman et al. (2020)	Liposuction	collagen and elastin-like polypeptide (ELP) scaffolds	Adipogenic study
Gurumurthy et al. (2017)	Liposuction (female) 80% confluence of 2D (N.A. cell/cm^2)	Polymer ELP conjugated to PEI coating of TCPS 50,000 cells	Osteogenic study
Fitzgerald et al. (2020)	Adipose tissue (female)	ELP-PEI method (two molecular weights: 800 and 25,000 g/mol) 26,000 cells/cm^2	Adipogenic study
Chuang et al. (2020)	Adipose tissue 2D (20,000 cells/well)	(AuNR)-PEG-PEI (APP)/chlorin e6 (Ce6) system	Cancer therapy

(Continues)

TABLE 3 (Continued)

Author	In vitro culture	Substrates/scaffolds	Results
Oliveira et al. (2018)	Commercially 2D (7000 cells/cm^2)	Matrigel	Cancer therapy
Liu et al. (2019)	Commercially (200,000 cells m/L)	PIC hydrogel conjugated with the adhesive peptide GRGDS	Spheroid formation
Kundu et al. (2019) [59]	Liposuction II passages 2D	3D hydrogel created from gellan gum (GG)-silk fibroin	Tumor stroma study in osteosarcoma model
S. Kim, Park, Kim, et al. (2019); S. Kim, Park, Byun, et al. (2019)	Commercially II-V passages 2D (0.5, 1, 2, and 4×10^5 cells/cm³)	all-in-one platform with HES or LoSH with Tet-TA polymers coniugated with fibronectin in a PDMS master mold	Spheroid formation
S. Kim, Han et al. (2018)	70% confluence of 2D (N.A. cell/cm^2)	StemFit 3D®: GMP 100 and 200 MPs/well, 1000 and 2000 cells/well	Spheroid formation
Ko et al. (2020)	Liposuction 5×10^5, 1×10^6, 1.5×10^6 cells/ml	StemFit 3D®: 200, 600 and 400 μm well diameter.	Osteoarthritis study
Y. Wu et al. (2018)	Adipose tissue N.A. Passages of 2D (N.A. cell/cm^2)	Microfabricated pTS 4% tubular alginate Porogens in 4% CaCl2. The cell/porogen mixture was 5:3 ratio.	Self-assembly, chondrogenic and osteogenic studies
G. Kim, Jung et al. (2020)	Commercially (1.2×10^6 cells/cm^3)	Loading spheroids onto acellular, lyophilized and sterile human dermis thin sectioned acellular dermal matrix (tsADM). 8 mm diameter round tsADM was fixed at the center of the coverslip.	Spheroid formation
Silva et al. (2016)	Liposuction 2.5×10^5 and 1×10^6 of 3D cells	Lockyballs: synthetic micro-scaffolds with porous wall, produced by two-photon polymerization of Zr-based hybrid-photopolymer. Micro-molded (2% agarose) hydrogel.	Spheroid formation
Iwazawa et al. (2018)	Commercially N.A. passage 2D (3×10^5 cells/ml)	CellSaic: cell- and -scaffold-forming mosaic scaffold with a bioabsorbable biomaterial RCP in EZ SPHERE, a micro-fabricated plastic vessel containing micro- wells	Cell therapy for colitis
Shima and Makino (2020)	Commercially V-VI passages 2D 5000 cells cm^{-2}	A plate with multicavity structures and bland adhesive properties due to a fluorinated polyimide film (MicoCell)	Spheroid formation Angiogenic study
J. Park et al. (2017)	Commercially 5×10^5 cells of 3D	CMS method: 100 microwells one spheroid per microwell. Internal surface is coated with pluronic copolymer solution. The top and bottom layers with PDMS. Initially 3000 RPM for 3 min rotation then 1000–2000 RPM for three days.	Spheroid formation
S. Zhang et al. (2015)	Adipose tissue 10^6 cells/ml of 3D	A microgravity bioreactor at 25 rpm with ASCs until 5 days	Spheroid formation
Ayan et al. (2020)	Adipose tissues 1×10^6 cells/ml	Aspiration-assisted bioprinting (AAB) technique	Osteochondral study
I. S. Park et al. (2015); I. S. Park et al. (2016)	Commercially V−VIII passage of 2D (7.5×10^4 cells/cm^2)	LLLI at 660 nm wavelength 10 min daily from Day 1 to 14	Angiogenic study
K. Shen et al. (2020)	IV passage of 2D (5000 cells per well)	liquid overlay, which involves coating the surface of the culture dish with a layer of agarose.	Studies of the adipose microenvironment surrounding the kidney

TABLE 3 (Continued)

Author	In vitro culture	Substrates/scaffolds	Results
Al-Ghadban et al. (2020)	Liposuction (thighs) III passage 2D	Orbital shaker at 50 rpm: 30×10^3 cells/cm^2 in 12-well plates coated with 1.5% Ultrapure Agarose solution	Studies on adipogenic potential, differentiation, and ECM remodeling
Hackenberg et al. (2013)	Liposuction 2D (2.000 cells/cm^2)	nanoparticles of titanium dioxide and zinc oxide	Nanoparticle cytotoxicity study on hMSCs

Abbreviations: AuNR, old nanorods; Ce6, chlorin e6; CMMPs, Cell mimicking microparticles; CMS, Centrifugal microfluidic-based spheroid; DCM, dichloromethane; DTS, Dodecylalkyltrichlorosilane; ELP, Elastin-like polypeptide; G-FF, Gelatin fragmented fibers; GMP, Gelatin neutral microparticles; GNF, Glycosyl-nucleosyl-fluorinated; GRGDS, Gly-Arg-Gly-Asp-Ser; HA, Hyaluronic Acid; HES, embossed surface; OEGs, Oligo (ethylene glycol)s; OPF, Oigo (poly(ethylene glycol) fumarate; PAAm, Polyacrylamide; PDMS, Polydimethylsiloxane; PEI, Polyethylenimine; Pd, Palladium; PDMS, Poly (dimethylsiloxane); PEG, poly ethylene glicol; PIC, Polyisocyanides; PLGA, Poly (L-glutamic acid); PLLA, Poly-lactic Acid fibers; pTS, Porous tissue strands; LLLI, Low-level light irradiation; LoSH: lotus seedpod-inspired; NWs, Nanowires; RCP, Recombinant protein; Si, Silicon; TCPS, Tissue culture polystyrene; Tet-TA, tyramine-conjugated Tetronic; TFE, trifluoroethanol.

et al., 2018). A further class of synthetic biomaterials used for spheroid formation is the PIC (polymeric hydrogels of polyisocyanides). By encapsulating several cellular lineages in PIC gel conjugated with the adhesive peptide Gly-Arg-Gly-Asp-Ser, and also varying length and concentration, Liu et al. observed that smooth muscle and tumor cells generated spheroids that proliferated in relation to the polymer density, while ASCs did not form spheroids but showed an elongated morphology, thus concluding that different cell behaviors can occur due to the extracellular matrix expression, organization and interaction with the hydrogel (Liu et al., 2019). Kundu et al. generated spheroids using a construct made with gellan gum (GG)-silk fibroin (S) hydrogels seeding both ASCs and cancer cells on the top to investigate if ASCs were capable of inducing cancer cells to form spheroids. Authors found cancer cell spheroids inside the core of the compartmentalized hydrogel system (Kundu et al., 2019).

Based on mechanical structure or new systems, several innovative techniques were developed to form spheroids of ASC characterized by controlled size, higher stemness, and improved differentiation abilities, such as the following:

- a method defined "all-in-one platform" with hydrogels with an embossed surface (HES) or lotus seedpod-inspired (LoSH) (S. J. Kim, Park, Byun, et al., 2019; S. J. Kim, Park, Kim, et al., 2019);
- StemFit 3D, based on a 389-microwell plate employed with gelatin microparticles (GMP) (Y. Kim, Baipaywad et al., 2018; Ko et al., 2020);
- microfabricated porous tissue strands (pTS) (Y. Wu et al., 2018);
- human dermis named thin sectioned acellular dermal matrix (tsADM) (J. H. Kim & Lee, 2020),
- lockyballs: microscaffolds with a porous wall and interlockable hooks produced by using two-photon polymerization (Silva et al., 2016);
- CellSaic platform, based on a biodegradable material, a recombinant Recombinant protein (Iwazawa et al., 2018);
- MicoCell, a plate with bland adhesive properties, due to a fluorinated polyimide film (Shima & Makino, 2020).

As opposed to the use of scaffolds, some studies developed novel scaffold-free methods to obtain spheroids:

- a centrifugal microfluidic-based spheroid formation method composed of a rotating platform for a dynamic culture (J. Park et al., 2017);
- a microgravity bioreactor (S. Zhang et al., 2015);
- an aspiration-assisted bioprinting technique (Ayan et al., 2020);
- LLLI (low-level light irradiation) in low adherence PS plates method (I. S. Park et al., 2015, 2016).

Another scaffold-free technique is the liquid overlay thanks to which spheroids can be generated through the use of nonadhesive plastic surfaces or adhesive surfaces functionalized with hydrophilic nonadhesive polymers such as agar or agarose.

By applying this technique for the first time, Shen et al. generated cocultures of adipocyte spheroids both with M0 macrofages to investigate their capability in invading the adipose tissue in vitro (K. Shen et al., 2020). Al-Ghadban et al. instead obtained ASC spheroids from both healthy and lipedema patient seeded at a density of 30×10^3 cells/cm^2 in 12-well plates coated with Ultrapure Agarose, and plating them on an orbital shaker at 50 rpm (Al-Ghadban et al., 2020). Coating a 96-multiwell plate with 0.1% soft agar and adding 6×10^3 cells to each well, Hackenberg et al. generated hMSC spheroids (Hackenberg et al., 2013).

4 | DISCUSSION

Spheroid is an element with its own defined and unique characteristics regardless of the method used for its formation. The size of the spheroid is critical because, increasing in size, the levels of expression of hypoxic factors stimulating angiogenesis and of antiapoptotic genes increase as well. Therefore, spheroids contrast the anoikis phenomena better than monolayer cultures. Another important factor to consider in in vitro cultures is that during the detachment process, the trypsin action on the single-layer of cells causes a great

loss of laminin, fibronectin and structural components of the extracellular matrix (Bhang et al., 2011). Nowadays, these 3D cell cultures have become a very attractive system for the scientific community (Abbott, 2003). Indeed, in the field of regenerative medicine, adherent cell cultures of ASCs are still traditionally used both in in vitro and in vivo studies. These cells were largely characterized and this was demonstrated by the fact that many factors can influence their properties. Amongst these factors, there are the characteristics of native adipose tissue (visceral or subcutaneous), of site donors (breast, thigh, abdomen and hip), patient characteristics (age, body mass index [BMI], and sex) as well as the ASC isolation and culture conditions (media, supplemented factors, and scaffolds) (Prieto González, 2019). These factors have not still been analyzed on spheroids yet, however they were subject to an in-depth examination in the 76 papers analyzed. In most of the articles, subcutaneous fat from the abdomen and thighs was used. Some did not describe the fat site donor, while others did not use fat from patients but employing commercial cell cultures. A single work used fat from the hip after arthroplasty (Winter et al., 2003). Moreover, very few authors detailed the BMI, whilst cell yields do not seem to be correlated with age and gender (only women). For the first time, we correlated the factors mentioned above with the yield of spheroids from ASCs, which we called SASCs. The cell yields of nine-two subcutaneous fat samples from abdomen, flanks, thighs and breast were statistically analyzed, also correlating age, sex, BMI, and the fat harvesting method. Male patients and thighs were the only two factors that affected the SASC yield (A. C. Di Stefano et al., 2022).

A fundamental question arises in this review; is it the spheroid that already exists in the tissue (spheroid isolation) or is it the result of a subsequent union or reorganization of individual cells (spheroid formation)? Regardless of the isolation/formation methods, the studies discussed here definitively established the better skills and potential of ASC spheroids when compared to the adherent cells in stemness and mesenchymal differentiation conditions. Results are controversial in the tumor microenvironment because ASCs seem to participate in tumor aggressiveness in osteosarcoma, but could also be a potential vehicle for antitumor therapies. We summarized different methods to generate 3D spheroids which are grouped in classic, canonical and innovative techniques. This proves that there is no standardized method for the isolation and in vitro culture of 3D-ASCs.

In the last 10 years, scientific literature has established that 3D spheroids properly represent the original cells condition in in vivo tissues (Abbott, 2003). This would lead us to assume that spheroids already exist in the tissue as a 3D structure and can therefore be directly isolated, most likely through tissue disintegration. We believe that the ideal technique would be to
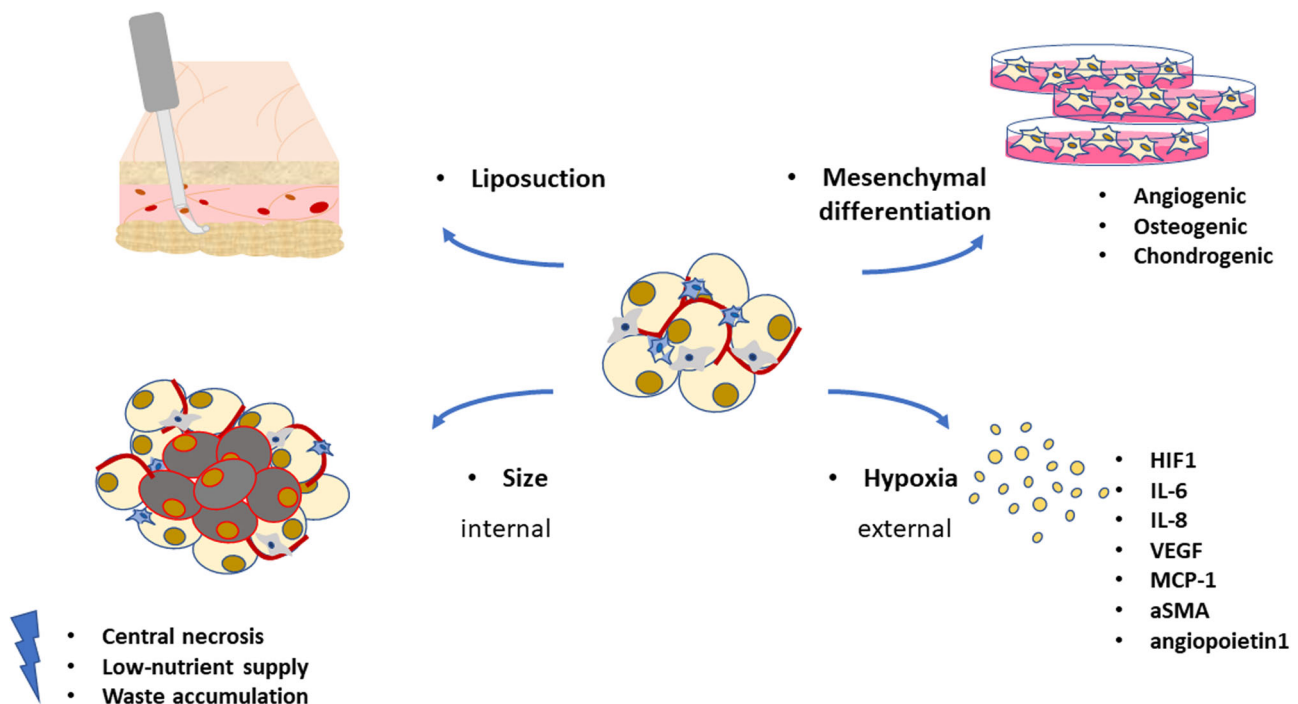

FIGURE 1   Summary of characteristics to form spheroids of adipose stem cells. Spheroids of adipose stem cells can derive from liposuction fat and can be differentiated in several mesenchymal lineages such as angiogenic, chondrogenic and osteogenic ones. Size and hypoxia effects are the major features concerning the formation and abilities of spheroids. Size mainly plays internal effects such as: central necrosis, low-nutrient supply and waste accumulation whilst hypoxia has external ones such as the autocrine and/or paracrine factors production of HIF1, IL-6, IL-8, VEGF, MCP-1, aSMA, and angiopoietin1 factors.
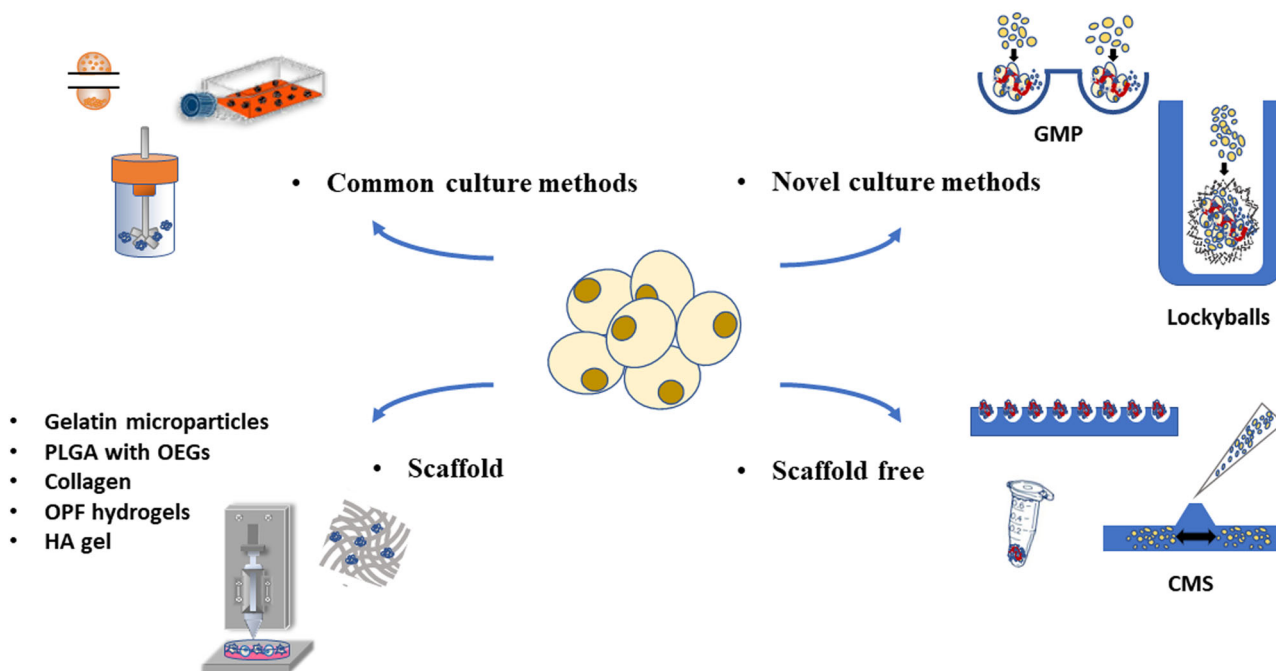
Spheroid formation techniques

FIGURE 2 Summary of methods to form spheroids of adipose stem cells. Representative culture methods listed in the text to form spheroids of adipose stem cells. Common culture methods include the use of ultralow adhesion flask, hanging drop and spinner flask. Novel culture methods, for example, include lockyballs (microscaffolds with a porous wall with interlockable hooks) and GMP (microwells plate employed with gelatin microparticles) techniques. Moreover, spheroid formation can take place through scaffold-free methods (e.g., CMS [centrifugal microfluidic-based spheroid] or plates treated with Pluronic F-127 aqueous solution) or by using several materials such as PLGA (Poly [L-glutamic acid]) with OEGs (Oligo(ethylene glycol), Collagen, OPF (oligo(poly(ethylene glycol) fumarate) hydrogels and HA (hyaluronic acid) gel.

culture cells in suspension without preliminary adhesion isolation or additional processes. In fact, this would lead to an upstream selection of cells that could form different spheroids. Among the classic techniques, only three studies (A. B. Di Stefano et al., 2015; Gimeno et al., 2017; Winter et al., 2003) and, amongst the canonical techniques, the hanging drop and spinner flasks, all obtain spheroids without requiring the first in vitro selection step under adherence conditions.

In the section concerning these innovative methods, we included multiple strategies for spheroid formation; from those featuring a physical nature such as LLLI, a bio-chemical-physical nature (PAAm with CMMPs), to scaffolds such as GNF hydrogel, PLLA-G/mff, PLGA-ADH hydrogel, PLGA-OEGs, HA and HA-chitosan, ELP-PEI, and Pd/Si NWs systems. Furthermore, there is the engineering-structural nature such as Bioreactors, Lockyballs, CellSaic, StemFit 3D, and pTS. Among these studies, only two involve the immediate use of 3D without passing through the adherence conditions such as the centrifugal microfluidic disk formulated to generate finely-controlled multicellular spheroids (Park et al. 2017) and the Pd/Si NWs system performed with 3D-ASCs obtained from the hanging drop method (Seo et al., 2014).

We believe that standardizing a single 3D-ASC isolation technique, such as the spontaneous formation in ultra-low culturing

conditions without the need of special instruments, would be more reliable and reproducible solution.

Although we propose an ideal spheroid isolation technique, it is crucial to evaluate two others important aspects in this discussion: one highlights the importance of these techniques for the in vitro characterization of spheroids, however, on the other hand, it is important to find innovative techniques that involve the least manipulation and the highest yield of cells for prompt use in the clinical field.

In the near future, clinical applications in regenerative medicine will feature the use of bio-printers and bioreactors capable of creating *ad personam* organ or tissue replacement. The results of this systematic review suggest that 3D-ASCs could represent the ideal candidates for clinical studies of regenerative medicine and, given their variety, ad hoc scaffolds could be chosen according to the specific requirements. Figure 1 and 2

AUTHOR CONTRIBUTIONS

Conceptualization: Di Stefano Anna Barbara. *Literature search and data analysis*: Di Stefano Anna Barbara, Urrata Valentina, Trapani Marco *Writing—original draft preparation*: Di Stefano Anna Barbara, Urrata Valentina, Trapani Marco; *Writing—review and editing*: Moschella Francesco, Cordova Adriana, and Toia Francesca.

CONFLICT OF INTEREST

The authors declare no conflict of interest.

ORCID

Anna Barbara Di Stefano 🆔 https://orcid.org/0000-0003-4323-8564

REFERENCES

Abbott, A. (2003). Biology's new dimension. *Nature*, *424*(6951), 870–872. https://doi.org/10.1038/424870a

Agrawal, H., Shang, H., Sattah, A. P., Yang, N., Peirce, S. M., & Katz, A. J. (2014). Human adipose-derived stromal/stem cells demonstrate short-lived persistence after implantation in both an immuno-competent and an immunocompromised murine model. *Stem Cell Research & Therapy*, *5*(6), 142. https://doi.org/10.1186/scrt532

Ahmad, T., Shin, H. J., Lee, J., Shin, Y. M., Perikamana, S. K. M., Park, S. Y., Jung, H. S., & Shin, H. (2018). Fabrication of in vitro 3D mineralized tissue by fusion of composite spheroids incorporating biomineral-coated nanofibers and human adipose-derived stem cells. *Acta Biomaterialia*, *74*, 464–477. https://doi.org/10.1016/j.actbio.2018.05.035

Al-Ghadban, S., Pursell, I. A., Diaz, Z. T., Herbst, K. L., & Bunnell, B. A. (2020). 3D spheroids derived from human lipedema ASCs demonstrated similar adipogenic differentiation potential and ECM remodeling to Non-Lipedema ASCs in vitro. *International Journal of Molecular Sciences*, *21*(21), 8350. https://doi.org/10.3390/ijms21218350

Ayan, B., Wu, Y., Karuppagounder, V., Kamal, F., & Ozbolat, I. T. (2020). Aspiration-assisted bioprinting of the osteochondral interface. *Scientific Reports*, *10*(1), 13148. https://doi.org/10.1038/s41598-020-69960-6

Berg, J., Roch, M., Altschüler, J., Winter, C., Schwerk, A., Kurtz, A., & Steiner, B. (2015). Human adipose-derived mesenchymal stem cells improve motor functions and are neuroprotective in the 6-hydroxydopamine-rat model for parkinson's disease when cultured in monolayer cultures but suppress hippocampal neurogenesis and hippocampal memory function when cultured in spheroids. *Stem Cell Reviews and Reports*, *11*(1), 133–149. https://doi.org/10.1007/s12015-014-9551-y

Bhang, S. H., Cho, S. W., La, W. G., Lee, T. J., Yang, H. S., Sun, A. Y., Baek, S. H., Rhie, J. W., & Kim, B. S. (2011). Angiogenesis in ischemic tissue produced by spheroid grafting of human adipose-derived stromal cells. *Biomaterials*, *32*(11), 2734–2747. https://doi.org/10.1016/j.biomaterials.2010.12.035

Chen, S. T., Wu, C. Y., & Chen, H. Y. (2018). Enhanced growth activities of stem cell spheroids based on a durable and chemically defined surface modification coating. *ACS Applied Materials & Interfaces*, *10*(38), 31882–31891. https://doi.org/10.1021/acsami.8b09103

Cheng, N. C., Wang, S., & Young, T. H. (2012). The influence of spheroid formation of human adipose-derived stem cells on chitosan films on stemness and differentiation capabilities. *Biomaterials*, *33*(6), 1748–1758. https://doi.org/10.1016/j.biomaterials.2011.11.049

Cheng, N. C., Chang, H. H., Tu, Y. K., & Young, T. H. (2012). Efficient transfer of human adipose-derived stem cells by chitosan/gelatin blend films. *Journal of Biomedical Materials Research, Part B: Applied Biomaterials*, *100*(5), 1369–1377. https://doi.org/10.1002/jbm.b.32706

Cho, R. J., Kim, Y. S., Kim, J. Y., & Oh, Y. M. (2017). Human adipose-derived mesenchymal stem cell spheroids improve recovery in a mouse model of elastase-induced emphysema. *BMB Reports*, *50*(2), 79–84. https://doi.org/10.5483/bmbrep.2017.50.2.101

Chuang, C. C., Chen, Y. N., Wang, Y. Y., Huang, Y. C., Lin, S. Y., Huang, R. Y., Jang, Y. Y., Yang, C. C., Huang, Y. F., & Chang, C. W. (2020). Stem Cell-Based delivery of Gold/Chlorin e6 nanocomplexes for combined photothermal and photodynamic therapy. *ACS Applied Materials & Interfaces*, *12*(27), 30021–30030. https://doi.org/10.1021/acsami.0c03446

Coyle, R., Yao, J., Richards, D., & Mei, Y. (2019). The effects of metabolic substrate availability on human Adipose-Derived stem cell spheroid survival. *Tissue Engineering. Part A*, *25*(7–8), 620–631. https://doi.org/10.1089/ten.TEA.2018.0163

Feng, J., Mineda, K., Wu, S. H., Mashiko, T., Doi, K., Kuno, S., Kinoshita, K., Kanayama, K., Asahi, R., Sunaga, A., & Yoshimura, K. (2017). An injectable non-cross-linked hyaluronic-acid gel containing therapeutic spheroids of human adipose-derived stem cells. *Scientific Reports*, *7*(1), 1548. https://doi.org/10.1038/s41598-017-01528-3

Fennema, E. M., Tchang, L. A. H., Yuan, H., van Blitterswijk, C. A., Martin, I., Scherberich, A., & de Boer, J. (2018). Ectopic bone formation by aggregated mesenchymal stem cells from bone marrow and adipose tissue: A comparative study. *Journal of Tissue Engineering and Regenerative Medicine*, *12*(1), e150–e158. https://doi.org/10.1002/term.2453

Fitzgerald, S. J., Cobb, J. S., & Janorkar, A. V. (2020). Comparison of the formation, adipogenic maturation, and retention of human adipose-derived stem cell spheroids in scaffold-free culture techniques. *Journal of Biomedical Materials Research, Part B: Applied Biomaterials*, *108*(7), 3022–3032. https://doi.org/10.1002/jbm.b.34631

Furuhata, Y., Kikuchi, Y., Tomita, S., & Yoshimoto, K. (2016). Small spheroids of adipose-derived stem cells with time-dependent enhancement of IL-8 and VEGF-A secretion. *Genes to Cells*, *21*(12), 1380–1386. https://doi.org/10.1111/gtc.12448

Gimeno, M. L., Fuertes, F., Barcala Tabarrozzi, A. E., Attorressi, A. I., Cucchiani, R., Corrales, L., Oliveira, T. C., Sogayar, M. C., Labriola, L., Dewey, R. A., & Perone, M. J. (2017). Pluripotent nontumorigenic adipose Tissue-Derived muse cells have immunomodulatory capacity mediated by transforming growth Factor-β1. *Stem Cells Translational Medicine*, *6*(1), 161–173. https://doi.org/10.5966/sctm.2016-0014

Guo, X., Li, S., Ji, Q., Lian, R., & Chen, J. (2015). Enhanced viability and neural differential potential in poor post-thaw hADSCs by agarose multi-well dishes and spheroid culture. *Human Cell*, *28*(4), 175–189. https://doi.org/10.1007/s13577-015-0116-4

Gurumurthy, B., Bierdeman, P. C., & Janorkar, A. V. (2017). Spheroid model for functional osteogenic evaluation of human adipose derived stem cells. *Journal of biomedical materials research. Part A*, *105*(4), 1230–1236. https://doi.org/10.1002/jbm.a.35974

Hackenberg, S., Scherzed, A., Technau, A., Froelich, K., Hagen, R., & Kleinsasser, N. (2013). Functional responses of human adipose Tissue-Derived mesenchymal stem cells to metal oxide nanoparticles In Vitro. *Journal of Biomedical Nanotechnology*, *9*(1), 86–95. https://doi.org/10.1166/jbn.2013.1473

Hoefner, C., Muhr, C., Horder, H., Wiesner, M., Wittmann, K., Lukaszyk, D., Radeloff, K., Winnefeld, M., Becker, M., Blunk, T., & Bauer-Kreisel, P. (2020). Human Adipose-Derived mesenchymal Stromal/Stem cell spheroids possess high adipogenic capacity and acquire an adipose tissue-like extracellular matrix pattern. *Tissue Engineering. Part A*, *26*(15–16), 915–926. https://doi.org/10.1089/ten.TEA.2019.0206

Hong, S., Oh, S. J., Choi, D., Hwang, Y., & Kim, S. H. (2020). Self-Organized liver microtissue on a Bio-Functional surface: The role of human Adipose-Derived stromal cells in hepatic function. *International Journal of Molecular Sciences*, 21(13), 4605. https://doi.org/10.3390/ijms21134605

Hsu, S., Ho, T. T., Huang, N. C., Yao, C. L., Peng, L. H., & Dai, N. T. (2014). Substrate-dependent modulation of 3D spheroid morphology self-assembled in mesenchymal stem cell-endothelial progenitor cell coculture. *Biomaterials*, 35(26), 7295–7307. https://doi.org/10.1016/j.biomaterials.2014.05.033

Hu, W., Zhu, S., Fanai, M. L., Wang, J., Cai, J., & Feng, J. (2020). 3D co-culture model of endothelial colony-forming cells (ECFCs) reverses late passage adipose-derived stem cell senescence for wound healing. *Stem Cell Research & Therapy*, 11(1), 355. https://doi.org/10.1186/s13287-020-01838-w

Huang, G. S., Dai, L. G., Yen, B. L., & Hsu, S. (2011). Spheroid formation of mesenchymal stem cells on chitosan and chitosan-hyaluronan membranes. *Biomaterials*, 32(29), 6929–6945. https://doi.org/10.1016/j.biomaterials.2011.05.092

Hutton, D. L., Moore, E. M., Gimble, J. M., & Grayson, W. L. (2013). Platelet-derived growth factor and spatiotemporal cues induce development of vascularized bone tissue by adipose-derived stem cells. *Tissue Engineering. Part A*, 19(17–18), 2076–2086. https://doi.org/10.1089/ten.TEA.2012.0752

Iwazawa, R., Kozakai, S., Kitahashi, T., Nakamura, K., & Hata, K. (2018). The therapeutic effects of Adipose-Derived stem cells and recombinant peptide pieces on mouse model of DSS colitis. *Cell Transplantation*, 27(9), 1390–1400. https://doi.org/10.1177/0963689718782442

Kapur, S. K., Wang, X., Shang, H., Yun, S., Li, X., Feng, G., Khurgel, M., & Katz, A. J. (2012). Human adipose stem cells maintain proliferative, synthetic and multipotential properties when suspension cultured as self-assembling spheroids. *Biofabrication*, 4(2), 025004. https://doi.org/10.1088/1758-5082/4/2/025004

Kim, G., Jung, Y., Cho, K., Lee, H. J., & Koh, W. G. (2020). Thermoresponsive poly(n-isopropylacrylamide) hydrogel substrates micropatterned with poly(ethylene glycol) hydrogel for adipose mesenchymal stem cell spheroid formation and retrieval. *Materials Science and Engineering: C*, 115, 111128. https://doi.org/10.1016/j.msec.2020.111128

Kim, J. H. & Lee, J. Y. (2020). Multi-Spheroid-Loaded human acellular dermal matrix carrier preserves its spheroid shape and improves in vivo Adipose-Derived stem cell delivery and engraftment. *Tissue Engineering and Regenerative Medicine*, 17(3), 271–283. https://doi.org/10.1007/s13770-020-00252-w

Kim, S., Han, Y. S., Lee, J. H., & Lee, S. H. (2018). Combination of MSC spheroids wrapped within autologous composite sheet dually protects against immune rejection and enhances stem cell trans-plantation efficacy. *Tissue and Cell*, 53, 93–103. https://doi.org/10.1016/j.tice.2018.06.005

Kim, S., Park, J., Byun, H., Park, Y. W., Major, L. G., Lee, D. Y., Choi, Y. S., & Shin, H. (2019). Hydrogels with an embossed surface: An all-in-one platform for mass production and culture of human adipose-derived stem cell spheroids. *Biomaterials*, 188, 198–212. https://doi.org/10.1016/j.biomaterials.2018.10.025

Kim, S., Park, J., Kim, E. M., Choi, J. J., Kim, H. N., Chin, I. L., Choi, Y. S., Moon, S. H., & Shin, H. (2019). Lotus seedpod-inspired hydrogels as an all-in-one platform for culture and delivery of stem cell spheroids. *Biomaterials*, 225, 119534. https://doi.org/10.1016/j.biomaterials.2019.119534

Kim, Y., Baipaywad, P., Jeong, Y., & Park, H. (2018). Incorporation of gelatin microparticles on the formation of adipose-derived stem cell spheroids. *International Journal of Biological Macromolecules*, 110, 472–478. https://doi.org/10.1016/j.ijbiomac.2018.01.046

Ko, J. Y., Park, J. W., Kim, J., & Im, G. I. (2020). Characterization of adipose-derived stromal/stem cell spheroids versus single-cell suspension in cell survival and arrest of osteoarthritis progression. *Journal of Biomedical Materials Research. Part A*, 109, 869–878. https://doi.org/10.1002/jbm.a.37078

Kundu, B., Bastos, A. R. F., Brancato, V., Cerqueira, M. T., Oliveira, J. M., Correlo, V. M., Reis, R. L., & Kundu, S. C. (2019). Mechanical property of hydrogels and the presence of adipose stem cells in tumor stroma affect spheroid formation in the 3D osteosarcoma model. *ACS Applied Materials & Interfaces*, 11(16), 14548–14559. https://doi.org/10.1021/acsami.8b22724

Labriola, N. R., Sadick, J. S., Morgan, J. R., Mathiowitz, E., & Darling, E. M. (2018). Cell mimicking microparticles influence the organization, growth, and mechanophenotype of stem cell spheroids. *Annals of Biomedical Engineering*, 46(8), 1146–1159. https://doi.org/10.1007/s10439-018-2028-4

Lee, G. H., Suh, Y., & Park, J. Y. (2018). A paired bead and magnet array for molding microwells with variable concave geometries. *Journal of Visualized Experiments*, (131), 1–10. https://doi.org/10.3791/55548

Lee, J., Lee, S., Ahmad, T., Madhurakkat Perikamana, S. K., Lee, J., Kim, E. M., & Shin, H. (2020). Human adipose-derived stem cell spheroids incorporating platelet-derived growth factor (PDGF) and bio-minerals for vascularized bone tissue engineering. *Biomaterials*, 255, 120192. https://doi.org/10.1016/j.biomaterials.2020.120192

Lin, I. C., Wang, T. J., Wu, C. L., Lu, D. H., Chen, Y. R., & Yang, K. C. (2020). Chitosan-cartilage extracellular matrix hybrid scaffold induces chon-drogenic differentiation to adipose-derived stem cells. *Regenerative Therapy*, 14, 238–244. https://doi.org/10.1016/j.reth.2020.03.014

Liu, K., Mihaila, S. M., Rowan, A., Oosterwijk, E., & Kouwer, P. H. J. (2019). Synthetic extracellular matrices with nonlinear elasticity regulate cellular organization. *Biomacromolecules*, 20(2), 826–834. https://doi.org/10.1021/acs.biomac.8b01445

Ma, J., Yang, F., Both, S. K., Kersten-Niessen, M., Bongio, M., Pan, J., Cui, F. Z., Kasper, F. K., Mikos, A. G., Jansen, J. A., & van den Beucken, J. J. J. P. (2014). Comparison of cell-loading methods in hydrogel systems. *Journal of Biomedical Materials Research. Part A*, 102(4), 935–946. https://doi.org/10.1002/jbm.a.34784

De Moor, L., Merovci, I., Baetens, S., Verstraeten, J., Kowalska, P., Krysko, D. V., De Vos, W. H., & Declercq, H. (2018). High-throughput fabrication of vascularized spheroids for bioprinting. *Biofabrication*, 10(3), 035009. https://doi.org/10.1088/1758-5090/aac7e6

Newman, K., Clark, K., Gurumurthy, B., Pal, P., & Janorkar, A. V. (2020). Elastin-Collagen based hydrogels as model scaffolds to induce three-dimensional adipocyte culture from adipose derived stem cells. *Bioengineering*, 7(3), 110. https://doi.org/10.3390/bioengineering7030110

No, dY., Lee, S. A., Choi, Y. Y., Park, D., Jang, J. Y., Kim, D. S., & Lee, S. H. (2012). Functional 3D human primary hepatocyte spheroids made by co-culturing hepatocytes from partial hepatectomy specimens and human adipose-derived stem cells. *PLoS One*, 7(12), e50723. https://doi.org/10.1371/journal.pone.0050723

Oberringer, M., Bubel, M., Jennewein, M., Guthörl, S., Morsch, T., Bachmann, S., Metzger, W., & Pohlemann, T. (2018). The role of adipose-derived stem cells in a self-organizing 3D model with regard to human soft tissue healing. *Molecular and Cellular Biochemistry*, 445(1–2), 195–210. https://doi.org/10.1007/s11010-017-3265-9

Oliveira, M. N., Pillat, M. M., Motaln, H., Ulrich, H., & Lah, T. T. (2018). Kinin-B1 receptor stimulation promotes invasion and is involved in Cell-Cell interaction of co-cultured glioblastoma and mesenchymal stem cells. *Scientific Reports*, 8(1), 1299. https://doi.org/10.1038/s41598-018-19359-1

Pappalardo, M., Montesano, L., Toia, F., Russo, A., Di Lorenzo, S., Dieli, F., Moschella, F., Leto Barone, A. A., Meraviglia, S., & Di Stefano, A. B. (2019). Immunomodulation in vascularized composite allotransplan-tation: what is the role for Adipose-Derived stem cells. *Annals of*

Plastic Surgery, 82(2), 245–251. https://doi.org/10.1097/SAP.0000 000000001763

Park, I. S., Chung, P. S., & Ahn, J. C. (2015). Enhancement of ischemic wound healing by spheroid grafting of human Adipose-Derived stem cells treated with Low-Level light irradiation. *PLoS One*, 10(6), e0122776. https://doi.org/10.1371/journal.pone. 0122776

Park, I. S., Chung, P. S., & Ahn, J. C. (2016). Angiogenic synergistic effect of Adipose-Derived stromal cell spheroids with Low-Level light therapy in a model of acute skin flap ischemia. *Cells Tissues Organs*, 202(5–6), 307–318. https://doi.org/10.1159/000445710

Park, J., Lee, G. H., Yull Park, J., Lee, J. C., & Kim, H. C. (2017). Hypergravity-induced multicellular spheroid generation with different morphological patterns precisely controlled on a centrifugal microfluidic platform. *Biofabrication*, 9(4), 045006. https://doi.org/ 10.1088/1758-5090/aa9472

Parshyna, I., Lehmann, S., Grahl, K., Pahlke, C., Frenzel, A., Weidlich, H., & Morawietz, H. (2017). Impact of omega-3 fatty acids on expression of angiogenic cytokines and angiogenesis by adipose-derived stem cells. *Atherosclerosis Supplements*, 30, 303–310. https://doi.org/10. 1016/j.atherosclerosissup.2017.05.040

Prieto González, E. A. (2019). Heterogeneity in adipose stem cells. *Advances in Experimental Medicine and Biology*, 1123, 119–150. https://doi.org/10.1007/978-3-030-11096-3_8

Rumiński, S., Kalaszczyńska, I., & Lewandowska-Szumieł, M. (2020). Effect of cAMP signaling regulation in osteogenic differentiation of adipose-derived mesenchymal stem cells. *Cells*, 9(7), 1587. https:// doi.org/10.3390/cells9071587

Rumiński, S., Kalaszczyńska, I., Długosz, A., & Lewandowska-Szumieł, M. (2019). Osteogenic differentiation of human adipose-derived stem cells in 3D conditions - comparison of spheroids and polystyrene scaffolds. *European Cells and Materials*, 37, 382–401. https://doi. org/10.22203/eCM.v037a23

Seo, J., Lee, J. S., Lee, K., Kim, D., Yang, K., Shin, S., Mahata, C., Jung, H. B., Lee, W., Cho, S. W., & Lee, T. (2014). Switchable water-adhesive, superhydrophobic palladium-layered silicon nanowires potentiate the angiogenic efficacy of human stem cell spheroids. *Advanced Materials*, 26(41), 7043–7050. https://doi.org/10.1002/adma.2014 02273

Shen, F. H., Werner, B. C., Liang, H., Shang, H., Yang, N., Li, X., Shimer, A. L., Balian, G., & Katz, A. J. (2013). Implications of adipose-derived stromal cells in a 3D culture system for osteogenic differentiation: an in vitro and in vivo investigation. *The Spine Journal*, 13(1), 32–43. https://doi.org/10.1016/j.spinee.2013.01.002

Shen, K., Vesey, D. A., Hasnain, S. Z., Zhao, K. N., Wang, H., Johnson, D. W., Saunders, N., Burgess, M., & Gobe, G. C. (2020). A cost-effective three-dimensional culture platform functionally mimics the adipose tissue microenvironment surrounding the kidney. *Biochemical and Biophysical Research Communications*, 522(3), 736–742. https://doi.org/10.1016/j.bbrc.2019.11.119

Shima, F. & Makino, T. (2020). Fabrication of spheroids with Dome-Shaped endothelial tube networks by an adhesive culture system. *Advanced Biosystems*, 4(10), 2000120. https://doi.org/10.1002/adbi. 202000120

Silva, K. R., Rezende, R. A., Pereira, F. D. A. S., Gruber, P., Stuart, M. P., Ovsianikov, A., Brakke, K., Kasyanov, V., da Silva, J. V. L., Granjeiro, J. M., Baptista, L. S., & Mironov, V. (2016). Delivery of human adipose stem cells spheroids into lockyballs. *PLoS One*, 11(11), e0166073. https://doi.org/10.1371/journal.pone.0166073

Skiles, M. L., Sahai, S., Rucker, L., & Blanchette, J. O. (2013). Use of culture geometry to control hypoxia-induced vascular endothelial growth factor secretion from adipose-derived stem cells: optimizing a cell-based approach to drive vascular growth. *Tissue Engineering. Part A*, 19(21–22), 2330–2338. https://doi.org/10. 1089/ten.TEA.2012.0750

Skiles, M. L., Hanna, B., Rucker, L., Tipton, A., Brougham-Cook, A., Jabbarzadeh, E., & Blanchette, J. O. (2015). ASC spheroid geometry and culture oxygenation differentially impact induction of preangiogenic behaviors in endothelial cells. *Cell Transplantation*, 24(11), 2323–2335. https://doi.org/10.3727/096368914X684051

Di Stefano, A., Montesano, L., Belmonte, B., Gulino, A., Gagliardo, C., Florena, A. M., Bilello, G., Moschella, F., Cordova, A., Leto Barone, A. A., & Toia, F. (2020). Human spheroids from adipose-derived stem cells induce calvarial bone production in AQ1 a xenogeneic rabbit model. *Annals of Plastic Surgery*.

Di Stefano, A. B., Leto Barone, A. A., Giammona, A., Apuzzo, T., Moschella, P., Franco, S., & Moschella, F. (2015). Identification and expansion of adipose stem cells with enhanced bone regeneration properties. *Journal of Regenerative Medicine*, 5(1), 1–11. https://doi. org/10.4172/2325-9620.1000124

Di Stefano, A. B., Grisafi, F., Perez-Alea, M., Castiglia, M., Di Simone, M., Meraviglia, S., Cordova, A., Moschella, F., & Toia, F. (2020). Cell quality evaluation with gene expression analysis of spheroids (3D) and adherent (2D) adipose stem cells. *Gene*, 768, 1–10. https://doi. org/10.1016/j.gene.2020.145269

Di Stefano, A. B., Grisafi, F., Castiglia, M., Perez, A., Montesano, L., Gulino, A., Toia, F., Fanale, D., Russo, A., Moschella, F., Leto Barone, A. A., & Cordova, A. (2018). Spheroids from adipose-derived stem cells exhibit an miRNA profile of highly undifferentiated cells. *Journal of Cellular Physiology*, 233(11), 8778–8789. https://doi.org/10.1002/jcp.26785

Di Stefano, A. C., Trapani, E., Pirrello, M., Montesano, R., Moschella, L., Cordova, F. A., & Toia, F. (2022). Correlation between tissue-harvesting method and donor-site with the yield of spheroids from adipose-derived stem cells. *Journal of Plastic, Reconstrucive & Aesthetic Surgery*, 22, S1748-6815(22)00412-0. https://doi.org/10. 1016/j.bjps.2022.06.091

Williams, S. K., Touroo, J. S., Church, K. H., & Hoying, J. B. (2013). Encapsulation of adipose stromal vascular fraction cells in alginate hydrogel spheroids using a direct-write three-dimensional printing system. *BioResearch Open Access*, 2(6), 448–454. https://doi.org/10. 1089/biores.2013.0046

Winter, A., Breit, S., Parsch, D., Benz, K., Steck, E., Hauner, H., Weber, R. M., Ewerbeck, V., & Richter, W. (2003). Cartilage-like gene expression in differentiated human stem cell spheroids: A comparison of bone marrow-derived and adipose tissue-derived stromal cells. *Arthritis & Rheumatism*, 48(2), 418–429. https://doi. org/10.1002/art.10767

Wu, J., Zhang, K., Yu, X., Ding, J., Cui, L., & Yin, J. (2017). Hydration of hydrogels regulates vascularization in vivo. *Biomaterials Science*, 5(11), 2251–2267. https://doi.org/10.1039/c7bm00268h

Wu, Y., Hospodiuk, M., Peng, W., Gudapati, H., Neuberger, T., Koduru, S., Ravnic, D. J., & Ozbolat, I. T. (2018). Porous tissue strands: avascular building blocks for scalable tissue fabrication. *Biofabrication*, 11(1), 015009. https://doi.org/10.1088/1758-5090/aaec22

Xu, Y., Shi, T., Xu, A., & Zhang, L. (2016). 3D spheroid culture enhances survival and therapeutic capacities of MSCs injected into ischemic kidney. *Journal of Cellular and Molecular Medicine*, 20(7), 1203–1213. https://doi.org/10.1111/jcmm.12651

Xu, Y., Yang, Y., Zheng, H., Huang, C., Zhu, X., Zhu, Y., Guan, R., Xin, Z., Liu, Z., & Tian, Y. (2020). Intracavernous injection of size-specific stem cell spheroids for neurogenic erectile dysfunction: efficacy and risk versus single cells. *EBioMedicine*, 52, 102656. https://doi.org/ 10.1016/j.ebiom.2020.102656

Yoon, H. H., Bhang, S. H., Shin, J. Y., Shin, J., & Kim, B. S. (2012). Enhanced cartilage formation via three-dimensional cell engineering of human adipose-derived stem cells. *Tissue Engineering. Part A*, 18(19–20), 1949–1956. https://doi.org/10.1089/ten.TEA.2011.0647

Zhang, K., Song, L., Wang, J., Yan, S., Li, G., Cui, L., & Yin, J. (2017). Strategy for constructing vascularized adipose units in poly(l-

glutamic acid) hydrogel porous scaffold through inducing in-situ formation of ASCs spheroids. *Acta Biomaterialia*, *51*, 246–257. https://doi.org/10.1016/j.actbio.2017.01.043

Zhang, S., Liu, P., Chen, L., Wang, Y., Wang, Z., & Zhang, B. (2015). The effects of spheroid formation of adipose-derived stem cells in a microgravity bioreactor on stemness properties and therapeutic potential. *Biomaterials*, *41*, 15–25. https://doi.org/10.1016/j.biomaterials.2014.11.019

Ziane, S., Schlaubitz, S., Miraux, S., Patwa, A., Lalande, C., Bilem, I., Lepreux, S., Rousseau, B., Le Meins, J. F., Latxague, L., Barthélémy, P., & Chassande, O. (2012). A thermosensitive low molecular weight hydrogel as scaffold for tissue engineering. *European Cells and Materials*, *23*, 147–160discussion 160. https://doi.org/10.22203/ecm.v023a11

Spheroids of adipose derived stem cells show their potential in differentiating towards the angiogenic lineage

Anna Barbara Di Stefano [a,*,1], Francesca Toia [a,b,c,1], Valentina Urrata [a], Marco Trapani [a], Luigi Montesano [b,c], Emanuele Cammarata [b,c], Francesco Moschella [a], Adriana Cordova [a,b,c]

[a] *BIOPLAST-Laboratory of BIOlogy and Regenerative Medicine-PLASTic Surgery, Plastic and Reconstructive Surgery Section, Department of Surgical, Oncological and Oral Sciences, University of Palermo, 90127 Palermo, Italy*
[b] *Section of Plastic and Reconstructive Surgery. Department of Surgical, Oncological and Oral Sciences, University of Palermo, Palermo, Italy*
[c] *Plastic and Reconstructive Unit, Department of D.A.I. Chirurgico, Azienda Ospedaliera Universitaria Policlinico "Paolo Giaccone", 90127 Palermo, Italy*

A B S T R A C T

Introduction: Adipose derived stem cells (ASCs) are a mesenchymal stem cell population of great scientific interest due to their abundance and easiness in obtaining them from adipose tissue. Recently, several techniques for three dimensional (3D) ASCs cultivation have been developed to obtain spheroids of adipose stem cells (SASCs). It was already proved that ASCs are able to differentiate towards the endothelial lineage thus, for the first time, we investigated the ability of our 3D SASCs to differentiate endothelially and the effects of not differentiated SASC secreted factors on specific cultured cells.
Materials and methods: SASCs were differentiated with a specific medium towards endothelial lineage. Cell viability, gene and protein expression of typical endothelial markers were analysed. Moreover, tube formation, wound healing and migration assays were performed to investigate the ability in migration and angiogenic networks formation of endothelially differentiated cells. SASCs secretome were also tested.
Results: We showed the ability of SASCs to differentiate towards the endothelial lineage with an increase in cell viability of 15-fold and 8-fold at 14 and 21 days of differentiation respectively. Moreover, we showed the upregulation of VEGF-A and CD31 mRNAs of 9-fold and 1300-fold in SASCs endothelially differentiated cells, whilst protein expression was different. VEGF-A protein expression was upregulated whilst CD31 protein wasn't translated. In addition, ICAM1, VCAM1, ANGPT1, CD62E protein levels remain unchanged. SASCs were also able to organize themselves into angiogenic networks after 7 days of culturing them on ECMatrix. Secreted factors from undifferentiated 3D SASCs acted in a paracrine way on HUVECs and endothelially differentiated ASCs seeded on ECMatrix to promote angiogenic events.
Conclusions: SASCs, thanks to their multilineage differentiation potential, also possess the ability to differentiate towards endothelial lineage and to organize themselves into angiogenic networks. Moreover, they are able to promote angiogenesis through their secreted factors.

1. Introduction

Mesenchymal stem cells are morphologically fibroblast-like cells (Denu et al., 2016), self-renewal cells (Yoon et al., 2014) and can be isolated from several sources such as bone marrow (Pittenger et al., 1999; Chu et al., 2020), dental pulp (Rajendran et al., 2013), adipose tissue (Mahmoudifar and Doran, 2015) and many others (Makhoul et al., 2013; Poltavtseva et al., 2014; Sahraei et al., 2022).

Recent literature studies proved that MSCs isolation from adipose tissue was advantageous if compared with bone marrow due to the lower invasiveness and higher safeness of the surgical liposuction procedures (Housman et al., 2002; Dhami and Agarwal, 2006) and the higher abundance of cells (Witkowska-Zimny and Walenko, 2011; Harasymiak-Krzyżanowska et al., 2013). It has already been proved that 2D cultures of adipose derived stem cells (ASCs), with the addition of specific culture media enriched with lineage-specific induction factors, are able to differentiate into multilineages such as chondrogenic, osteogenic, adipogenic (Kuca-Warnawin et al., 2023), cardiomyogenic, angiogenic (Shang et al., 2019), myogenic and others cell lines (Si et al., 2019).

Recently, new advances in 3D ASCs cultivation have been developed, leading to obtain spheroids of adipose stem cells (SASCs). Today, there is still no standardised technique to obtain spheroids of ASCs, but all researchers agree that 3D cultures represent better the *in vivo* condition and possess higher capacity to differentiate towards mesenchymal lineages compared to 2D-ASCs (Di Stefano et al., 2022). We showed that SASCs possess higher stemness properties than 2D ASCs (Di Stefano et al., 2021), exhibiting a typical miRNAs profile similar to the one of the induced pluripotent stem cells (iPSCs) (Di Stefano et al., 2018). It has already been proved that they have an increased differentiation potential towards chondrogenic, osteogenic and adipogenic lineages if compared to 2D ASCs (Di Stefano et al., 2015) and their ability in inducing osteogenesis in *in vivo* rabbit calvaria models. SASCs implanted with Integra at the site of injury, through the release of paracrine factors, stimulated rabbit cells to repair the bone injury and also to enhance neoangiogenesis processes (Di Stefano et al., 2020). This could due to the fact that SASCs mimic better than 2D cells what happens inside the living tissue where the cells are in three dimensions and not in two. Nowadays, only one study investigated the angiogenic differentiation potential of ASC spheroids, proving that 3D spheroids formed with a different technique showed a quick spontaneous over-expression of some osteogenic and angiogenic markers, respectively RUNX2 and CD31 compared to 2D adherent cells. Then, an increased cell differentiation was performed through the simultaneous addition of specific osteo and angio-inductive factors, finding a predominance in osteogenic differentiation (Gorkun et al., 2021).

In addition, literature shows that ASCs can play a role in tissue repair by promoting angiogenesis and neovascularisation in various pathologies such as myocardial and various types of ischemia (Gimble et al., 2007; Ma et al., 2017; Katagiri et al., 2020; Lee et al., 2020).

The aim of this work was to show the differentiation potential of SASCs towards the angiogenic lineage, not yet investigated in detail. Then, we also studied SASCs ability, or their released paracrine factors, to form tube networks and stimulate the cell proliferation.

2. Materials and methods

2.1. Cell culture

Lipoaspirates and subcutaneous adipose tissue samples were taken from healthy patients which underwent surgery in the Department of Plastic and Reconstructive Surgery at the University Hospital of Palermo, following informed consent. The samples were treated both enzymatically with collagenase (150 mg/ml, Gibco, Carlsbad, CA) and hyaluronidase (20 mg/ml, Sigma) and mechanically thanks to a thermomixer at 37 °C (30–60 min). After centrifugation at 1200 rpm for 5 min, the SVF (stromal vascular fraction) was cultured under different conditions: in suspension (3D) and in adhesion (2D).

In 3D conditions, the stem cell medium (SCM) together with growth factors as bFGF (10 ng/ml, Sigma, St. Louis, MO) and EGF (20 ng/mL, Sigma, St. Louis, MO) were added and the cells were seeded in ultralow adhesion flasks (Corning, NY). On average, the generated spheroids are composed of 30 to 100 cells. In 2D conditions, Dulbecco's Modified Eagle Medium (DMEM) supplemented with 10% FBS was used in traditional adhesion flasks. In addition, HUVEC population was cultured in 2D adhesion conditions with Vascular Cell Basal Medium (VCBM) (MesenPRO RS, Gibco, 2337037). All the cell cultures were synchronized, by culturing them concurrently for up to 21 days. They were stored in an incubator at 37 °C and 5% CO_2 and periodically washed. In order to analyse the growth of ASCs, SASCs and HUVECs cultured in specific inductive endothelial conditions, 350.000 cells were seeded and a cell count was performed after 0, 14 and 21 days of *in vitro* differentiation.

2.2. RNA extraction and mRNA assay

RNA extraction was performed through the RNeasy Mini Kit (Qiagen). High quality RNA was quantified with Qubit 4 (Thermofisher). Then, 350 ng of RNA was reverse transcribed into cDNA using the High capacity cDNA reverse transcription kit (Applied Biosystems). Relative mRNA expression values were calculated through the Livak method from the equation $2^{-\Delta\Delta Ct}$. HIF1α (Hs00153153_m1), VEGF (Hs0090054_m1) and CD31 (Hs00169777_m1) genes were analysed on VCBM-treated cells and GAPDH (Hs02758991_g1) was used as housekeeping gene.

2.3. In vitro angiogenesis assay

After culturing ASCs, SASCs and HUVECs in VCBM for 21 days, cells were seeded on an extracellular matrix (ECMatrix™ ECM625, Sigma-Aldrich). It consists of laminin, collagen type IV, heparan sulfate proteoglycans, entactin and nidogen and several growth factors such as TGF-beta and FGF and proteolytic enzymes such as plasminogen, tPA and MMPs.

It was generated *in vitro* by mixing a solution of ECMatrix™ and cold buffer which was seeded on 96-well plates and kept in the incubator at 37 °C to solidify. After 1 h, 10,000 cells per well were added and incubated overnight. After 12 h all media were changed by adding the conditioned media from ASC and SASC cultured in their own media for 28 days. The experimental conditions for this analysis were the following: VCBM as control and conditioned medium from 3D SASCs and 2D ASCs maintained respectively in their specific media for 28 days. Then, we tested the angiogenic sprouting of the cells and also analysed the expression of angiogenic markers on cells seeded on matrix through an immunofluorescence assay. Anti-VEGF antibody (ab185238, Abcam) and anti-CD31 antibody (ab9498, Abcam) were used. In addition, Hoechst (33342, Thermofisher) was used to detect cell nuclei.

2.4. Wound healing assay

After 21 days of endothelial differentiation, the proliferation and migration of ASCs, SASCs and HUVECs were evaluated in two different assays in VCBM and experimental conditioned media. Firstly, cells were cultured into a 24-well plate until confluence and, subsequently, a scratch was performed. *ImageJ* software was used to measure the migration distance and the covered area. Secondly, 15.000 cells were seeded into the upper chamber with pore sizes of 8 μm in a 24well plate (Thermofisher) and, after 24 h, the migrated cells on the bottom of the well were counted.

2.5. Luminex investigation

By Luminex plate (BioRad), we analysed the presence of 7

endothelial analytes in SASCs, ASCs and HUVECs conditioned medium. Firstly, for each analyte, we subtracted the average value of each cell conditioned medium to the blank after that the average between the data of SASCs and ASCs samples was calculated. Finally, data were processed as intensity value in log10.

2.6. Statistical analysis

Data are expressed as mean ± standard deviation (SD) of three independent experiments conducted in triplicate. Statistical significance was observed using the One Way Anova test, followed by Bonferroni's multiple comparison test. Significance levels are indicated as p values: * $p < 0,001$.

3. Results

3.1. Investigation on the angiogenic differentiation potential of 3D SASCs

In order to investigate the angiogenic differentiation potential of SASCs, we performed several analyses comparing them with HUVECs and endothelially differentiated 2D ASCs, whose endothelial properties were already known. Morphological observations showed that the addition of endothelial differentiation stimuli on cell cultures led to a change in SASCs shape. In fact, the cells take on the fibroblastic-like shape characteristic of the endothelial population (Fig. 1A) if compared with the original spheroidal organization as well as mesenchymal 2D shape. The analysis of cell viability showed a different proliferation of SASCs, at the same medium condition and time period, compared to ASC and HUVEC ones. Although the latter maintained the same pattern with an increase in growth at 14 and 21 days of approximately 2.5-fold compared to baseline, SASCs showed an increase of approximately 15-fold at 14 days and 8-fold at 21 days compared to time 0. Comparison analysis amongst the three cell cultures showed that SASCs grew up approximately 6-fold more at 14 days and 3-fold more at 21 days if compared to ASCs and HUVECs (Fig. 1B). A Real-Time PCR analysis of several angiogenic mRNAs was performed on the cell cultures after 21 days of induction of endothelial differentiation in comparison to HUVEC expression. The results showed an up-regulation of VEGF-A expression levels approximately of 9-fold on SASCs and 5-fold on ASCs and CD31 up-regulation of 1300-fold on SASCs and 800-fold on ASCs. VEGFR2 and HIF1-α (data not shown) were instead reduced on SASCs (750-fold and 2-fold, respectively) and ASCs (180-fold and 1-fold, respectively) compared with HUVECs expression (Fig. 1C). We also quantified several angiogenic factors through Luminex assay, finding that VEGF-A was 6-fold up-regulated in both samples whilst VEGFR2 and CD31 were 3-fold down-regulated. In addition, ICAM1, VCAM1, ANGPT1 and CD62E (data not shown) did not change in all samples (Fig. 1D).

3.2. Investigation of cell differentiation on ECM matrix

To evaluate the ability to form angiogenic networks, SASCs previously induced to differentiate towards the endothelial lineage, were seeded on ECMatrix^TM. Similarly, ASCs and HUVECs were placed on the matrix as control. These tests showed different behaviours of cells. Although the specific protocol indicated the first sprouting events within 4 h followed by apoptosis phenomena, HUVECs maintained their angiogenic networks up to 24 h. In contrast, after 24 h SASCs and ASCs had not yet shown any angiogenic network and only single sprouting events were visible, so that they were maintained on ECMatrix^TM for longer time. After being cultured for 7 days on matrix, both populations started to generate angiogenic networks that were maintained and observed until 14 days (Fig. 2).

3.3. Analysis of SASCs secreted factors on angiogenic networks formation

To investigate the potential stimulatory effects of secreted SASCs paracrine factors for angiogenic networks formation, the cells were
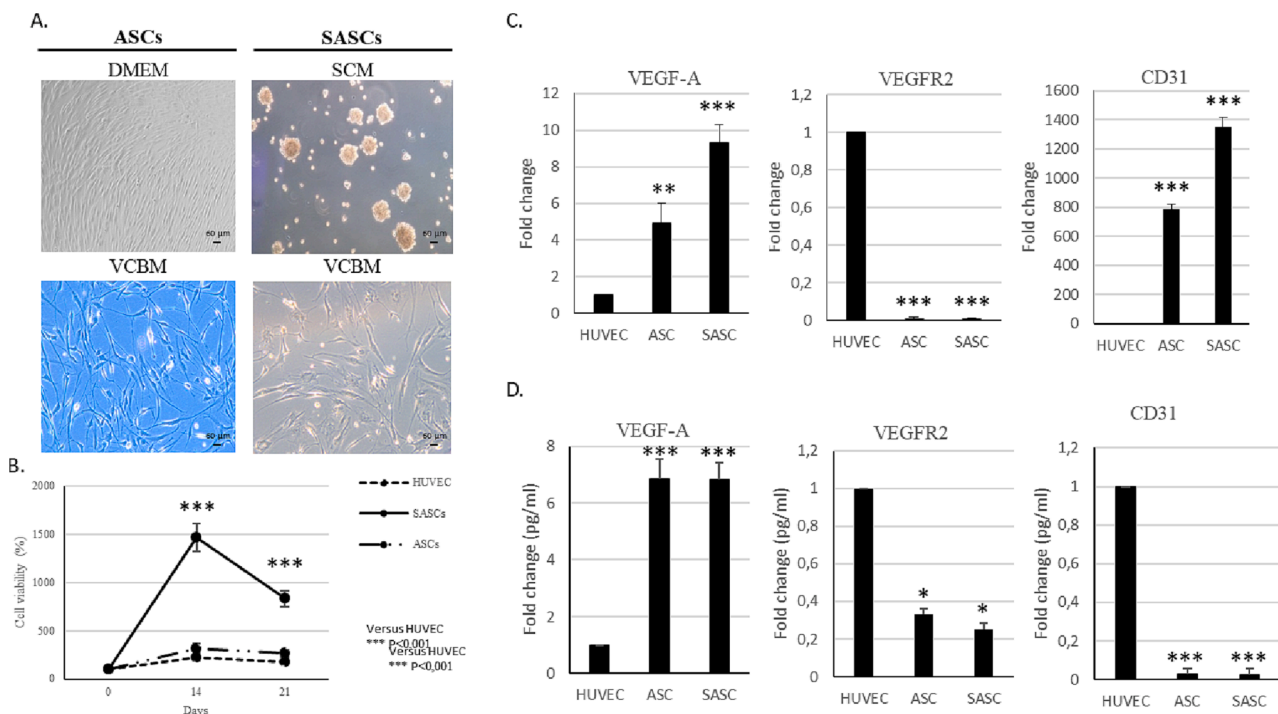
Fig. 1. Cell analysis during endothelial differentiation. A. Morphological analysis of ASCs and SASCs endothelially differentiated cells at 21 days in culture condition. On the top: cells in their own growth medium. On the bottom: cells cultured in VCBM. HUVECs and ASCs were used as control. B. Cell viability analysis of ASCs, SASCs and HUVECs in VCBM at 0, 14 and 21 days. C. Real-time PCR analysis of VEGF-A, VEGFR2 and CD31 mRNAs and D. Angiogenic Luminex assay in SASCs, ASCs and HUVECs at 21 days of endothelial differentiation.
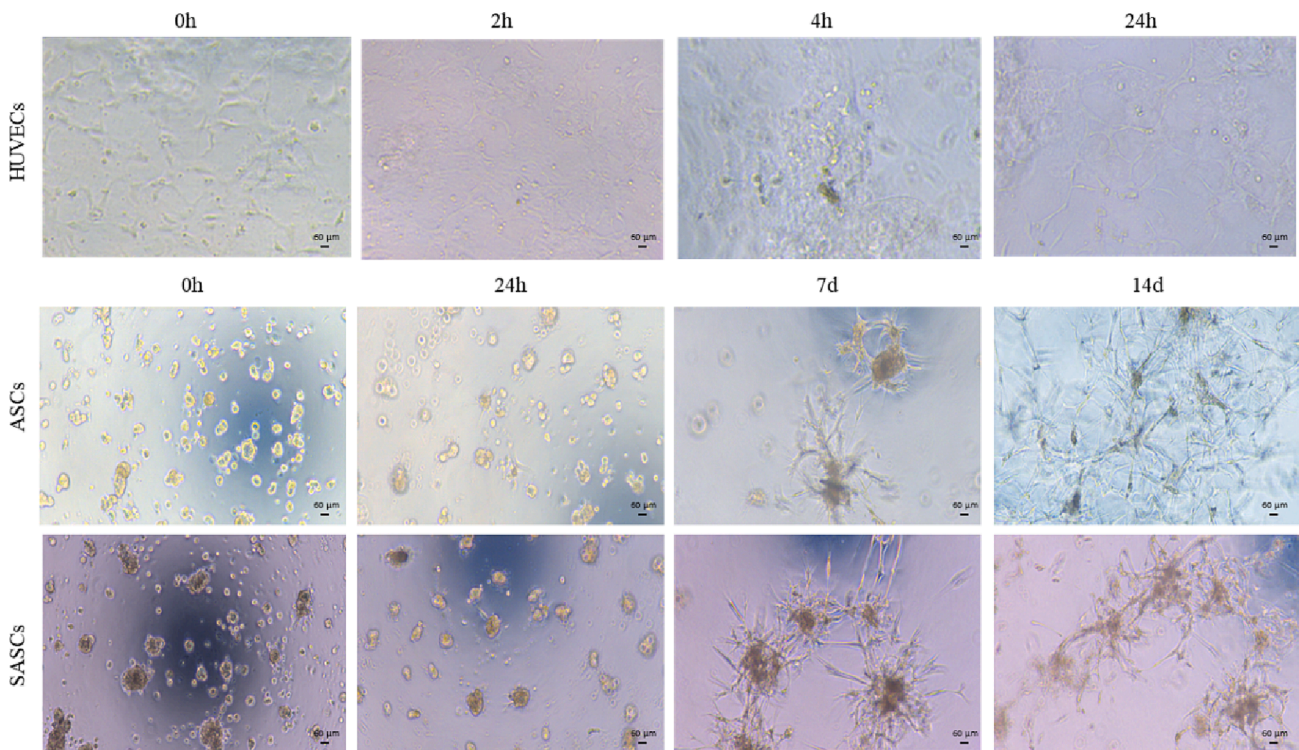
Fig. 2. Analysis of angiogenic networks on ECMatrix^TM. In the first lane, angiogenic network formation by HUVECs at 0 h, 2 h, 4 h and 24 h. In the second and third lanes, respectively, angiogenic network formation by ASCs and SASCs at 0 h, 24 h, 7d and 14d.
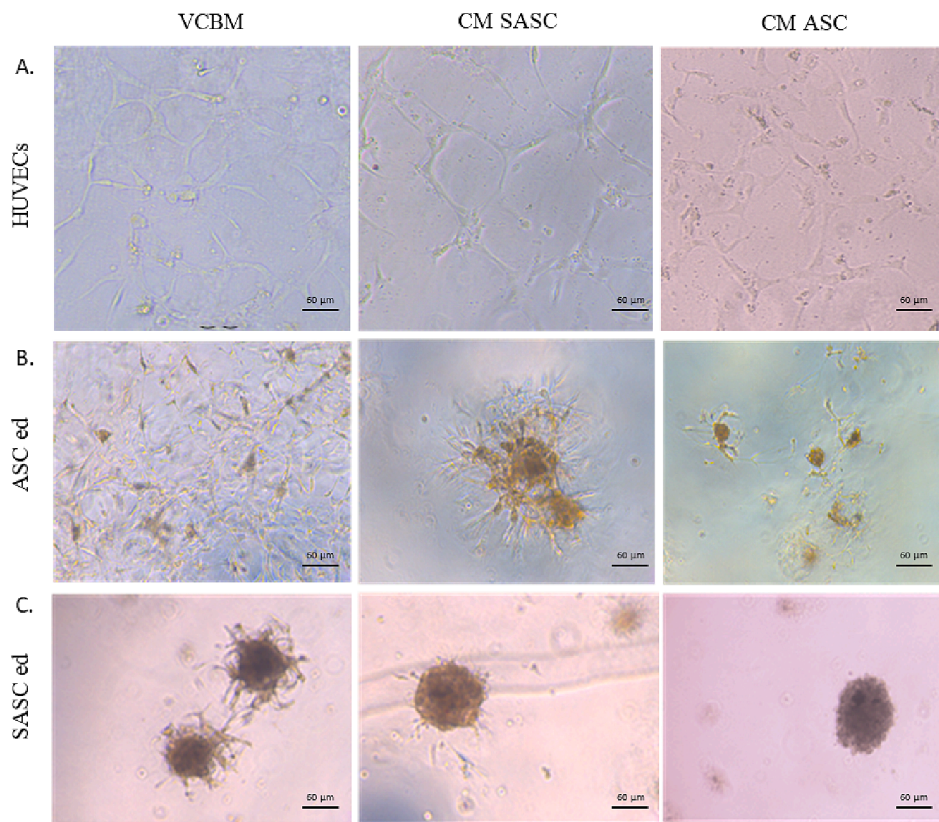
Fig. 3. In vitro assay of angiogenic networks formation on ECMatrix^TM. A. HUVECs in VCBM, CM SASCs and CM ASCs on ECMatrix^TM at 24 h. B. ASCs endothelially differentiated cells in VCBM, CM SASCs and CM ASCs on ECMatrix^TM at 7d. C. SASCs endothelially differentiated cells in VCBM, CM SASCs and CM ASCs on ECMatrix^TM at 7d.

cultured in their own medium for 28 days and their secretomes were added on HUVECs, ASCs and SASCs endothelially differentiated cells seeded on ECMatrix™. The same analysis was performed with ASC secretomes, as control. The results of the assay performed on HUVECs showed the beginning of the sprouting already after the first hour, leading to the development of a more evoluted angiogenic network at 24 h, but only in the condition of SASCs secretome addition and not of ASCs' one (Fig. 3A). The analysis of angiogenic networks formation through morphological evaluation of ASCs differentiated endothelial cells showed that any sprouting event was happening at 24 h (data not shown), whilst after 7 days of SASCs secretome treatment, detectable ramifications appeared (Fig. 3B). On the contrary, the addition of ASCs CM led to very few and thin ramifications at 7 days of culture (Fig. 3B). The same treatment on SASCs endothelially differentiated cells proved that already after 24 h (data not shown), CM SASCs stimulated the beginning of sprouting phenomena, but after 7 days the cells lost this condition (Fig. 3C).

In addition, we performed immunofluorescence analysis on SASCs and ASCs endothelially differentiated cells seeded on ECMatrixTM at 7d, showing positive cells to VEGF and CD31, two typical angiogenic markers (Fig. 4).

With the aim of investigate the effect of SASCs secretome on proliferation and migration of endothelial cells, wound healing assays respectively on HUVECs, ASCs and SASCs endothelially differentiated cells were performed. The end point was fixed at 4 h for HUVEC but the others cell cultures were analysed until 72 h. The fresh conditioned media (SCM and DMEM) were used as control to analyse if their effect was due to the paracrine factors secreted by the stem cells or by the fresh medium factors. A morphological analysis revealed that CM SASC had any effect on HUVECs proliferation, in comparison to CM ASCs that stimulated a greater proliferation and migration of HUVECs after 4 h in an *in vitro* assay (Fig. 5A).

In ASC endothelially differentiated cells, no effect was visible with conditioned media but an increased wound closure was observed in SCM and DMEM conditions (Fig. 5C). The treatment of SASC endothelially differentiated cells, instead, showed an higher proliferation and migration in CM SASCs condition at 72 h (Fig. 5E). These data were quantified by ImageJ analysis (Fig. 5B,5D,5F).

In addition, to investigate if endothelially pre-differentiated cells were able to migrate, we performed a transwell migration assay. We found that respectively 20% of HUVECs in the control condition, 13% in the CM SASCs and 7% in the CM ASCs migrated. 7% of pre-differentiated SASCs migrated only in the control condition whilst in CM ASCs and

SASCs both endothelially differentiated SASCs and ASCs didn't show a relevant migration (Fig. 6).

4. Discussion

Vascularization is an essential process for tissue and organ physiological functions, such as for bone and cartilage maintenance (Chiesa et al., 2020; Apelgren et al., 2021), as well as remodelling and healing of injuries. Vessels help to ensure the cell viability by supplying them with the nutrients they need to survive. In regenerative medicine field, several studies investigated the angiogenic properties of the traditional 2D ASCs for the generation of functional vascularized new tissues (Fischer et al., 2009). The capacity and role of 3D ASCs has not yet been investigated. Today, spheroids of adipose stem cells could represent a revolution in this field. In recent years, they have been extensively characterised both for their capacity to maintain stemness and for their ability to differentiate into adipocytes, chondrocytes and osteoblasts, making them suitable for the use in regeneration of bone and cartilage lesions. In particular, in an *in vivo* calvaria study with SASCs, we demonstrated that the paracrine production of specific factors has led to osteoblastic but also angiogenic regeneration. SASCs actively participated in neoangiogenesis process at the site of the lesion. Furthermore, we showed the expression of miRNAs (miR-126, miR-21, and miR-20a) and mRNAs (VEGF and HIF-1a) typically involved in angiogenesis in SASCs cultures (Di Stefano et al., 2021). From these observations, we first asked whether SASCs themselves are capable of differentiating into endothelial cells but, more importantly, what molecules they produced to stimulate vascular regeneration.

At first, we showed the capacity of SASCs to differentiate towards the endothelial lineage. Interestingly, SASCs grew up much more than HUVECs or 2D ASCs, showing a visible morphological change at 21 days of *in vitro* differentiation. Then, we confirmed the differentiation through mRNA analysis observing an increased expression of typical endothelial genes, such as VEGF-A and CD31. In addition, the hypoxia marker HIF1-α and VEGF receptor 2 (VEGFR2) gene expression were down-regulated. We hypothesized that HIF1-α lower expression could indicate that SASCs differentiated endothelial cells were not in a hypoxic condition. Moreover, several studies proved that VEGFR2 expression is down-regulated by MMP-2 and MMP-14 metalloproteases and that endothelial cells secrete high levels of MMP-2 until they create stable cell–cell contacts and tubular structures. Thus, we hypothesized that we found a VEGFR2 down-regulation probably because our differentiated cells were still at the beginning of their cell–cell contacts and tubular

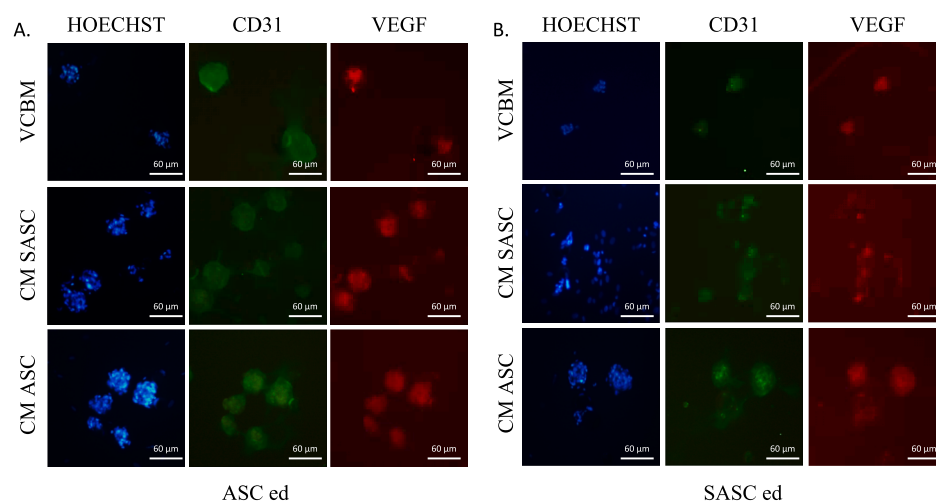**Fig. 4.** Analysis of angiogenic markers on ECMatrix™. Hoechst (blue), CD31 (green) and VEGF (red) expression on A. endothelially differentiated ASCs in VCBM, CM SASCs and CM ASCs condition and on B. endothelially differentiated SASCs in VCBM, CM SASCs and CM ASCs condition. (For interpretation of the references to colour in this figure legend, the reader is referred to the web version of this article.)
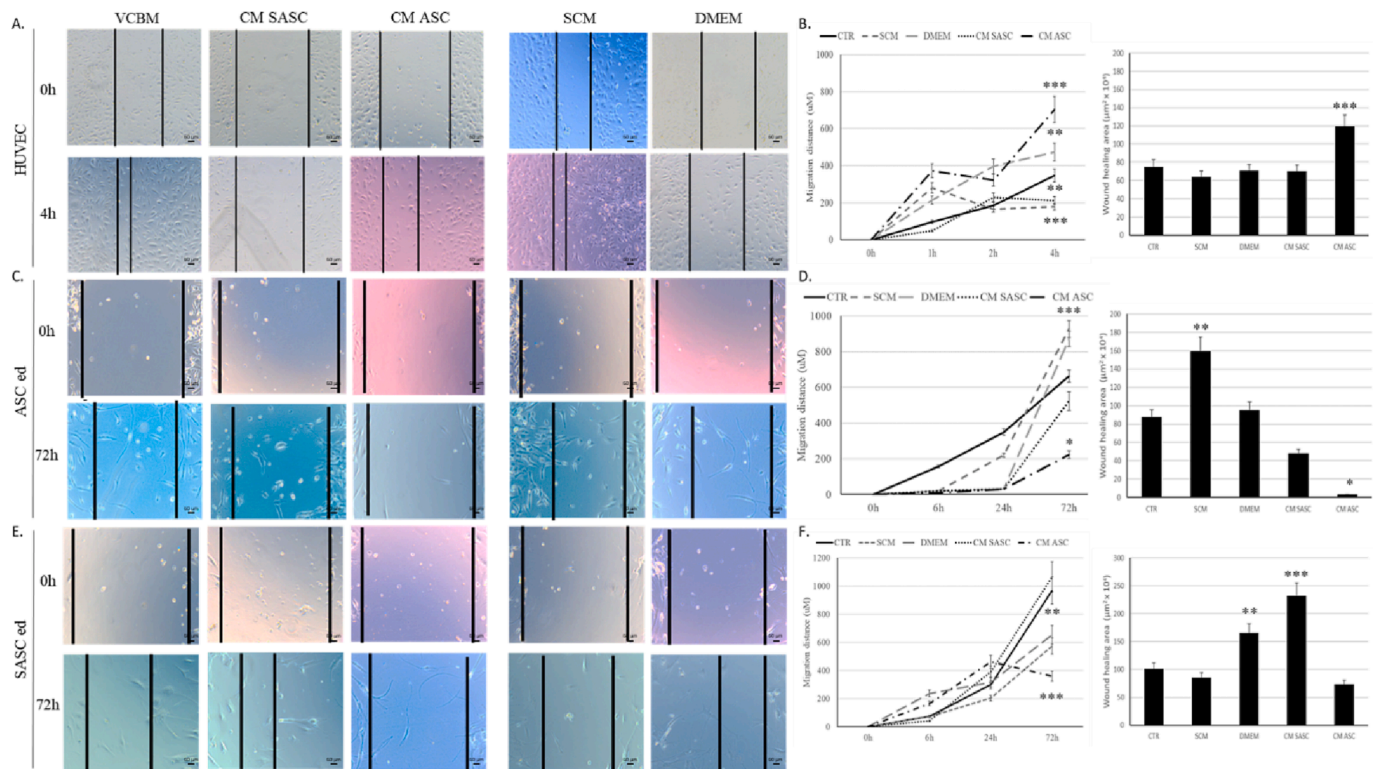
Fig. 5. Wound healing assay. A. observation of the conditioned media on HUVECs and SCM/DMEM as controls. B. Analysis of migration distance and determination of covered area at 4 h. C. Observation of the conditioned media on ASCs endothelially differentiated cells and SCM/DMEM as controls. D. Analysis of migration distance and determination of covered area at 72 h. E. Observation of the conditioned media on SASCs endothelially differentiated cells and SCM/DMEM as controls. F. Analysis of migration distance and determination of covered area at 72 h.
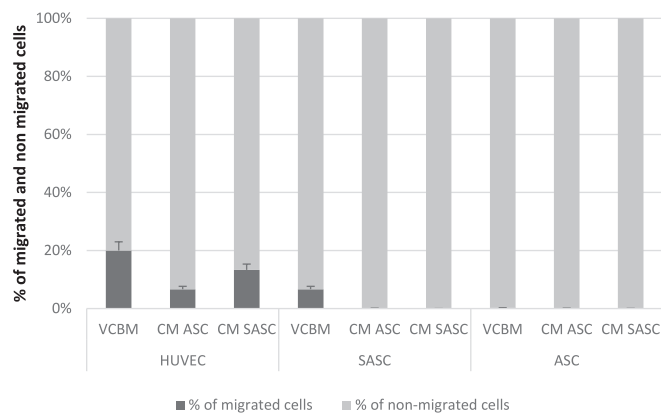

Fig. 6. Transwell migration assay. The percentage of migrated (dark grey) and non-migrated (light grey) cells after 24 h is shown.

structures formation (Rautiainen et al., 2021). VEGFR2 is not the main VEGF-A binding pathway in SASCs differentiated endothelial cells. VEGF-A ligand can bind also the less characterized VEGFR1 receptor (Weddell et al., 2018).

We also investigated the protein concentration of seven typical endothelial proteins, observing VEGF-A up-regulation and CD31 and VEGFR2 down-regulation. ICAM1, VCAM1, ANGPT1 and CD62E did not change. We hypothesized the activation of alternative post-transcriptional regulatory mechanisms that did not translate the high expression of CD31 mRNA into protein, while VEGFR2 maintains a constant trend of low gene and protein expression in both adipose cultures. These aspects find no correspondence in literature. In 2D ASCs, only a study investigated the mRNA or protein expression of VEGFR2

and CD31. In fact, Amerion et al. analysed VEGFR2 expression during the endothelial differentiation of rat ASCs, observing a constant up regulation of its mRNA for three weeks of differentiation and a lack of CD31 expression in EPCs compared to undifferentiated ASCs (Amerion et al., 2018). In addition, a study demonstrated how after 14 days of ASCs culturing in endothelial growth medium enriched with growth factors such as VEGF, hFGF-b (human basic fibroblast growth factor), EGF (epidermal growth factor) and IGF-1 (insulin like growth factor-1), ASCs expressed typical endothelial markers and presented an evident formation of angiogenic networks; ASCs plated onto Matrigel formed capillary-like structures after 24 h (Zhang et al., 2011). Similarly, pre-differentiated ASCs for 10 days with VEGF, FGF or VEGF/FGF media, showed the ability of forming tube structures during 12 h if plated on Matrigel but only in FGF and VEGF/FGF conditions (Khan et al., 2017). Moreover, co-cultures of ASCs and HUVECs respectively in a ratio 1:6 were able to organize themselves to form angiogenic networks, already after three hours (Parshyna et al., 2017). Based on these results, in order to better characterise the endothelial differentiation capacity of SASCs, we seeded cells on ECM Matrix™ showing that they formed angiogenic branches and networks already at 7 days, and that they were maintained up to 14 days.

A final important factor that we analysed in this study was the cell capacity to release factors in the culture medium. Thanks to the secreted factors, cells can exert a paracrine signalling on the other cells by conveying promoting or inhibiting messages. Many studies showed the importance of mesenchymal stem cell paracrine factors in promoting migration and proliferation of endothelial or progenitor endothelial cells (Suga et al., 2014; Kato et al., 2020; Gan et al., 2022) as well as the involvement of mesenchymal stem cell secreted factors in angiogenesis stimulation (Kuchroo et al., 2015; Maacha et al., 2020).

In this regard, we analysed the effects of SASCs released paracrine factors, defined also as secretome, on three endothelial cell lines,

through a wound healing assay. Our preliminary results showed that SASCs released factors increased the proliferation of SASCs endothelially differentiated cells, while ASCs secretome had an opposite effect, stimulating HUVECs and inhibiting ASCs endothelially differentiated cells. Data showed that this effect was probably due to the presence of stimulatory factors released by the cultured SASCs rather than by those already present in the fresh medium. Instead, the transwell migration assay showed migration ability of HUVEC treated in all media conditions and SASC endothelially differentiated cells in VCBM. ASC endothelially differentiated cells weren't able to migrate in all media conditions. In particular, the CM SASC seems to stimulate HUVECs to migrate more if compared to CM ASC, confirming a different effect of 2D and 3D cell released factors.

Further investigations on the possibility of recreate a vascularized tissue using adipose stem cell spheroids are desirable. The future perspectives will be directed to the generation of bio-mould biocompatible scaffolds where spheroids can be seeded for tissue regeneration.

CRediT authorship contribution statement

Anna Barbara Di Stefano: Conceptualization, Methodology, Validation, Formal analysis, Writing – original draft, Visualization. **Francesca Toia:** Writing – review & editing, Supervision, Funding acquisition. **Valentina Urrata:** Methodology, Validation, Investigation, Writing – original draft. **Marco Trapani:** Methodology, Investigation, Writing – original draft. **Luigi Montesano:** . **Emanuele Cammarata:** . **Francesco Moschella:** Writing – review & editing, Supervision, Funding acquisition. **Adriana Cordova:** Writing – review & editing, Supervision, Funding acquisition.

Declaration of Competing Interest

The authors declare that they have no known competing financial interests or personal relationships that could have appeared to influence the work reported in this paper.

Data availability

The authors are unable or have chosen not to specify which data has been used.

Acknowledgments

References

Amerion, M., Valojerdi, M.R., Abroun, S., Totonchi, M., 2018. Long term culture and differentiation of endothelial progenitor like cells from rat adipose derived stem cells. Cytotechnology 70, 397–413.

Apelgren, P., Amoroso, M., Säljö, K., Montelius, M., Lindahl, A., Stridh Orrhult, L., Gatenholm, P., Kölby, L., 2021. Vascularization of tissue engineered cartilage - Sequential in vivo MRI display functional blood circulation. Biomaterials 276, 121002.

Chiesa, I., De Maria, C., Lapomarda, A., Fortunato, G.M., Montemurro, F., Di Gesù, R., Tuan, R.S., Vozzi, G., Gottardi, R., 2020. Endothelial cells support osteogenesis in an in vitro vascularized bone model developed by 3D bioprinting. Biofabrication 12, 025013.

Chu, D.T., Phuong, T.N.T., Tien, N.L.B., Tran, D.K., Thanh, V.V., Quang, T.L., Truong, D. T., Pham, V.H., Ngoc, V.T.N., Chu-Dinh, T., Kushekhar, K., 2020. An update on the progress of isolation, culture, storage, and clinical application of human bone marrow mesenchymal stem/stromal cells. Int. J. Mol. Sci. 21.

Denu, R.A., Nemcek, S., Bloom, D.D., Goodrich, A.D., Kim, J., Mosher, D.F., Hematti, P., 2016. Fibroblasts and mesenchymal stromal/stem cells are phenotypically indistinguishable. Acta Haematol. 136, 85–97.

Dhami, L.D., Agarwal, M., 2006. Safe total corporal contouring with large-volume liposuction for the obese patient. Aesthetic Plast. Surg. 30, 574–588.

Di Stefano, A., Leto Barone, A., Giammona, A., Apuzzo, T., Moschella, P., Di Franco, S., Giunta, G., Carmisciano, M., Eleuteri, C., Todaro, M., Dieli, F., Cordova, A., Stassi, G.

and Moschella, F., 2015. Identification and Expansion of Adipose Stem Cells with Enhanced Bone Regeneration Properties. J Regen Med.

Di Stefano, A.B., Urrata, V., Trapani, M., Moschella, F., Cordova, A., Toia, F., 2022. Systematic review on spheroids from adipose-derived stem cells: Spontaneous or artefact state? J. Cell Physiol.

Di Stefano, A.B., Grisafi, F., Castiglia, M., Perez, A., Montesano, L., Gulino, A., Toia, F., Fanale, D., Russo, A., Moschella, F., Leto Barone, A.A., Cordova, A., 2018. Spheroids from adipose-derived stem cells exhibit an miRNA profile of highly undifferentiated cells. J. Cell. Physiol. 233, 8778–8789.

Di Stefano, A.B., Montesano, L., Belmonte, B., Gulino, A., Gagliardo, C., Florena, A.M., Bilello, G., Moschella, F., Cordova, A., Leto Barone, A.A., Toia, F., 2020. Human spheroids from adipose-derived stem cells induce calvarial bone production in a xenogeneic rabbit model. Ann. Plast. Surg.

Di Stefano, A.B., Montesano, L., Belmonte, B., Gulino, A., Gagliardo, C., Florena, A.M., Bilello, G., Moschella, F., Cordova, A., Leto Barone, A.A., Toia, F., 2021. Human spheroids from adipose-derived stem cells induce calvarial bone production in a xenogeneic rabbit model. Ann. Plast. Surg. 86, 714–720.

Fischer, L.J., McIlhenny, S., Tulenko, T., Golesorkhi, N., Zhang, P., Larson, R., Lombardi, J., Shapiro, I., DiMuzio, P.J., 2009. Endothelial differentiation of adipose-derived stem cells: effects of endothelial cell growth supplement and shear force. J. Surg. Res. 152, 157–166.

Gan, F., Liu, L., Zhou, Q., Huang, W., Huang, X., Zhao, X., 2022. Effects of adipose-derived stromal cells and endothelial progenitor cells on adipose transplant survival and angiogenesis. PLoS One 17, e0261498.

Gimble, J.M., Katz, A.J., Bunnell, B.A., 2007. Adipose-derived stem cells for regenerative medicine. Circ. Res. 100, 1249–1260.

Gorkun, A.A., Revokatova, D.P., Zurina, I.M., Nikishin, D.A., Bikmulina, P.Y., Timashev, P.S., Shpichka, A.I., Kosheleva, N.V., Kolokoltsova, T.D., Saburina, I.N., 2021. The Duo of Osteogenic and Angiogenic differentiation in ADSC-derived spheroids. Front. Cell Dev. Biol. 9, 572727.

Harasymiak-Krzyżanowska, I., Niedojadło, A., Karwat, J., Kotuła, L., Gil-Kulik, P., Sawiuk, M., Kocki, J., 2013. Adipose tissue-derived stem cells show considerable promise for regenerative medicine applications. Cell. Mol. Biol. Lett. 18, 479–493.

Housman, T.S., Lawrence, N., Mellen, B.G., George, M.N., Filippo, J.S., Cerveny, K.A., DeMarco, M., Feldman, S.R., Fleischer, A.B., 2002. The safety of liposuction: results of a national survey. Dermatol. Surg. 28, 971–978.

Katagiri, T., Kondo, K., Shibata, R., Hayashida, R., Shintani, S., Yamaguchi, S., Shimizu, Y., Unno, K., Kikuchi, R., Kodama, A., Takanari, K., Kamei, Y., Komori, K., Murohara, T., 2020. Therapeutic angiogenesis using autologous adipose-derived regenerative cells in patients with critical limb ischaemia in Japan: a clinical pilot study. Sci. Rep. 10, 16045.

Kato, M., Tsunekawa, S., Nakamura, N., Miura-Yura, E., Yamada, Y., Hayashi, Y., Nakai-Shimoda, H., Asano, S., Hayami, T., Motegi, M., Asano-Hayami, E., Sasajima, S., Morishita, Y., Himeno, T., Kondo, M., Kato, Y., Izumoto-Akita, T., Yamamoto, A., Naruse, K., Nakamura, J. and Kamiya, H., 2020. Secreted Factors from Stem Cells of Human Exfoliated Deciduous Teeth Directly Activate Endothelial Cells to Promote All Processes of Angiogenesis. Cells 9.

Khan, S., Villalobos, M.A., Choron, R.L., Chang, S., Brown, S.A., Carpenter, J.P., Tulenko, T.N., Zhang, P., 2017. Fibroblast growth factor and vascular endothelial growth factor play a critical role in endotheliogenesis from human adipose-derived stem cells. J. Vasc. Surg. 65, 1483–1492.

Kuca-Warnawin, E., Kurowska, W., Plebańczyk, M., Wajda, A., Kornatka, A., Burakowski, T., Janicka, I., Syrówka, P., Skalska, U., 2023. Basic properties of adipose-derived mesenchymal stem cells of rheumatoid arthritis and osteoarthritis patients. Pharmaceutics 15.

Kuchroo, P., Dave, V., Vijayan, A., Viswanathan, C., Ghosh, D., 2015. Paracrine factors secreted by umbilical cord-derived mesenchymal stem cells induce angiogenesis in vitro by a VEGF-independent pathway. Stem Cells Dev. 24, 437–450.

Lee, H.B., Park, S.W., Kim, I.K., Kim, J.H., Kim, D.Y., Hwang, K.C., 2020. Adipose tissue derived stromal vascular fraction as an adjuvant therapy in stroke rehabilitation: Case reports. Medicine (Baltimore) 99, e21846.

Ma, T., Sun, J., Zhao, Z., Lei, W., Chen, Y., Wang, X., Yang, J., Shen, Z., 2017. A brief review: adipose-derived stem cells and their therapeutic potential in cardiovascular diseases. Stem Cell Res Ther 8, 124.

Maacha, S., Sidahmed, H., Jacob, S., Gentilcore, G., Calzone, R., Grivel, J.C., Cugno, C., 2020. Paracrine mechanisms of mesenchymal stromal cells in angiogenesis. Stem Cells Int. 2020, 4356359.

Mahmoudifar, N., Doran, P.M., 2015. Mesenchymal stem cells derived from human adipose tissue. Methods Mol. Biol. 1340, 53–64.

Makhoul, G., Chiu, R.C., Cecere, R., 2013. Placental mesenchymal stem cells: a unique source for cellular cardiomyoplasty. Ann. Thorac. Surg. 95, 1827–1833.

Parshyna, I., Lehmann, S., Grahl, K., Pahlke, C., Frenzel, A., Weidlich, H., Morawietz, H., 2017. Impact of omega-3 fatty acids on expression of angiogenic cytokines and angiogenesis by adipose-derived stem cells. Atheroscler. Suppl. 30, 303–310.

Pittenger, M.F., Mackay, A.M., Beck, S.C., Jaiswal, R.K., Douglas, R., Mosca, J.D., Moorman, M.A., Simonetti, D.W., Craig, S., Marshak, D.R., 1999. Multilineage potential of adult human mesenchymal stem cells. Science 284, 143–147.

Poltavtseva, R.A., Nikonova, Y.A., Selezneva, I.I., Yaroslavtseva, A.K., Stepanenko, V.N., Esipov, R.S., Pavlovich, S.V., Klimantsev, I.V., Tyutyunnik, N.V., Grebennik, T.K., Nikolaeva, A.V., Sukhikh, G.T., 2014. Mesenchymal stem cells from human dental pulp: isolation, characteristics, and potencies of targeted differentiation. Bull. Exp. Biol. Med. 158, 164–169.

Rajendran, R., Gopal, S., Masood, H., Vivek, P. and Deb, K., 2013. Regenerative Potential of Dental Pulp Mesenchymal Stem Cells Harvested from High Caries Patient's Teeth Journal of Stem Cells.

Rautiainen, S., Laaksonen, T., Koivuniemi, R., 2021. Angiogenic effects and crosstalk of adipose-derived mesenchymal stem/stromal cells and their extracellular vesicles with endothelial cells. Int. J. Mol. Sci. 22.

Sahraei, S.S., Davoodi Asl, F., Kalhor, N., Sheykhhasan, M., Fazaeli, H., Moud, S.S., Sheikholeslami, A., 2022. A comparative study of gene expression in menstrual blood-derived stromal cells between endometriosis and healthy women. Biomed Res. Int. 2022, 7053521.

Shang, T., Li, S., Zhang, Y., Lu, L., Cui, L., Guo, F.F., 2019. Hypoxia promotes differentiation of adipose-derived stem cells into endothelial cells through demethylation of ephrinB2. Stem Cell Res Ther 10, 133.

Si, Z., Wang, X., Sun, C., Kang, Y., Xu, J., Hui, Y., 2019. Adipose-derived stem cells: Sources, potency, and implications for regenerative therapies. Biomed. Pharmacother. 114, 108765.

Suga, H., Glotzbach, J.P., Sorkin, M., Longaker, M.T., Gurtner, G.C., 2014. Paracrine mechanism of angiogenesis in adipose-derived stem cell transplantation. Ann. Plast. Surg. 72, 234–241.

Weddell, J.C., Chen, S., Imoukhuede, P.I., 2018. VEGFR1 promotes cell migration and proliferation through PLCγ and PI3K pathways. NPJ Syst. Biol. Appl. 4, 1.

Witkowska-Zimny, M., Walenko, K., 2011. Stem cells from adipose tissue. Cell. Mol. Biol. Lett. 16, 236–257.

Yoon, D.S., Choi, Y., Jang, Y., Lee, M., Choi, W.J., Kim, S.H., Lee, J.W., 2014. SIRT1 directly regulates SOX2 to maintain self-renewal and multipotency in bone marrow-derived mesenchymal stem cells. Stem Cells 32, 3219–3231.

Zhang, P., Moudgill, N., Hager, E., Tarola, N., Dimatteo, C., McIlhenny, S., Tulenko, T., DiMuzio, P.J., 2011. Endothelial differentiation of adipose-derived stem cells from elderly patients with cardiovascular disease. Stem Cells Dev. 20, 977–988.
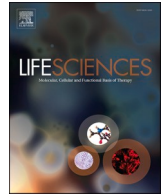
Review article

Analysis of MSCs' secretome and EVs cargo: Evaluation of functions and applications

Valentina Urrata [a], Marco Trapani [a,b], Mara Franza [b,c], Francesco Moschella [a], Anna Barbara Di Stefano [a,*,1], Francesca Toia [a,b,c,1]

[a] BIOPLAST-Laboratory of BIOlogy and Regenerative Medicine-PLASTic Surgery, Plastic and Reconstructive Surgery, Department of Surgical, Oncological and Oral Sciences, University of Palermo, 90127 Palermo, Italy
[b] Plastic and Reconstructive Surgery, Department of Oncology, Azienda Ospedaliera Universitaria Policlinico "Paolo Giaccone", 90127 Palermo, Italy
[c] Plastic and Reconstructive Surgery, Department of Surgical, Oncological and Oral Sciences, University of Palermo, 90127 Palermo, Italy

A B S T R A C T

Mesenchymal stem cells (MSCs) can exert different functions and can be used in several medical fields. In the last years, MSC properties have been attributed to their secreted factors such as soluble proteins, cytokines and growth factors. Moreover, a key role is played by the extracellular vesicles (EVs) which lead a heterogeneous *cargo* of proteins, lipids and small and long non-coding RNAs that interfere with the pathways of the recipient cells. Due to the safeness and easiness in obtaining the secretome, its use is becoming a turning point for the application in physiological and pathological fields. This review summarizes the most recent studies on the use of MSCs secretome, focusing on some physiological (angiogenesis and osteogenesis) and pathological (cancer, cardiovascular and autoimmune diseases) applications. The secreted analyzed factors are listed in a table. In addition, the different characteristics of the fetal MSCs derived secretome and the differences in the secretome composition of three-dimensionally (3D) cultured cells are discussed. As very innovative aspects, recent studies on some applications of engineered vesicles, embedded or not in three-dimensional structures, are treated and the influence of some epigenetic modifications on cells and EVs is investigated.

1. Introduction

Mesenchymal stem cells (MSCs) are multipotent and undifferentiated cells with the ability to differentiate into several mesenchymal lineages such as osteoblasts, chondrocytes, adipocytes, myocytes [1,2] and also neuron-like [3]. Although it is known that MSCs are responsible of several cell functions, such as pro-angiogenesis [4], anti-apoptosis [5], neuro-protection and regulation [6], anti-inflammation [7], immunomodulation [8] and others, several studies showed that these functions are mainly exerted by MSCs secreted paracrine factors [9–13].

In fact, cells need to communicate between each other and to exchange information not only through a direct cell-cell interaction but also through an indirect way as the endocrine, autocrine and paracrine signalling [14]. In particular, paracrine signalling can occur through a set of soluble factors and/or extracellular vesicles (EVs) secreted by the cells in the culture medium, called 'conditioned medium'. The set of secreted factors with EVs is called 'secretome'.

Amongst the main components of the soluble fraction, there are proteins, cytokines, chemokines and growth factors [15], whilst EVs are distinguished into exosomes, microvesicles (MVs) and apoptotic bodies, according to their size and biogenesis. About that, exosomes are 30–150 nm in size and derive by multivesicular bodies generated by the early endosomes, whilst microvesicles are 100–1000 nm in size and derive by plasma membrane shedding. Both of them are enriched in small and long non-coding RNAs, mRNAs, lipid and proteins which exert specific functions in the recipient cells [16,17]. Finally, apoptotic bodies are 1–3 μm in size and derive from apoptotic cells that disassemble themselves and close their content into vesicles, protecting the neighbouring cells. They contain cytosolic fragments and proteins as well as nuclear fragments, such as DNA and histones, or even organelles [18,19].

It has been proved that the secretome has a higher safety profile if compared to cell engrafting due to its reduced possibility of neoplastic transformation [20] and a better ease of storage with the use of natural and non-toxic agents such as the trehalose, a natural disaccharide found

---

in many foods [21]. Moreover, in the last few years, the analysis of factors contained in the secretome and/or extracellular vesicles made possible for researchers to engineer EVs for a controlled drug delivery [22–25] or also to defeat viruses [26] but also to evaluate the risks and/or benefits of exposure to certain substances (*e.g.*, chemical agents, environmental pollutants, *etc.*) [27,28].

This review aims to summarize current literature on secretome derived from different MSCs with the purpose of creating a compendium of the most recently discovered proteins and non-coding RNAs as components of the soluble fraction or EVs.

Starting from these goals, the applications of the secretome from MSCs from different sources, analyzed in its totality or in its specific components, have been characterized in a broad range of physiological and pathological conditions both in *in vitro* and *in vivo* studies.

2. Applications and factors of secretome from MSCs in physiological fields

2.1. Angiogenesis

Tissue and organ regeneration is nowadays a field of interest for many worldwide researchers. Although cell applications, together or not with a scaffold, were interestingly investigated [29–33], recently the attention was focused on the cells released paracrine factors and their regenerative properties. For example, studies concerning the secretome characterization from bone marrow MSCs (BM-MSCs) showed that the highest percentage of secreted proteins were involved in cell growth, maintenance and communication. In detail, extracellular matrix laminins and several collagen isoforms were identified together with factors such as IGFBP-3, -4, -5, -6, TGF-β1, TGF-β2 and VEGFC (see Table 1). Moreover, a rich presence of angiotensin (AGT), a protein involved in maintaining the blood pressure, and serpinE1, a fibrinolysis inhibitor, were found [34]. Instead, with the aim of analyzing the micro-RNA (miRNA) and transfer-RNA (tRNA) content of exosomes from BM-MSCs and adipose-derived stem cells (ASCs), Baglio et al. found that miR-486-5p, miR-10a-5p, miR-10b-5p, miR-191-5p, miR-222-3p were amongst the most expressed miRNAs in ASC exosomes, from a higher to a lower value respectively, whilst miR-143-3p, miR-10b-5p, miR-486-5p, miR-22-3p, miR-21-5p were amongst the most expressed in BM-MSC exosomes. Investigations on the most expressed tRNAs in ASC and BM-MSC exosomes showed the over-expression of tRNA Gly in ASC exosomes and tRNA Glu in BM-MSC ones [35].

The authors did not describe the roles of these factors, but in literature their involvement in the angiogenic processes has been investigated in several oncological (miR-10a-5p, miR-143-3p) and angiogenic (miR-486-5p, miR-21-5p) studies. In physiological content: miR-486-5p promoted the angiogenesis in human microvascular endothelial cells (HMECs), leading to an increased length of vessels and new branches formation [36]; similarly, miR-21-5p stimulated the angiogenic process, increasing the number of blood vessels and sprouting events, in chicken embryos. It acted targeting Spry1 factor and thus leading to MMP-13 and VEGF over-expression and ERK/MAPK signalling pathway activation [50]. On the contrary, tRNA Gly did not stimulate the angiogenic processes on HUVECs plated on a Matrigel [51].

MiR-31 was also investigated in the secretome for its ability in inducing neovessels formation. Zhu et al. investigated the pathway of miR-31, an over-expressed miRNA in ASC derived exosomes, in *in vivo* experiments. miR-31 was considered as a pro-angiogenic factor due to its pathway: miR-31/FIH1 (factor inhibiting hypoxia inducible factor-1)/HIF-1α.

In detail, FIH1 was targeted by miR-31 and therefore could no longer inhibit HIF-1α. The *in vivo* injections of ASC derived exosomes in mice myocardial infarction models proved the improving of cardiac function and the neo-angiogenesis induction [37].

In addition, MVs isolated from EDM (endothelial differentiation medium)-preconditioned ASCs were rich in miR-31 and able to induce

Table 1
Summary of the secreted factors in physiological fields.

Authors	Soluble fraction	EVs Fraction
● Angiogenesis		
[34]	BM-MSCs: IGFBP3, 4, 5, 6, TGF-β1, TGF-β2, VEGFC, COL6A2, COL4A2, COL6A1, COL10A1, COL5A2, COL15A1, COL8A1, COL11A1, COL1A1, COL3A1, COL5A1, COL1A2, COL5A3, COL4A1, LAMA2, LAMA4, LAMB, AGT, serpinE1.	
[35]		ASCs exosomes: miR-486-5p, miR-10a-5p, miR-10b-5p, miR-191-5p, miR-222-3p; tRNA Gly over-expressed. BM-MSCs exosomes: miR-143-3p, miR-10b-5p, miR-486-5p, miR-22-3p, miR-21-5p; tRNA Glu over-expressed.
[36]		ASCs EVs: miR-486-5p
[37]		ASC exosomes: miR-31
[38]		ASC microvesicles: miR-378, miR-31, miR-320, miR-130, miR-26, let-7f
[39]		Exosomes from the vertebral body MSCs: miR-18b-5p, miR-654-5p, miR-202-3p, miR-200a-5p, miR-367-3p, miR-423-3p, miR-122-5p, miR-302a-5p, miR-127-5p, miR-340-5p, miR-541-3p, miR-935, miR-135b-5p, miR-139-3p, miR-29c-5p, miR-582-5p, miR-491-5p, miR-590-3p, miR-31-5p, miR-32-5p
[40]		hUC-MSCs: VEGF, SDF-1, IGF-1, Ang-1, HGF, IGF-1, PGE2, TGF-b1, VCAM-1
[41]	Replicative senescent ASCs: MMP-8, IL-1b, Ang-1, PF4, uPA, DPPIV, Activin A, GM-CSF, IL-8, MCP-1, MCP-3, IL-4, IP-10, GRO, RANTES, IFN-a2, FGF-2, MDC, MCP-1, IL-8, IL-6 Replicative young ASCs: PAI-1.	
[42]		EVs from young MSCs: miR-27a, miR-27b, miR-106a, miR-335-5p, miR-199-5p, miR-294, miR-872-3p, miR-let-7 g, miR-17 EVs from aged/senescent MSCs: miR-17, miR-335-5p, miR-34, miR-140, miR-146a, miR-195, miR-183-5p, miR-452, miR-141-3p
● Osteogenesis		
[43]		BM-MSCs: miR-196a, miR-122-5p, miR-27a, miR-206, MALAT1
[44]		BM-MSCs: miR27a, miR206, miR196a
[45]		MSC exosomes: hsa-let-7a-5p, hsa-miR-630, hsa-miR-199a-3p+hsa-miR-199b-3p, hsa-miR-100-5p, hsa-miR-145-5p, hsa-miR-518b, hsa-miR-23a-3p, hsa-miR-4443, hsa-let-7i-5p, hsa-miR-4286, hsa-miR-1183, hsa-miR-495, hsa-miR-21-5p, hsa-miR-222-3p, hsa-miR-302d-3p, hsa-miR-378e, hsa-miR-29b-3p, hsa-miR-4532, hsa-miR-4516, hsa-miR-4454, hsa-miR-29a-3p, hsa-miR-187-3p, hsa-miR-125b-5p, hsa-miR-720, hsa-let-7g-5p, hsa-miR-4488, hsa-miR-598, hsa-miR-548al, hsa-miR-16-5p
[46]	BM-MSCs with HOP (High Osteogenic Potential): SMOC1,	

Table 1 (*continued*)

Authors	Soluble fraction	EVs Fraction
	RPS17, RPS19, RPS20, RPS8, RPS24, RPS25, RPS3, RPS11, RPS13, RPS2, LDHAL6A, ALDOC, HMG1L10, ANG, DCD, PRPH, TPM3, CAPZB, TOR1B, RPL18, RPS14, TTLL3, VTN, TPI1, GLIPR2, HELZ, CTGF,PGAM4, THBS2, LOC387867, PRDX2, ZNF677, RNASE4, SEMA7A, KRT24, CHI3L1, ARPC4, FSCN1, RPL10A, EEF2, MMP1, PSMB3, HIST2H2BE, MFAP2, ARPC2, PSMA1, RPL5, GLO1, HAPLN1, STC1, PDIA6, EFEMP1, HNRNPA1, RPL8, RALB, TGFB1, ARPC1B, TBCA, PXDN, TIMP3, POSTN	
[47]	MSCs: IGF-1, VEGF	
[48]	PMSCs (periosteum-derived MSCs): CSF1, COL1A2M ACTN4, CHI3L1, FBN2, PRDX1, COL12A1, FBN1, ANXA2, LRP1, CTSK, CHI3L1, MMP2, SERPINE1, CALR, THBS1, SERPING1, DPP4, COL4A1, COL3A1, NRP1, ANXA1, KRT1, HSPG2, GPNMB, CST3, FBN1, SERPINE2, LRP1, COL3A1, COL4A1, S100A6, CALR, DPP4, PTX3, SERPINB1, SERPINB2, SERPINB6, CALR, ANXA1, ANXA4, PSMA6, SERPINE1, A2M, ANXA2, S100A11, GNS, LGALS3BP, PDIA3, NMLRC3, PRDX1, FTL, FTH1, CD109, KRT1, CTSS, CTSD, PSAP, PPIA, C1R, LAMP1, CHI3L1, PSMA1, ANXA5, C4A, LGALS3	
[49]	preA (prelamin A)-hMSCs-CM: FN1, TGFBI, IGFBP7 and PAI-1	

cell migration and tube formation if compared to MVs from canonically *in vitro* cultured ASCs [38] (see Table 1). In particular, miR-31-5p was amongst the 20 over-expressed miRNAs in the exosomes from the vertebral body MSCs (see Table 1). It was negatively related to apoptosis and calcification in fact, agomiR-31-5p transfection in MSC-exosomes, caused a significant apoptosis and calcification inhibition of the oxidative-stressed endplate chondrocytes (EPCs) in *in vitro* experiments.

These effects were reverted when exosomes were transfected with antagomir-31-5p. The authors found that miR-31-5p acted through the down-regulation of ATF6, CHOP, XBP1, and GRP78, all factors involved in the endoplasmic reticulum (ER) - oxidative stress pathways. They confirmed the results through the sub-endplate injection of MSC-exosomes in the tail of intervertebral disc degeneration (IVDD) rat models where they observed the decrease of IVDD [39].

The secretome by human umbilical cord blood (hUCB) also promoted neoangiogenesis; in fact, a study demonstrated that at different doses (from 2 % to 20 %) and in combination with atorvastatin (a statin), it could enhance endothelial progenitor cells (EPCs) proliferation and migration. In particular, the enhanced EPCs migration and proliferation was obtained after the treatment with hUCB-MSCs secretome (20 %) plus atorvastatin. The EPCs proliferation stimulating factors in the hUCB-MSCs secretome were VEGF, SDF-1 and IGF-1, whilst that stimulating angiogenesis were Ang-1, HGF, IGF-1, PGE2, TGF-β1, VCAM-1 and VEGF [40].

Moreover, it is easy to hypothesize that a young replicative cell could express some different factors if compared with an older one. Ratushnyy et al. analyzed the secretome from replicative senescent ASCs compared to young replicative ones, revealing an increased release of angiogenic factors but a decreased potential in inducing new vessels formation of

replicative senescent cells. Angiogenesis related proteins as MMP-8, IL-1b, Ang-1, PF4, uPA, DPPIV, Activin A, GM-CSF, IL-8, MCP-1 and cytokines as MCP-3, IL-4, IP-10, GRO, RANTES, IFN-a2, FGF-2, MDC, MCP-1, IL-8, IL-6 were released by senescent ASCs, whilst PAI-1 by younger ones [41].

Boulestreau et al. also summarized the MSC-EVs content comparing EVs by cells from young and aged subjects. They identified an amount of miRNAs such as miR-183-5p, miR-141-3p, miR-195, miR-452, miR-17, miR-140, miR-335-5p, miR-34 and miR-146a in EVs from senescent MSCs and an amount of miRNAs such as, let-7g, miR-27a, miR-27b, miR-199-5p, miR-335-5p, miR-106a, miR-294, miR-872-3p and miR-17 in EVs from young MSCs [42].

Amongst these, miR-146a showed a role in promoting HUVECs angiogenesis through FGFBP1/FG2 up-regulation, mediated by miRNA direct targeting of CREB3L1 [52] or TGF-β1 mRNA [53]; Similarly, miR-27a/b induced HUVECs angiogenesis and sprouting phenomena in *in vitro* assays and new vessels formation in *in vivo* Zebrafish model, indicating it was a pro-angiogenic miRNA. Moreover, *in vitro* assays proved that SEMA6A, an anti-angiogenic and pro-repulsive factor for cell to cell interactions, was a putative miR-27a/b target. The identification of angiogenesis-related miRNAs, as well as their targets, could be important to disrupt the angiogenic phenomena for therapeutic purposes [54].

2.2. Osteogenesis

Bone regeneration is another important field where the use of the secretome can find several applications. In fact, in extended fracture or bone removal conditions, it could be important to stimulate osteogenesis, together with angiogenesis, for the induction of a regenerated vascularized bone. Several studies characterized BM-MSC exosomes as able in inducing osteogenesis. The exosomes stimulated the expression of several mRNAs such as OPN, OCN and ALP as osteogenesis promoting factors and COL1, ANG1, ANG2, VEGF as angiogenesis inducing factors [55]. BM-MSC EVs were also enriched with microRNAs as miR-196a, miR-122-5p, miR-27a, miR-206 and lncRNA MALAT1, all osteogenesis involved factors [43]. Investigations on the role of these factors found that miR-196a promoted hASCs osteogenic differentiation through HOXC8 transcription factor targeting [56] and if inserted in a hydrogel stimulated the bone repair in calvarial rat models [44]. LncRNA MALAT1 promoted osteogenic differentiation by sponging miR-129-5p [57]. On the contrary, miR-206 suppressed BM-MSCs osteogenic differentiation directly targeting glutaminase mRNA, thus inducing the negative regulation of glutamine metabolism that, physiologically, has a stimulatory role in the induction of osteogenic differentiation [58].

The role of BM-MSC derived exosomes was also investigated in *in vivo* experiments using CD9$^{-/-}$ mice with a femur fracture. The cells of this strain of mice produced low levels of exosomes and their injection was responsible for the enhancement of endochondral ossification of wounded mice. The exosomes expressed thirty up-regulated miRNAs as hsa-let-7a-5p, hsa-miR-630, hsa-miR-199a-3p, hsa-miR-199b-3p, hsa-miR-100-5p and others (see Table 1) [45].

BM-MSCs with high and low osteogenic potential (HOP and LOP respectively) secreted different factors after treatment with the osteogenic medium. BM-MSCs with HOP secreted 64 proteins involved in intracellular and extracellular functions (see Table 1) and, amongst them, the authors proved the critical role of SMOC1. SMOC1 was up-regulated in response to the osteogenic medium and was involved in the positive regulation of osteoblastic differentiation through the induction of the expression of typical osteoblastic genes [46]. As further confirmation of the MSC-conditioned medium (CM) ability in inducing bone regeneration, Osugi et al. proved that MSC-CM contained several chemokines and cytokines, such as IGF-1 and VEGF, in a high concentration and many others in a lower concentration in *in vitro* and *in vivo* studies. All of them contributed to trigger the bone regeneration processes through the endogenous stem cells stimulation [47]. In the regenerative context, it is also important the research of factors able to

induce a complete regeneration not only in the angiogenic field but also in a broad range of processes such as neurogenesis, immune system stimulation, *etc*.

Rabbit periosteum MSCs derived secretome contained several factors involved in osteogenic, angiogenic, neurogenic and immune-response processes (see Table 1) [48].

Focusing on a model of human aging cell phenotype, factors secreted by human MSCs (hMSCs) accumulating prelamin-A (preA-hMSCs), the immature form of lamin-A, were investigated. The authors found that amongst the proteins secreted in the preA-hMSCs conditioned medium, IGFBP-7, TGFBI, PAI-1 and FN1 were up-regulated. In particular, they demonstrated the crucial role of IGFBP-7 in maintaining the hMSCs viability during the early osteogenic differentiation. Moreover, the preA-hMSCs-CM induced the up-regulation of Runx2 and ALP, thus having a pro-osteogenic effect exerted through a paracrine signalling [49].

3. Applications and factors of secretome from MSCs in pathological fields

3.1. Cancer

Cancer diseases are nowadays amongst the most diffused and lethal diseases in the world. Moreover, several studies predicted an increase in the number of affected people by 2040 [59,60]; thus, it can be important to identify new tumor markers as well as to characterize cancer cells secretome to provide a tool to target specific cancer pathways. In this regard, several studies analyzed the secretome of cancer cells to find some specific factors that could be considered as biomarkers of disease or could actively partecipate to cancer disease. For the first instance, some proteins composing the secretome of pancreatic cancer cells were individuated as putative biomarkers due to their involvement in tumor proliferation, migration and apoptosis inhibition as erb-B2 Receptor Tyrosine Kinase 2 (ERBB2), extracellular regulated kinase (ERK), protein kinase B (AKT) and epidermal growth factor (EGF), [61]. Similarly, factors as nucleolin, PTMA, biotinidase, clusterin and enolase1 were firstly identified in the secretome of two thyroid cancer cell lines, TPC-1 and CAL62, and secondly in the thyroid cancer patient serum making them as potential biomarkers to detect a patient with thyroid cancer [62]. In the second instance, negatively involved factors in tumor development were identified. For example, in the secretome of human breast cancer, an high amount of CD44 antigen was found. It is a soluble factor creating a pro-inflammatory microenvironment, favorable to tumor growth and able to trigger the IL1β pro-inflammatory pathway led by macrophages. So the CD44 antigen targeting could be a possible valid strategy to disrupt a way of communication between tumor and immune system [63]. Cervical cancer cells secretome showed the expression of 67 differentially expressed proteins if compared to normal cells. Amongst them, the usually secreted protein βig-h3 (transforming growth factor beta-induced protein), a growth factor involved in the cell-matrix interactions, and the unusually secreted protein PRDX2 (peroxiredoxin-2), an antioxidant enzyme involved in regulating redox reactions, were found. They were selected for further studies due to their altered expression in the secretome of other cancer cells, opening to the discovery of new putative tumor targets [64].

Several studies analyzed the composition and the effects of the secretome from mesenchymal stem cells (HUCPVCs, DPMSCs, WJMSCs) on the treatment of different cancer cells. For example, the secretome from human umbilical cord perivascular cells (HUCPVCs) stimulated cancer cell viability, proliferation and migration of glioblciastoma cells and promoted an increase in glioblciastoma vessels density in the chicken chorioallantoic membrane. A more detailed analysis revealed the presence of 699 proteins such as NRP2, SPOCK1, SEMA7A, ADAM10 (see Table 2), involved in several cancer pathways [65]. The secretome from dental pulp mesenchymal stem cell (DPMSCs) increased the oral cancer cells (AW123516) proliferation if tested at a low concentration (20 %), whilst attenuated cancer progression if tested at an high concentration

Table 2
Summary of the secreted factors in pathological fields.

Field	Authors	Soluble fraction	EVs fraction
• Cancer	[65]	HUCPVCs (human umbilical cord perivascular cells): NRP2, SPOCK1, SEMA7A, ADAM10, TPT1, PDGFC, SERPINE1, IL6, POSTN, CCL2, ACTN4, TGFBI, APRC5.	
	[66]	DPMSC-S (dental pulp mesenchymal stem cell secretome): VEGF, Ang-2, TGF-a, SCF, PDGF-BB, HCF, bFGF, EPO, CXCL8, TNF-a, IL-4, TGF-β1, IL-10, IL-2, CXCL10, MCP-1, IL-17A, IL-6, IL-12p70	
• Cardiovascular diseases	[67]		MSCs: miR-210
	[68]		MSCs: miR-29a-3p
	[69]		MSCs: miR-4732-3p miR-200b3p
	[70]		MSCs: miR-200b-3p

(100 %). This secretome was enriched in growth factors (VEGF, Ang-2, TGF-a, SCF, PDGF-BB, HCF, bFGF, EPO), proinflammatory (CXCL8 and TNF-a) and anti-inflammatory cytokines (IL-4, TGF-β1 and IL-10) (see Table 2) [66].

In addition, the effect of Wharton's Jelly (WJ) MSCs secretome on A549 lung cancer cells was investigated. In particular, WJ-MSCs treated or not with IFNγ, an inflammatory cytokine, produced a secretome which induced neither an increased cell proliferation nor a pro-apoptotic effect and doxorubicin resistance [71]. Similarly, the secretome from cultured human neonatal MSCs combined with Doxorubicin did not influence neither positively nor negatively the cytotoxic effects of the drug on the human breast cancer cells MDA-MB-231 [72] whilst the combination of secretome from hADMSCs (higher doses) and Paclitaxel (lower doses) was able to kill triple negative breast cancer cells (TNBCs) on a paclitaxel-resistant population [73]. These results opened a new perspective for a safe potential cancer or cancer-associated diseases treatment.

Due to the spreading of resistance phenomena against conventional therapies and thanks to EVs ability in vehiculating information, the most recent studies focused on generating engineered EVs, functionalizing them to reduce tumor growth and stimulate cancer cell apoptosis. In addition, they opened the way on new strategies to inhibit the drug resistance phenomena in cancer cells. For example, in a study on colon cancer cells, exosomes were purified and uploaded with a co-combination of factors: an anticancer drug (5-Fluorouracil (5-FU)) and miR-21 inhibitor (miR21i). The inhibition of miR21 caused the cell-cycle arrest and increased apoptosis. In an *in vivo* colon cancer mouse model with 5-FU resistant cells, the engineered exosomes were able to revert the drug resistance and tumor growth (Fig. 1) [24].

Similarly, exosomes uploaded with the antisense lncRNA PGM5-AS1 and oxaliplatin, an anticancer drug, were able to significantly inhibit the tumor growth in oxaliplatin resistant colon cancer mice models. Indeed, the study showed that these resistant cells expressed low levels of PGM5-AS1, able to inhibit cell proliferation and migration (Fig. 1) [23]. A new approach to fight cancer could be to enhance the specific immune response. In this regard, the study of Huang et al. formulated a vaccine with engineered breast cancer-derived exosomes. They uploaded the TLR3 agonist (Hiltonol), as immunogenic cell death (ICD) inducer, and the human neutrophil elastase (HELANE) into α-lactalbumin engineered breast cancer derived exosomes (HELA-Exos). These induced a potent ICD in breast cancer cells, a significant growth inhibition of patient-derived breast cancer organoids and an increased activation of
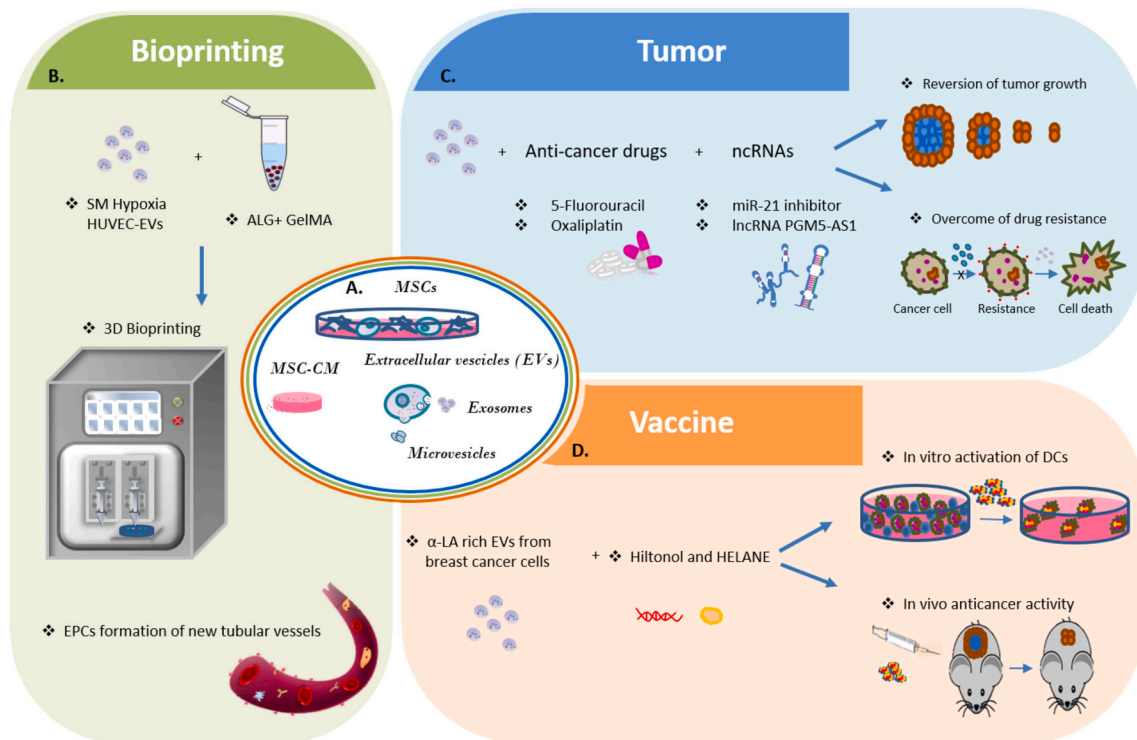
Fig. 1. Schematic illustration of the engineered EVs function.

A. Mesenchymal Stem Cells (MSCs) cultured in a specific medium, so called 'conditioned medium' (MSC-CM), secrete extracellular vesicles (EVs) as exosomes and microvesicles. B. [Bioprinting]: EVs derived from HUVECs (HUVEC-EVs) cultured in serum free medium (SM) and hypoxia conditions were 3D bioprinted together with a bioink composed by alginate [ALG (4 % *w/v*)] and gelatin methacrylamide [GelMA (6 % w/v)]. The bioprinted structure led the endothelial progenitor cells to form new angiogenic vessels. C. [Tumor]: Exosomes functionalized with anti-cancer drugs (5-Fluorouracil and Oxaliplatin) and non-coding RNAs (ncRNAs) (miR-21 inhibitor and the antisense long ncRNA PGM5-AS1) were able to revert the tumor growth and to overcome the drug resistance phenomena leading to the cancer cells death. D. [Vaccine]: EVs rich in α-lactalbumin (α-LA) levels derived from genetically engineered breast cancer cells were uploaded with Hiltonol (immunogenic cell death inducer) and Human Neutrophil Elastase (HELANE). The engineered EVs induced: -*in vitro* activation of dendritic cells (DCs) in patient-derived breast cancer organoid-Peripheral Blood Mononuclear Cell (PBMC) co-cultures; -the decrease of the tumor size in *in vivo* mice model.

dendritic cells in organoid-Peripheral Blood Mononuclear Cell (PBMC) co-cultures. HELA-Exos exhibited a potent anticancer activity in *in vivo* mice model, drastically decreasing the tumor sizes (Fig. 1) [22].

4. Cardiovascular diseases

Cardiovascular diseases (CVDs) are heart and circulatory system disorders with an extremely high incidence. CVDs are classified as chronic diseases and evolve gradually over a lifetime, generating numerous symptoms in the patients. They can also lead to sudden death. EVs seem to be excellent candidates for the treatment of myocardial damage, as shown by some recent studies. The treatment with MSC-EVs by hypoxic cardiomyocytes caused a marked improvement in cell invasion, proliferation and migration compared to the treatment of miR-497 alone. In fact, these EVs expressed SMAD7, a miR-497 target, that influenced the improvement in myocardial infarction due to its ability to regulate TGF-β, VEGF, collagen type 1, and αSMA, all factors involved in the advancement of cardiac fibrosis and thus its degeneration [74]. In another study, MSC-EVs were intravenously injected into rats with myocardial infarction (MI). Due to the release of miR210, they were able to increase angiogenesis and decrease fibrotic area, leading to the improvement of myocardial function (see Table 2) [67]. Likewise, in the condition of myocardial damage induced by severe acute pancreatitis (SAP), the use of MSC-EVs induced the decrease of the inflammatory response (TNF-α, IL-1β and IL-6) thanks to miR-29a-3p release (see Table 2). It acted by blocking HMGB1 and consequently the TL4/akt response, which played a key role in the development and exacerbation of cardiovascular disease [68]. MSC-EVs vehiculated also miR-4732-3p and miR-200b-3p (see Table 2), responsible in activating

cardioprotective mechanisms in myocardial infarction (MI) models. Neonatal rat cardiomyocytes (NRCMs) were deprived of oxygen-glucose (OGD) to induce ischemia and, after miR-4732-3p transfection, an increased connexin 3 expression was observed. It was related to improved contraction, decreased extracellular matrix deposition and myofibroblastic markers expression, related to fibrosis [69]. Moreover, miR-200b-3p injected into MI mice, reduced the inflammatory response (IL-1β and IL-18) and oxidative stress in myocardium and improved cardiac function [70].

5. Autoimmune diseases

Autoimmune diseases are characterized by a misreaction of the immune system, which attacks and destroys healthy tissues in the body by mistakenly recognizing them as foreign. These disorders are multifaceted and the causes are not entirely clear but several external factors seem to play a role. Recently, it was discovered that EVs derived from mesenchymal stem cells play a role in the progression or otherwise of the disease. In this regard, over-expressing programmed cell death-ligand 1 + (PD-L1) MSC-EVs (MSC-EVs-PD-L1) showed the ability to reconfigure the immune microenvironment in mouse models when ulcerative colitis and psoriasis were induced. They significantly reduced the expression of IFN-γ$^+$ CD4$^+$ T cells CD3$^+$ Ki-67$^+$, CD80, IL1-β and TNF-α (pro-inflammatory markers) and increased the expression of FOX3, CD206+, IL10 (anti-inflammatory markers). In ulcerative colitis, there was an improvement of the disease activity index in the colon as well as the blockage of tissue lesions confirmed by histological analysis. In psoriasis, MSC-sEVs-PD-L1 administration caused to significantly relieve symptoms by inhibiting acanthosis, parakeratosis and stratum corneum

thickening [75]. BM-MSC-EVs also exerted therapeutic effects on type 1 diabetes (T1D) and experimental autoimmune uveoretinitis (EAU). The intravenously MSC-EVs administration in T1D mice preserved the ability to produce insulin thus avoiding hyperglycemia compared with PBS injection. EAU mice treatment with the same EVs, showed an appearance to normal retinas without induction of the disease. In addition, there was a reduction in CD3$^+$ T cells and pro-inflammatory cytokines expression levels such as IL-2, IL-1b, IL-6, IL-12A, IFN-g and IL-17A [76]. EVs isolated from hUCMSCs were also tested in other autoimmune diseases such as for autoimmune encephalomyelitis (EAE) treatment. It is a central nervous system disease that involves the cells of the immune system (T lymphocytes, B lymphocytes, macrophages and microglia). After the disease induction in C57Bl/6 mice, Koohsari et al. intravenously injected hUCMSC-EVs, obtaining the reduction of IFN-γ, TNFα and IL-17a expression levels. There was also the decrease of leukocytes infiltration in mice spinal cord and bone marrow inflammation, and the increase of Treg cells frequency [77]. Another study applied hUCMSC-EVs on a systemic lupus erythematosus (SLE) condition. It is a connective tissue disease characterized by erythematous skin, mucosal manifestations and systemic involvement of almost all organs. The results showed that hUCMSC-EVs inhibited CD4$^+$ T cells and CD19$^+$ B cells frequencies whilst increased the production of T helper (Th)17 cells, IL-17, IL-4, IFN-γ and TGF-β1[78].

6. Characterization of secretome from fetal MSCs

Several studies have already proved that there are important differences amongst adult and fetal MSCs. Indeed, fetal MSCs showed better abilities as immune-modulators [79] and are more proliferative with longer telomeres and less predestined, with an higher expression of the pluripotency markers than adult ones [80,81]. Moreover, they showed enhanced neuroprotective abilities also in *in vivo* models [82].

Due to the differences in the cell properties at different stages of life, it was easy to speculate that their secreted factors might also show substantial differences. Thus, Lobov et al., for the first time, analyzed the protein composition of the secretome from human fetal multipotent MSCs (FetMSCs) isolated by early human embryo bone marrow. The authors identified 236 proteins amongst whom an higher quantity was involved in ECM organization, signal transduction and cell adhesion. In particular, an enrichment of anti-apoptotic proteins such as CD44, metalloproteinase inhibitor 1 and filamin-A was found in FetMSCs secretome. Moreover, positive regulators of angiogenesis such as annexin A2, ECM protein 1, connective tissue growth factor, aminopeptidase N and lactadherin and negative regulators as plasminogen activator inhibitor-1 and TGFBI were found. The authors also revealed the expression of proteins involved in activating and inhibiting osteogenic differentiation, respectively semaphorin-7A, stanniocalcin-1, tenascin, exostosin-1 and 2, COL6-A1 and MMP2 as activators whilst twisted gastrulation protein homolog 1, gremlin-1 and insulin-like

growth factor binding protein-3 as inhibitors (see Table 3). In addition, FetMSCs secretome analysis showed an enrichment in proteins involved in anti-viral processes, such as: heterogeneous nuclear ribonucleoprotein A1 (hnRNPA1), fibulin-1, heat shock 70 kDa protein 8 (HSPA8), matrix metalloproteinase-1 (MMP-1), talin-1, major histocompatibility complex class I, C (HLA―C), milk fat globule-EGF factor 8 protein (lactadherin) and vimentin [83].

Gaetani et al. investigated the different protein expression amongst the secretome of fetal and adult MSCs. Multipotent fetal dermal cells (MFDCs) were isolated from small fetus and adult dermal cells (ADCs) from adult subjects. Fetal skin is the most able tissue to induce regeneration processes avoiding fibrosis formation, typical of reparative processes. Fetal skin fibroblasts are the main effectors of regeneration, producing an ECM matrix with a different composition than the adult one. The MFDCs secretome was composed by several over-expressed proteins mainly involved in the positive regulation of wound healing and angiogenesis such as EPHA2, NRP2, DCBLD2, PDGFC and IGFBP2. In addition, proteins involved in basal membrane organization such as laminin α1, agrin, EDIL3, CPA4 and EFEMP1 or in ECM composition and remodelling as collagen chains Va2, VIIa1, IVa2 and XVIIIa1 were up-regulated together with ApoE and FABP5, involved in cellular metabolism processes. Negative angiogenesis regulators, pro-fibrotic and pro-inflammatory factors and ECM remodelling factors involved in inducing skin reparation instead of regeneration were down-regulated in MFDCs secretome rather than in ADCs one [84].

Xu et al. investigated the effects of human fetal MSCs (hFMSCs) secretome compared to human adult MSCs (hAMSCs) one on rat BM-MSCs (rBMSCs) through *in vivo* experiments. They analyzed the stimulation of rats' immunological system and the osteogenic differentiation of rBMSCs. HFMSCs secretome did not induce a significative immune response compared with hAMSCs one. Moreover, hFMSCs secretome at a dose of 100 μg/μl led to the up-regulation of typical osteogenic markers like OSX, OPN, OCN and Runx2 [86].

Shin et al. compared the proteins secreted from adult and fetal MSCs. In adult MSCs, BM-MSCs and AD-MSCs, they identified respectively 253 and 265 secreted proteins, whilst in fetal MSCs, Wharton's Jelly-MSCs (WJ) and Placenta-MSCs (PL), they identified respectively 440 and 511 proteins.

Fetal MSCs secretome was enriched in angiogenesis related factors such as VEGF, PDGF, CSF, TIMP, IL-6, HGF and TGF-β. Moreover, WJ-MSCs secretome was enriched in cytokines and growth factors such as IL-6, IL-11, LIF, ICAM and CXCL. Proteins related to the anti-apoptotic activity such as PPIA, PPIB and PPIC were found in all AD, WJ and PL-MSCs secretome [85].

7. Analysis of secretome from 3D cultured MSCs

Several scientific studies proved that cells cultured under 3D conditions were able to better mimic the properties of their native tissues [87,88] both in oncological and regenerative studies. In this last field, until ten years ago, mesenchymal stem cells were only cultured in 2D adhesion conditions. Recently, several studies were performed on 3D cultures, demonstrating their effective superiority. Although to date there is still no standardized technique to obtain 3D spheroids, many studies compared 2D and 3D cultures of adipose derived stem cells proving the higher multilineage differentiation potential of 3D cultured cells as well as their abilities in maintaining stemness until 28 days and better regenerative abilities in *in vitro* and *in vivo* experiments [89,90]. Moreover, 3D cultured cells are closer to their physiological condition and do not express altered surface molecules compared to 2D cultured ones. In fact, in adhesion conditions cells have to adhere to plastic in an artificial manner and it alters the expression of their surface molecules [91]. Different techniques were performed to form spheroids [92,93] or also to obtain a 3D structure through the use of specific scaffolds [94–96].

It is easy to speculate that differences in cell properties may be

Table 3

Summary of the secreted factors from fetal MSCs.

Authors	Soluble fraction	EVs fraction
[83]	Fetal MSCs: CD44, metalloproteinase inhibitor 1, filamin-A, annexin A2, ECM protein 1, connective tissue growth factor, aminopeptidase N, lactadherin, plasminogen activator inhibitor-1, TGFBI, semaphorin-7A, stanniocalcin-1, tenascin, exostosin-1 and 2, COL6-A1, MMP2, twisted gastrulation protein homolog 1, gremlin-1, insulin-like growth factor binding protein-3, hnRNPA1, fibulin-1, HSPA8, MMP-1, talin-1, HLA-C, lactadherin, vimentin	
[84]	Fetal MSCs: EPHA2, NRP2, DCBLD2, PDGFC and IGFBP2, laminin α1, agrin, EDIL3, CPA4 and EFEMP1, Va2, VIIa1, IVa2 and XVIIIa1, ApoE and FABP5	
[85]	Fetal MSCs: VEGF, PDGF, CSF, TIMP, IL-6, HGF, TGF-β	

reflected in the secretion of different factors and thus in the formation of a particular secretome, but few studies have been done on this issue. The secretome from 3D adipose tissue MSCs (AT-MSCs) was enriched with some growth factors (HGF and PDGF-AB) and cytokines (IL-1, SFD-1, IL-6, TGF-β1) with pro and anti-inflammatory functions when compared to the one from 2D-AT-MSCs cultures [94]. Similarly, the secretome from 3D BM-MSCs spheroids, was richer of G-CSF (a factor stimulating the bone marrow to produce more white blood cells), IL-1Ra (an anti-inflammatory protein that inhibits IL-1 pro-inflammatory effects) and VEGF (an important regulator of angiogenesis) secreted factors than the secretome from 2D cultured cells [93]; hBM-MSC 3D spheroids also secreted a higher amount of TSG-6, STC-1 and LIF, anti-inflammatory proteins, IL-24 and TRAIL, two anti-cancer genes and CXCR4, a receptor for MSC homing, compared to cells grown in adhesion conditions. Thus, spheroids can exert anti-inflammatory effects through their secreted factors [92]. hUC-MSCs cultured in 3D and 2D also showed differences in secreted factors. In fact, 3D cells secreted a higher amount of anti-inflammatory cytokines, such as IL-10 and LIF, and factors involved in tissue regeneration mechanisms, such as PDGF-BB, FGF-2, I-309-SCF and GM-CSF, compared to 2D cultured cells. On the other hand, IL-6, MCP-1 AND IL-21 expression levels were increased in 2D cultures and played a role in pro-inflammation and progression of joint diseases as rheumatoid arthritis (RA) [97].

In addition, the secretome from BM-MSCs cultured in canonical 2D adhesion conditions or in a 3D environment, such as 3D electrospun fiber scaffolds (polycaprolactone and gelatin), revealed substantial differences. The analysis of secretome from 3D cultured MSCs showed the over-expression of 14 proteins related to different functions (HGF, IL-6, LIF, Eotaxin, MCP-1, FGF-b, MCP-3, VCAM-1, ICAM-1, resistin, VEGF, IL-8, IL-9, and TGF-β1) and the down-regulation of PAI-1 (Plasminogen activator inhibitor-1, involved in a wide range of processes such as the physiological hemostasis but also the pathological atherosclerosis, insulin resistance, obesity). On the contrary, SDF1-α (Stromal cell derived factor-1 aplha), a chemokine involved in a variety of functions as immune cell regulation, tumorigenesis, wound healing, stem cell survival and development and regulation of osteogenic differentiation, was unically expressed in the secretome from 2D cultured MSCs [95].

Moreover, BM-MSC spheroids trapped in RGD modified alginate hydrogels showed a higher cell viability and secreted a significant amount of VEGF as well as of IL-8, MCP-1 and GRO, all factors with a critical positive role in stimulating angiogenesis [96].

The role of human endothelial umbilical cord (HUVEC) – EVs was investigated in 3D-printed structures made by an innovative bioink of alginate (ALG) (4 % *w/v*) and gelatin methacrylamide (GelMA) (6 % w/v). HUVECs cultured in serum-free and hypoxia (SM Hypoxia) conditions released a high amount of EVs, especially exosomes, with high CD9, CD81, VEGFR2 and PIGF expression levels. *In vitro* and *in vivo* experiments confirmed that EVs derived from HUVECs cultured in SM Hypoxia had a great ability in stimulating EPCs to differentiate and form new tubular vessels and that the 3D bioprinted structure functioned as a guide for the new angiogenic network organization (Fig. 1) [98]. A similar approach with goat articular chondrocytes derived exosomes and CGC (chitosan-gelatin-chondroitin sulphate) cryogel was used in an articular cartilage repair study. The treatment with exosomes (20 μg/ml) and a cryogel extract rich in chondroitin sulfate led to a high cell proliferation and a complete wound closure of a chondrocyte monolayer. This treatment could be important to vehicle inductive informations for cell proliferation [25].

Similarly, hUC-MSCs secretome was adsorbed in 3D printed structures of collagen and silk fibroin (3D-C/S). Analysis showed an improved secretome stability when it was trapped in this 3D printed structure as well as a good biocompatibility with neural stem cells *in vitro*. Then, the implantation of these systems in rats with complete spinal cord transection, led to a significant recovery of locomotor function thanks to a suitable microenvironment for the regeneration of remyelinate nerve fibers and the restoration of synaptic connections [99] (see Table 4).

Table 4
Summary of the secreted factors from 3D-cultured MSCs.

Authors	Soluble fraction	EVs fraction
[94]	3D cultured AT-MSCs: PDGF, TGFβ1, HGF, SDF-1, IL-1, IL-6	
[93]	3D cultured BM-MSCs: G-CSF, IL-1Ra, VEGF	
[92]	3D cultured BM-MSCs: TSG-6, STC-1, LIF, IL-24, TRAIL, CXCR4	
[97]	3D cultured UC-MSCs: IL-10, LIF, PDGF-BB, FGF-2, I-309, SCF e GM-CSF	
[95]	3D cultured BM-MSCs: HGF, IL-6, LIF, Eotaxin, MCP-1, FGF-b, MCP-3, VCAM-1, ICAM-1, resistin, VEGF, IL-8, IL-9, and TGF-β1. Very low expression of PAI-1	

8. Secretome and epigenetic modifications

In recent years, science has focused much of its interest on studying the environmental effects on cells. The outdoor and indoor air pollution is amongst the increasingly significant issues, resulting in the death of more than 6 millions of people [100]. Moreover, the exposure to chemical compounds (for example phthalates and phenols, perfluorinated chemicals, ethyl paraben) as well as ionizing radiations, metals or cigarette smoke, lead cells to side effects [101]. It was already known that cells receiving an environmental stimulus affect their extracellular vesicles in content and number [102]. Starting from this knowledge, science is now paying attention on how environmental factors affect the message carried by EVs or how EVs induce epigenetic modifications in recipient cells.

A recent study showed the role of extracellular vesicles in contributing to the pathogenesis triggered by the environmental pollution. In fact, particulate inhalation leads bronchial epithelial cells and macrophages to secrete pro-inflammatory factors which are also enclosed in their produced EVs. Meanwhile, these ultrafine particles reach the bloodstream stimulating endothelial and circulating cells to secrete other pro-inflammatory EVs. It was showed that all of these vesicles, enriched with pro-inflammatory factors, can contribute to trigger or amplify systemic diseases such as cancer, neurodegenerative and cardiovascular ones [101]. UV exposure, air pollution but also physical exercise and diet can affect the EVs content, influencing the aging process. In fact, the few studies carried out to date demonstrated that a low-calorie diet can lead to an EV *cargo* poor in pro-inflammatory and pro-aging factors as well as an unsatured fatty acid and antioxidant factors rich diet can be associated with low levels of pro-inflammatory and pro-thrombotic circulating EVs. Similarly, it was proved that a constant physical exercise can slow down the aging processes [102]. In addition, some recent studies focused in more detail whether specific epigenetic modifications can affect the message carried by EVs or how epigenetic modifications EV-induced can influence the cellular fate. In this regard, osteoblasts treated with Thricostatin A (TSA), a histone deacetylase inhibitor (HDACi), were investigated to evaluate if their secreted EVs showed enhanced osteo regenerative properties. The results showed that EVs from treated cells induced BSP1, COL1A, ALP and OCN mRNAs up-regulation as well as the increased expression of ALP, COL1A and OCN intercellular proteins in hBM-MSCs. Effectively, TSA-EVs *cargo* was enriched in transcriptional regulators and specific miRNAs involved in pro-osteogenic pathways [27].

Similarly, osteosarcoma-derived EVs (OS-EVs) were tested for their ability in inducing MSCs or pre-osteoblasts to acquire malignant characteristics. The epigenetic effects induced by OS-EVs on these cells were tested analyzing LINE-1 (long interspersed element) and tumor suppressor genes methylation. The results showed that only MSCs exposed to OS-EVs, already within a short time after treatment, presented LINE-1 hypomethylation and this contributed to cancer development. By contrast, they did not show alterations in the methylation status of tumor suppressor genes, thus indicating that a later promotor hyper-methylation probably occurred to mute their function [103].

The role of lncRNA UFC1 was also investigated in oncogenic field. It is highly expressed in serum and serum exosomes isolated from serum samples of non-small cell lung cancer (NSCLC) patients. The results showed that UFC1 exerted a pivotal role in promoting NSCLC progression due to its binding to EZH2, a histone methyltransferase that targeted PTEN promoter region. PTEN is a tumor suppressor gene and EZH2 induced histone 3 lysine 27 trimethylation (H3K27me3) in PTEN promoter region, inhibited its transcription and thus its activation. Simultaneously, EZH2 activated the Akt pathway stimulating migration and proliferation of malignant cells [104].

The epigenetic effect induced by ethanol treatment was analyzed on organotypic brain slice cultures (OBSCs). It was known that microglia promoted adult ippocampal neurogenesis (AHN) thanks to its secreted EVs. Thus, OBSCs were used to generate microglia derived EVs after ethanol (EtOH) treatment or not (pro-neurogenic control). The results showed that EtOH-EVs did not promote neurogenesis and were enriched with proinflammatory cytokines. The authors found that methyltransferase G9a mRNA was 3-fold increase in EtOH-EVs compared to non-treated ones. Moreover, histone 3-lysine 9 dimethylation (H3K9me2) epigenetic modification was higher in OBSCs treated with EtOH-EVs compared to the pro-neurogenic control thus leading to identify G9a-GLP complex (G9a formed a complex with G9a-like protein, GLP, to exert its enzymatic activities) as the main author in AHN inhibition [28].

The effect of exosomes generated by engineered cells was also tested to fight HIV virus. Cells were programmed through the fusion of a gene encoding for a Zinc Finger Protein, which binds to site 362 on HIV-1 LTR (ZFP-362), and a DNA methyltransferase 3 domain (DNMT3A). Firstly, the authors transfected ZD3A fusion protein into chronically HIV-1 infected Jurkat cells (CHI-Ju), showing that it was able to selectively bind 5′ LTR promoter region of HIV-1. In this site, it induced CpG methylation, an epigenetic modification that led to the inhibition of virus expression. Secondly, they generated new fusion proteins and, amongst them, ZPAMt (ZFP fused to PWWP, ADD, and Methyltransferase domains) was tested, due to its long and stable virus repression in Chi-Ju HIV-1 infected cells. Therefore, ZPAMt packaged into the exosomes made possible the repression of HIV-1 infection in humanized NSG mice engrafted with HIV-1-infected PBMCs (hu-PBMCNSG) in *in vivo* experiments. After having refined the way of application of these engineered exosomes, their use could be an important supportive therapy to the current cART, in the way to block HIV infection and improve the life quality of infected people [26].

9. Conclusion

Mesenchymal stem cells are multipotent cells with different functions [1–3]. Recently, several studies attributed these abilities to their secreted factors that act in a paracrine manner on the neighbouring cells [9–13]. In fact, paracrine signalling happens through the so-called "secretome", formed by soluble factors, released by the cells in the culture medium, and extracellular vesicles (EVs), which are vehicles of small and long non-coding RNAs, proteins and lipids that influence the pathways of the recipient cells [15–17].

The angiogenic and osteogenic regenerative processes play a key role in new tissue formation, especially in avoiding the activation of reparative processes after extensive damage, resulting in the formation of scar tissue. About that, miR-31, over-expressed in ASC derived EVs, was able to stimulate neo-vessels formation [37,38] as well as miR-146a [52,53] and miR-27a/b [54], whilst miR-196a, miR-27a, miR-122-5p, miR-206 and lncRNA MALAT1 were involved in osteogenic pathways [43,56–58].

Several studies discovered some specific factors contained into the secretome from cancer cells that could be used as tumor biomarkers [61,62] and others actively involved in cancer progression [63–65]. In addition, MSC-EVs were enriched in miRNAs involved in improving myocardial function such as miR-210, miR-29a-3p, miR-4732-3p and miR-200b-3p [67–70].

MSC-EVs-PD-L1, BM-MSC-EVs and hUCMSCs-EVs also showed a therapeutic role on autoimmune disorders [75–78].

A first consideration can be made regarding all stem cells that, through the pre-stimulation with specific factors, can be induced to generate a differentially composed secretome. The most commonly studied factors are: - IFNγ, tested in oncological field [71]; - IL-1α, IL1-β, TNF-α and IFNγ, tested on LPS-stimulated microglial cells [93] and - TNFα and IL-10, tested on macrophages immunomodulation [105]. Effectively, all these studies proved that modified secretome could be used for different applications as the inhibition of cell migration, proliferation or the progression of autoimmune, neurodegenerative or cardiovascular complications. Moreover, a modified secretome could contain pro-apoptotic factors useful, for example, in case of tumor or higher levels of pro-angiogenic and pro-osteogenic factors useful for regenerative applications. Thus, a more in-depth study on secretome and the factors that may mostly influence its composition could contribute to the enhancement of secretome for regenerative applications whilst, in the pathological field, it could allow for the identification of new biomarkers, also present in patients' blood, allowing for more rapid diagnosis and, on the other hand, it could enable to discover new targets for new therapies.

With reference to the cited studies, a second consideration can be made regarding the difference in the secretome function and composition depending on the condition of cell culturing.

Few studies compared the secretome from 2D and 3D cultured cells opening up the possibility of culturing cells under 3D conditions in the way to better mimic their *in vivo* environment and likely give to secretome better characteristics. In this regard, some of these studies provided a new perspective on the dynamic use of secretome from 3D-cultured MSCs. In fact, the static addition of conditioned medium to cells leads to the consumption of its soluble factors without giving them the opportunity to produce new ones in terms of quantity and quality. A dynamic communication amongst the cells could, instead, allow them to continuously modify their secretome in response to received stimuli [95]. In addition, supporting 3D cell growth with modified or unmodified scaffolds could generate a microenvironment able to induce the secretome enhancement for specific applications [96].

The human fetal MSCs expressed more primitive developmental genes and possessed better properties than adult ones, and their secretome was enriched in anti-apoptotic factors [83] as well as pro and anti angiogenic and osteogenic differentiative proteins [83,85]. Instead, MFDCs secretome was full of over-expressed proteins involved in angiogenesis, wound healing processes and cellular metabolism [84]. All of these studies led us to speculate that the secretome from fetal MSCs could be considered the most useful for regenerative applications if compared to the secretome from adult cells and, in accordance with the studies on the secretome derived from 3D cultured cells, we suggest it might also be interesting to understand whether fetal cells cultured under three-dimensional conditions could further enhance the therapeutic capabilities of their secretome.

In addition, we focused on the latest techniques for engineering extracellular vesicles and their applications. One of the most significant is the targeted drug delivery. In fact, in the highly investigated oncological field, exosomes were specifically engineered to overcome the drug resistances [23,24] as well as for the generation of a new *in situ* vaccine able to enhance the DC immune response in an *in vivo* breast cancer model [22]. Instead, in the regenerative field, Nikhil et al. investigated the role of exosomes in mediating the communication of chondrocytes plated in a porous scaffold. Similarly, Maiullari et al. generated a 3D printed structure with EVs inserted in a polymeric scaffold to confine them into a specific site of interest. Effectively, this complex was an inductor and a guide for neo-vessels organization. Analogously, Chen et al. made the secretome by hUC-MSCs adsorbed in a 3D printed structure of collagen and silk fibroin, proving the enhanced secretome stability as well as the ability of this structure in inducing the

spinal cord regeneration in *in vivo* rat spinal cord injured models. All these studies led us to speculate that the new 3D technologies, together with the discovering of new biocompatible materials, could be the new frontiers for several medical applications. They would overcome the drug resistances, the loss of nanoparticles in the circulating body fluids, the stimulation of the immune-response and the risk of tumorigenesis. Moreover, a scaffold can confine the secretome and/or EVs in a specific injured site thus stabilizing it and allowing the neighbouring cells to colonize it and differentiate or also to receive stable signals for a specific tissue regeneration. Finally, we summarized some recent studies on how epigenetic modifications can affect the message carried by EVs or how EVs can influence the cellular fate inducing them. In fact, although it is still a new field to explore, some recent studies focused on how exposure to substances, such as Thricostatin A or ethanol, can induce cell modifications and thus a change in the EVs *cargo*. For example, the epigenetic modification induced by HDAC inhibition TSA-induced in osteoblasts made EVs acquire better osteo-inductive abilities [27] whilst ethanol treated organotipic brain slice cultures changed microglia-EVs function from pro- to anti-neurogenic, thus inhibiting adult ippocampal neurogenesis [28]. In addition, with regard to the oncological field, osteosarcoma derived EVs were found able to induce LINE-1 hypomethylation in MSCs and thus tumor progression through an epigenetic modification [103]. Similarly, lncRNA UFC1 contained in serum exosomes from non-small cell lung cancer patients induced PTEN suppression through H3K27me3 EZH2-mediated [104]. Although few studies on this topic have been done to date, it can be already clear that environmental exposure to pollutants but also factors such as diet and physical activity, radiations and chemical substances can interfere with the expression of certain genes within cells. Consequently, it leads to changes in the messages vehiculated by cell secreted EVs. This opens up new perspectives to investigate a new kind of cell modifications, due to the crosstalk between healthy and cancer cells, but also the safety on the use of specific chemical substances and the effects of some environmental pollutants with the goal of finding new strategies to have a minor environmental impact and lower risks on the human health.

Funding

Data availability

No data was used for the research described in the article.

CRediT authorship contribution statement

Valentina Urrata: Conceptualization, Writing – original draft, Writing – review & editing. **Marco Trapani:** Writing – original draft. **Mara Franza:** Writing – original draft. **Francesco Moschella:** Supervision, Writing – review & editing. **Anna Barbara Di Stefano:** Conceptualization, Supervision, Writing – original draft, Writing – review & editing. **Francesca Toia:** Supervision, Writing – review & editing.

Declaration of competing interest

The authors declare that there are no conflicts of interest.

Acknowledgements

References

[1] A.A. Khan, T.J. Huat, A. Al Mutery, A.T. El-Serafi, H.H. Kacem, S.H. Abdallah, et al., Significant transcriptomic changes are associated with differentiation of bone marrow-derived mesenchymal stem cells into neural progenitor-like cells in the presence of bFGF and EGF, Cell Biosci. 10 (2020) 126.

[2] M.F. Pittenger, A.M. Mackay, S.C. Beck, R.K. Jaiswal, R. Douglas, J.D. Mosca, et al., Multilineage potential of adult human mesenchymal stem cells, Science 284 (1999) 143–147.

[3] K.S. Bae, J.B. Park, H.S. Kim, D.S. Kim, D.J. Park, S.J. Kang, Neuron-like differentiation of bone marrow-derived mesenchymal stem cells, Yonsei Med. J. 52 (2011) 401–412.

[4] W.H. Huang, M.C. Chang, K.S. Tsai, M.C. Hung, H.L. Chen, S.C. Hung, Mesenchymal stem cells promote growth and angiogenesis of tumors in mice, Oncogene 32 (2013) 4343–4354.

[5] J. Kossl, P. Bohacova, B. Hermankova, E. Javorkova, A. Zajicova, V. Holan, Antiapoptotic properties of mesenchymal stem cells in a mouse model of corneal inflammation, Stem Cells Dev. 30 (2021) 418–427.

[6] I. Papazian, V. Kyrargyri, M. Evangelidou, A. Voulgari-Kokota, L. Probert, Mesenchymal stem cell protection of neurons against glutamate excitotoxicity involves reduction of NMDA-triggered calcium responses and surface GluR1, and is partly mediated by TNF, Int. J. Mol. Sci. 19 (2018).

[7] P. Huang, N. Gebhart, E. Richelson, T.G. Brott, J.F. Meschia, A.C. Zubair, Mechanism of mesenchymal stem cell-induced neuron recovery and anti-inflammation, Cytotherapy 16 (2014) 1336–1344.

[8] A.R.R. Weiss, M.H. Dahlke, Immunomodulation by Mesenchymal Stem Cells (MSCs): mechanisms of action of living, apoptotic, and dead MSCs, Front. Immunol. 10 (2019) 1191.

[9] L. Chen, E.E. Tredget, P.Y. Wu, Y. Wu, Paracrine factors of mesenchymal stem cells recruit macrophages and endothelial lineage cells and enhance wound healing, PLoS One 3 (2008), e1886.

[10] W. Huang, B. Lv, H. Zeng, D. Shi, Y. Liu, F. Chen, et al., Paracrine factors secreted by MSCs promote astrocyte survival associated with GFAP downregulation after ischemic stroke via p38 MAPK and JNK, J. Cell. Physiol. 230 (2015) 2461–2475.

[11] P. Kuchroo, V. Dave, A. Vijayan, C. Viswanathan, D. Ghosh, Paracrine factors secreted by umbilical cord-derived mesenchymal stem cells induce angiogenesis in vitro by a VEGF-independent pathway, Stem Cells Dev. 24 (2015) 437–450.

[12] H.M. Kwon, S.M. Hur, K.Y. Park, C.K. Kim, Y.M. Kim, H.S. Kim, et al., Multiple paracrine factors secreted by mesenchymal stem cells contribute to angiogenesis, Vasc. Pharmacol. 63 (2014) 19–28.

[13] D. Pankajakshan, D.K. Agrawal, Mesenchymal stem cell paracrine factors in vascular repair and regeneration, J. Biomed. Technol. Res. 1 (2014).

[14] G.H. Lee, S.H. Kim, A. Kang, S. Takayama, S.H. Lee, J.Y. Park, Deformable L-shaped microwell array for trapping pairs of heterogeneous cells, J. Micromech. Microeng. 25 (2015) 1–11.

[15] J. Driscoll, T. Patel, The mesenchymal stem cell secretome as an acellular regenerative therapy for liver disease, J. Gastroenterol. 54 (2019) 763–773.

[16] F.T. Borges, L.A. Reis, N. Schor, Extracellular vesicles: structure, function, and potential clinical uses in renal diseases, Braz. J. Med. Biol. Res. 46 (2013) 824–830.

[17] X. Zhou, F. Xie, L. Wang, L. Zhang, S. Zhang, M. Fang, et al., The function and clinical application of extracellular vesicles in innate immune regulation, Cell Mol Immunol. 17 (2020) 323–334.

[18] M. Battistelli, E. Falcieri, Apoptotic bodies: particular extracellular vesicles involved in intercellular communication, Biology (Basel) 9 (2020).

[19] Y.B. Haddad, S. Robert, P. Salers, L. Zekraoui, C. Farnarier, C.A. Dinarello, et al., Sterile inflammation of endothelial cell-derived apoptotic bodies is mediated by interleukin-1α, PNAS 51 (2011) 20684–20689.

[20] C. Théry, K.W. Witwer, E. Aikawa, M.J. Alcaraz, J.D. Anderson, R. Andriantsitohaina, et al., Minimal information for studies of extracellular vesicles 2018 (MISEV2018): a position statement of the International Society for Extracellular Vesicles and update of the MISEV2014 guidelines, J. Extracell Vesicles 7 (2018) 1535750.

[21] A. Jeyaram, S.M. Jay, Preservation and storage stability of extracellular vesicles for therapeutic applications, AAPS J. 20 (2017) 1.

[22] L. Huang, Y. Rong, X. Tang, K. Yi, P. Qi, J. Hou, et al., Engineered exosomes as an in situ DC-primed vaccine to boost antitumor immunity in breast cancer, Mol. Cancer 21 (2022) 45.

[23] B. Hui, C. Lu, J. Wang, Y. Xu, Y. Yang, H. Ji, et al., Engineered exosomes for co-delivery of PGM5-AS1 and oxaliplatin to reverse drug resistance in colon cancer, J. Cell. Physiol. 1 (2022) 911–933.

[24] G. Liang, Y. Zhu, D.J. Ali, T. Tian, H. Xu, K. Si, et al., Engineered exosomes for targeted co-delivery of miR-21 inhibitor and chemotherapeutics to reverse drug resistance in colon cancer, J. Nanobiotechnol. 18 (2020) 10.

[25] A. Nikhil, A. Kumar, Evaluating potential of tissue-engineered cryogels and chondrocyte derived exosomes in articular cartilage repair, Biotechnol. Bioeng. 119 (2022) 605–625.

[26] S. Shrivastava, R.M. Ray, L. Holguin, L. Echavarria, N. Grepo, T.A. Scott, et al., Exosome-mediated stable epigenetic repression of HIV-1, Nat. Commun. 12 (2021) 5541.

[27] K. Man, M.Y. Brunet, M. Fernandez-Rhodes, S. Williams, L.M. Heaney, L. A. Gethings, et al., Epigenetic reprogramming enhances the therapeutic efficacy of osteoblast-derived extracellular vesicles to promote human bone marrow stem cell osteogenic differentiation, J. Extracell Vesicles 10 (2021), e12118.

[28] J. Zou, T.J. Walter, A. Barnett, A. Rohlman, F.T. Crews, L.G. Coleman, Ethanol induces secretion of proinflammatory extracellular vesicles that inhibit adult

hippocampal neurogenesis through G9a/GLP-epigenetic signaling, Front. Immunol. 13 (2022), 866073.

[29] C. Amnael Orozco-Díaz, R. Moorehead, G.C. Reilly, F. Gilchrist, C. Miller, Characterization of a composite polylactic acid-hydroxyapatite 3D-printing filament for bone-regeneration, Biomed. Phys. Eng. Express 6 (2020), 025007.

[30] S.Y. Hann, H. Cui, T. Esworthy, X. Zhou, S.J. Lee, M.W. Plesniak, et al., Dual 3D printing for vascularized bone tissue regeneration, Acta Biomater. 123 (2021) 263–274.

[31] G.G. Walmsley, R.C. Ransom, E.R. Zielins, T. Leavitt, J.S. Flacco, M.S. Hu, et al., Stem cells in bone regeneration, Stem Cell Rev. Rep. 5 (2016) 524–529.

[32] Y. Xiao, S. Mareddu, R. Crawford, Clonal characterization of bone marrow derived stem cells and their application for bone regeneration, Int. J. Oral Sci. 2 (2010) 127–135.

[33] Y. Yan, H. Chen, H. Zhang, C. Guo, K. Yang, K. Chen, et al., Vascularized 3D printed scaffolds for promoting bone regeneration, Biomaterials 190–191 (2019) 97–110.

[34] F. Baberg, S. Geyh, D. Waldera-Lupa, A. Stefanski, C. Zilkens, R. Haas, et al., Secretome analysis of human bone marrow derived mesenchymal stromal cells, Biochim. Biophys. Acta, Proteins Proteomics 1867 (2019) 434–441.

[35] S.R. Baglio, K. Rooijers, D. Koppers-Lalic, F.J. Verweij, M. Pérez Lanzón, N. Zini, et al., Human bone marrow- and adipose-mesenchymal stem cells secrete exosomes enriched in distinctive miRNA and tRNA species, Stem Cell Res Ther 6 (2015) 127.

[36] Y. Lu, H. Wen, J. Huang, P. Liao, H. Liao, J. Tu, et al., Extracellular vesicle-enclosed miR-486-5p mediates wound healing with adipose-derived stem cells by promoting angiogenesis, J. Cell. Mol. Med. 24 (2020) 9590–9604.

[37] D. Zhu, Y. Wang, M. Thomas, K. McLaughlin, B. Ogüljahan, J. Henderson, et al., Exosomes from adipose-derived stem cells alleviate myocardial infarction via microRNA-31/FIH1/HIF-1α pathway, J. Mol. Cell. Cardiol. 162 (2022) 10–19.

[38] T. Kang, T.M. Jones, C. Naddell, M. Bacanamwo, J.W. Calvert, W.E. Thompson, et al., Adipose-derived stem cells induce angiogenesis via microvesicle transport of miRNA-31, Stem Cells Transl. Med. 5 (2016) 440–450.

[39] L. Xie, Z. Chen, M. Liu, W. Huang, F. Zou, X. Ma, et al., MSC-derived exosomes protect vertebral endplate chondrocytes against apoptosis and calcification via the mir-31-5p/ATF6 axis, Mol. Ther.–Nucleic Acids 22 (2020) 601–614.

[40] Y.H. Oktaviono, S.A. Hutomo, M.J. Al-Farabi, A. Chouw, F. Sandra, Human umbilical cord blood-mesenchymal stem cell-derived secretome in combination with atorvastatin enhances endothelial progenitor cells proliferation and migration, F1000Research 9:537 (2021) 1–23.

[41] A. Ratushnyy, M. Ezdakova, L. Buravkova, Secretome of senescent adipose-derived mesenchymal stem cells negatively regulates angiogenesis, Int. J. Mol. Sci. 21 (2020).

[42] J. Boulestreau, M. Maumus, P. Rozier, C. Jorgensen, D. Noël, Mesenchymal stem cell derived extracellular vesicles in aging, Front. Cell Dev. Biol. 8 (2020) 1–9.

[43] S. Bianciardi, D. Merlotti, M. Materozzi, Vescicole extracellulari e metabolismo Osseo: ruolo e possibili implicazioni cliniche, L'Endocrinologo 22 (2021) 28–33.

[44] Y. Qin, L. Wang, Z. Gao, G. Chen, C. Zhang, Bone marrow stromal/stem cell-derived extracellular vesicles regulate osteoblast activity and differentiation in vitro and promote bone regeneration in vivo, Sci. Rep. 6 (2016) 21961.

[45] T. Furuta, S. Miyaki, H. Ishitobi, T. Ogura, Y. Kato, N. Kamei, et al., Mesenchymal stem cell-derived exosomes promote fracture healing in a mouse model, Stem Cells Transl. Med. 5 (2016) 1620–1630.

[46] Y.A. Choi, J. Lim, K.M. Kim, B. Acharya, J.Y. Cho, Y.C. Bae, et al., Secretome analysis of human BMSCs and identification of SMOC1 as an important ECM protein in osteoblast differentiation, J. Proteome Res. 9 (2010) 2946–2956.

[47] M. Osugi, W. Katagiri, R. Yoshimi, T. Inukai, H. Hibi, M. Ueda, Conditioned media from mesenchymal stem cells enhanced bone regeneration in rat calvarial bone defects, Tissue Eng. A 18 (2012) 1479–1489.

[48] M. Pranskunas, E. Simoliunas, M. Alksne, A. Kaupinis, G. Juodzbalys, Periosteum-derived mesenchymal stem cells secretome - cell-free strategy for endogenous bone regeneration: proteomic analysis, J. Oral Maxillofac. Res. 12 (2021), e2.

[49] A. Infante, C.I. Rodríguez, Secretome analysis of in vitro aged human mesenchymal stem cells reveals IGFBP7 as a putative factor for promoting osteogenesis, Sci. Rep. 8 (2018) 4632.

[50] S. Ma, A. Zhang, X. Li, S. Zhang, S. Liu, H. Zhao, et al., MiR-21-5p regulates extracellular matrix degradation and angiogenesis in TMJOA by targeting Spry1, Arthritis Res. Ther. 22 (2020) 99.

[51] Q. Li, B. Hu, G.W. Hu, C.Y. Chen, X. Niu, J. Liu, et al., tRNA-derived small non-coding RNAs in response to ischemia inhibit angiogenesis, Sci. Rep. 6 (2016) 20850.

[52] H.Y. Zhu, W.D. Bai, J.Q. Liu, Z. Zheng, H. Guan, Q. Zhou, et al., Up-regulation of FGFBP1 signaling contributes to miR-146a-induced angiogenesis in human umbilical vein endothelial cells, Sci. Rep. 6 (2016) 25272.

[53] Y. Li, H. Zhu, X. Wei, H. Li, Z. Yu, H. Zhang, LPS induces HUVEC angiogenesis in vitro through miR-146a-mediated TGF-β1 inhibition, Am. J. Transl. Res. 9 (2) (2017) 591–600.

[54] C. Urbich, D. Kaluza, T. Frömel, A. Knau, K. Bennewitz, R.A. Boon, et al., MicroRNA-27a/b controls endothelial cell repulsion and angiogenesis by targeting semaphorin 6A, Blood 119 (2012) 1607–1616.

[55] R. Takeuchi, W. Katagiri, S. Endo, T. Kobayashi, Exosomes from conditioned media of bone marrow-derived mesenchymal stem cells promote bone regeneration by enhancing angiogenesis, PLoS One 14 (2019), e0225472.

[56] Y.J. Kim, S.W. Bae, S.S. Yu, Y.C. Bae, J.S. Jung, miR-196a regulates proliferation and osteogenic differentiation in mesenchymal stem cells derived from human adipose tissue, J. Bone Miner. Res. 24 (2009) 816–825.

[57] J. Yin, Z. Zheng, X. Zeng, Y. Zhao, Z. Ai, M. Yu, et al., lncRNA MALAT1 mediates osteogenic differentiation of bone mesenchymal stem cells by sponging miR-129-5p, PeerJ 10 (2022), e13355.

[58] Y. Chen, Y.R. Yang, X.L. Fan, P. Lin, H. Yang, X.Z. Chen, et al., miR-206 inhibits osteogenic differentiation of bone marrow mesenchymal stem cells by targetting glutaminase, Biosci. Rep. 39 (2019).

[59] T. Holecki, M. Węgrzyn, A. Frączkiewicz-Wronka, K. Sobczyk, Oncological diseases and social costs considerations on undertaken health policy interventions, Int. J. Environ. Res. Public Health 17 (2020).

[60] C. Wang, J. Guo, N. Zhao, Y. Liu, X. Liu, G. Liu, et al., A cancer survival prediction method based on graph convolutional network, IEEE Trans. Nanobiosci. 19 (2020) 117–126.

[61] X. Li, H. Liu, M.D. Dun, S. Faulkner, X. Liu, C.C. Jiang, et al., Proteome and secretome analysis of pancreatic cancer cells, Proteomics 22 (2022) 1–8.

[62] L. Kashat, A.K. So, O. Masui, X.S. Wang, J. Cao, X. Meng, et al., Secretome-based identification and characterization of potential biomarkers in thyroid cancer, J. Proteome Res. 9 (2010) 5757–5769.

[63] J.H. Jang, D.H. Kim, J.M. Lim, J.W. Lee, S.J. Jeong, K.P. Kim, et al., Breast cancer cell-derived soluble CD44 promotes tumor progression by triggering macrophage IL1β production, Cancer Res. 80 (2020) 1342–1356.

[64] G. Kontostathi, J. Zoidakis, M. Makridakis, V. Lygirou, G. Mermelekas, T. Papadopoulos, et al., Cervical cancer cell line secretome highlights the roles of transforming growth factor-Beta-induced protein ig-h3, Peroxiredoxin-2, and NRF2 on cervical carcinogenesis, Biomed. Res. Int. 2017 (2017), 4180703.

[65] J. Vieira de Castro, E.D. Gomes, S. Granja, S.I. Anjo, F. Baltazar, B. Manadas, et al., Impact of mesenchymal stem cells' secretome on glioblastoma pathophysiology, J. Transl. Med. 15 (2017) 200.

[66] A.T. Raj, S. Kheur, Z. Khurshid, M.E. Sayed, M.H. Mugri, M.A. Almasri, et al., The growth factors and cytokines of dental pulp mesenchymal stem cell secretome may potentially aid in Oral cancer proliferation, Molecules 26 (2021).

[67] N. Wang, C. Chen, D. Yang, Q. Liao, H. Luo, X. Wang, et al., Mesenchymal stem cells-derived extracellular vesicles, via miR-210, improve infarcted cardiac function by promotion of angiogenesis, Biochim. Biophys. Acta Mol. basis Dis. 1863 (2017) 2085–2092.

[68] S. Ren, L. Pan, L. Yang, Z. Niu, L. Wang, H. Feng, et al., miR-29a-3p transferred by mesenchymal stem cells-derived extracellular vesicles protects against myocardial injury after severe acute pancreatitis, Life Sci. 272 (2021), 119189.

[69] R. Sánchez-Sánchez, M. Gómez-Ferrer, I. Reinal, M. Buigues, E. Villanueva-Bádenas, I. Ontoria-Oviedo, et al., miR-4732-3p in extracellular vesicles from mesenchymal stromal cells is cardioprotective during myocardial ischemia, Front. Cell Dev. Biol. 9 (2021), 734143.

[70] J. Wan, S. Lin, Z. Yu, Z. Song, X. Lin, R. Xu, et al., Protective effects of MicroRNA-200b-3p encapsulated by mesenchymal stem cells-secreted extracellular vesicles in myocardial infarction via regulating BCL2L11, J. Am. Heart Assoc. 11 (2022), e024330.

[71] F. Hendijani, S.H. Javanmard, L. Rafiee, H. Sadeghi-Aliabadi, Effect of human Wharton's jelly mesenchymal stem cell secretome on proliferation, apoptosis and drug resistance of lung cancer cells, Res. Pharm. Sci. 10 (2015) 134–142.

[72] A.S. Serras, S.P. Camões, B. Antunes, V.M. Costa, F. Dionísio, V. Yazar, et al., The secretome of human neonatal mesenchymal stem cells modulates doxorubicin-induced cytotoxicity: impact in non-tumor cells, Int. J. Mol. Sci. 22 (2021).

[73] R. Nadesh, K.N. Menon, L. Biswas, U. Mony, K. Subramania Iyer, S. Vijayaraghavan, et al., Adipose derived mesenchymal stem cell secretome formulation as a biotherapeutic to inhibit growth of drug resistant triple negative breast cancer, Sci. Rep. 11 (2021) 23435.

[74] M. Chen, J. Chen, C. Li, R. Yu, W. Chen, C. Chen, Improvement of cardiac function by mesenchymal stem cells derived extracellular vesicles through targeting miR-497/Smad7 axis, Aging (Albany NY) 13 (2021) 22276–22285.

[75] F. Xu, Z. Fei, H. Dai, J. Xu, Q. Fan, S. Shen, et al., Mesenchymal stem cell-derived extracellular vesicles with high PD-L1 expression for autoimmune diseases treatment, Adv. Mater. 34 (2022), e2106265.

[76] T. Shigemoto-Kuroda, J.Y. Oh, D.K. Kim, H.J. Jeong, S.Y. Park, H.J. Lee, et al., MSC-derived extracellular vesicles attenuate immune responses in two autoimmune murine models: type 1 diabetes and uveoretinitis, Stem Cell Rep. 8 (2017) 1214–1225.

[77] S. Ahmadvand Koohsari, A. Absalan, D. Azadi, Human umbilical cord mesenchymal stem cell-derived extracellular vesicles attenuate experimental autoimmune encephalomyelitis via regulating pro and anti-inflammatory cytokines, Sci. Rep. 11 (2021) 11658.

[78] M. Xie, C. Li, Z. She, F. Wu, J. Mao, M. Hun, et al., Human umbilical cord mesenchymal stem cells derived extracellular vesicles regulate acquired immune response of lupus mouse in vitro, Sci. Rep. 12 (2022) 13101.

[79] Y. Yu, A.V. Valderrama, Z. Han, G. Uzan, S. Naserian, E. Oberlin, Human fetal liver MSCs are more effective than adult bone marrow MSCs for their immunosuppressive, immunomodulatory, and Foxp3, Stem Cell Res Ther 12 (2021) 138.

[80] P.V. Guillot, C. Gotherstrom, J. Chan, H. Kurata, N.M. Fisk, Human first-trimester fetal MSC express pluripotency markers and grow faster and have longer telomeres than adult MSC, Stem Cells 25 (2007) 646–654.

[81] C. Götherström, A. West, J. Liden, M. Uzunel, R. Lahesmaa, K. Le Blanc, Difference in gene expression between human fetal liver and adult bone marrow mesenchymal stem cells, Haematologica 90 (2005) 1017–1026.

[82] K.E. Hawkins, M. Corcelli, K. Dowding, A.M. Ranzoni, F. Vlahova, K.L. Hau, et al., Embryonic stem cell-derived mesenchymal stem cells (MSCs) have a superior neuroprotective capacity over fetal MSCs in the hypoxic-ischemic mouse brain, Stem Cells Transl. Med. 7 (2018) 439–449.

[83] A.A. Lobov, N.M. Yudintceva, A.G. Mittenberg, S.V. Shabelnikov, N. A. Mikhailova, A.B. Malashicheva, et al., Proteomic profiling of the human fetal multipotent mesenchymal stromal cells secretome, Molecules 25 (2020).

[84] M. Gaetani, C.M. Chinnici, A.P. Carreca, C. Di Pasquale, G. Amico, P.G. Conaldi, Unbiased and quantitative proteomics reveals highly increased angiogenesis induction by the secretome of mesenchymal stromal cells isolated from fetal rather than adult skin, J. Tissue Eng. Regen. Med. 12 (2018) e949–e961.

[85] S. Shin, J. Lee, Y. Kwon, K.S. Park, J.H. Jeong, S.J. Choi, et al., Comparative proteomic analysis of the mesenchymal stem cells secretome from adipose, bone marrow, placenta and Wharton's Jelly, Int. J. Mol. Sci. 22 (2021).

[86] J. Xu, B. Wang, Y. Sun, T. Wu, Y. Liu, J. Zhang, et al., Human fetal mesenchymal stem cell secretome enhances bone consolidation in distraction osteogenesis, Stem Cell Res Ther 7 (2016) 134.

[87] A. Jauković, D. Abadjieva, D. Trivanović, E. Stoyanova, M. Kostadinova, S. Pashova, et al., Specificity of 3D MSC spheroids microenvironment: impact on MSC behavior and properties, Stem Cell Rev. Rep. 16 (2020) 853–875.

[88] Z. Koledova, 3D Cell Culture: An Introduction, Springer Nature, 2017.

[89] A. Di Stefano, A. Leto Barone, A. Giammona, T. Apuzzo, P. Moschella, S. Di Franco, et al., Identification and expansion of adipose stem cells with enhanced bone regeneration properties, J. Regen. Med. 4:2 (2015) 1–11.

[90] A.B. Di Stefano, F. Grisafi, M. Castiglia, A. Perez, L. Montesano, A. Gulino, et al., Spheroids from adipose-derived stem cells exhibit an miRNA profile of highly undifferentiated cells, J. Cell. Physiol. 233 (2018) 8778–8789.

[91] M. Pappalardo, L. Montesano, F. Toia, A. Russo, S. Di Lorenzo, F. Dieli, et al., Immunomodulation in vascularized composite allotransplantation: what is the role for adipose-derived stem cells? Ann. Plast. Surg. 82 (2019) 245–251.

[92] T.J. Bartosh, J.H. Ylöstalo, A. Mohammadipoor, N. Bazhanov, K. Coble, K. Claypool, et al., Aggregation of human mesenchymal stromal cells (MSCs) into 3D spheroids enhances their antiinflammatory properties, Proc. Natl. Acad. Sci. U. S. A. 107 (2010) 13724–13729.

[93] E. Redondo-Castro, C.J. Cunningham, J. Miller, H. Brown, S.M. Allan, E. Pinteaux, Changes in the secretome of tridimensional spheroid-cultured human mesenchymal stem cells in vitro by interleukin-1 priming, Stem Cell Res Ther 9 (2018) 1–11.

[94] M.B.H. Al-Shaibani, Three-dimensional cell culture (3DCC) improves secretion of signaling molecules of mesenchymal stem cells (MSCs), Biotechnol. Lett. 44 (1) (2022) 143–155.

[95] K. Carter, H.J. Lee, K.S. Na, G.M. Fernandes-Cunha, I.J. Blanco, A. Djalilian, et al., Characterizing the impact of 2D and 3D culture conditions on the therapeutic effects of human mesenchymal stem cell secretome on corneal wound healing in vitro and ex vivo, Acta Biomater. 99 (2019) 247–257.

[96] S.S. Ho, K.C. Murphy, B.Y. Binder, C.B. Vissers, J.K. Leach, Increased survival and function of mesenchymal stem cell spheroids entrapped in instructive alginate hydrogels, Stem Cells Transl. Med. 5 (2016) 773–781.

[97] J.P. Miranda, S.P. Camões, M.M. Gaspar, J.S. Rodrigues, M. Carvalheiro, R. N. Bárcia, et al., The secretome derived from 3D-cultured umbilical cord tissue MSCs counteracts manifestations typifying rheumatoid arthritis, Front. Immunol. 10 (2019) 18.

[98] F. Maiullari, M. Chirivì, M. Costantini, A.M. Ferretti, S. Recchia, S. Maiullari, et al., In vivo organized neovascularization induced by 3D bioprinted endothelial-derived extracellular vesicles, Biofabrication 13 (2021) 1–19.

[99] C. Chen, H.-H. Xu, X.-Y. Liu, Y.-S. Zhang, L. Zhong, Y.-W. Wang, 3D printed collagen/silk fibroin scaffolds carrying the secretome of human umbilical mesenchymal stem cells ameliorated neurological dysfunction after spinal cord injury in rats, Regen. Biomater. 9 (2022) 1–15.

[100] S. Alkoussa, S. Hulo, D. Courcot, S. Billet, P.J. Martin, Extracellular vesicles as actors in the air pollution related cardiopulmonary diseases, Crit. Rev. Toxicol. 50 (2020) 402–423.

[101] C.M. Eckhardt, A.A. Baccarelli, H. Wu, Environmental exposures and extracellular vesicles: indicators of systemic effects and human disease, Curr. Environ. Health Rep. 9) (3) (2022) 465–476.

[102] P. Monti, G. Solazzo, L. Ferrari, V. Bollati, Extracellular vesicles: footprints of environmental exposures in the aging process? Curr. Environ. Health Rep. 8 (2021) 309–322.

[103] B. Mannerström, R. Kornilov, A.G. Abu-Shahba, I.M. Chowdhury, S. Sinha, R. Seppänen-Kaijansinkko, et al., Epigenetic alterations in mesenchymal stem cells by osteosarcoma-derived extracellular vesicles, Epigenetics 14 (2019) 352–364.

[104] X. Zang, J. Gu, J. Zhang, H. Shi, S. Hou, X. Xu, et al., Exosome-transmitted lncRNA UFC1 promotes non-small-cell lung cancer progression by EZH2-mediated epigenetic silencing of PTEN expression, Cell Death Dis. 11 (2020) 215.

[105] L. Saldaña, F. Bensiamar, G. Vallés, F.J. Mancebo, E. García-Rey, N. Vilaboa, Immunoregulatory potential of mesenchymal stem cells following activation by macrophage-derived soluble factors, Stem Cell Res Ther 10 (2019) 58.

Aknowledgements

Ringrazio:

- Il ***Prof. Francesco Moschella*** e la ***Prof. Adriana Cordova*** che hanno creduto in me, supportandomi nel mio lavoro e permettendomi di raggiungere i miei obiettivi professionali all'interno del reparto di Chirurgia Plastica e Ricostruttiva del Policlinico Universitario Paolo Giaccone, Palermo.

- La ***Dott.ssa Anna Barbara Di Stefano*** e la ***Prof. Francesca Toia*** per la disponibilità che mi hanno dimostrato nella realizzazione del mio progetto.

- Mio marito ***Francesco***, per avermi supportata durante tutto il mio percorso.